

# **STRUCTURE, EXPRESSION AND FUNCTION OF THE NOVEL KIND DOMAIN FAMILY PROTEIN**

**very-KIND**



**Anaid Bedrossian**

Thesis submitted in fulfillment of the requirements for the  
Doctor of Philosophy in Biology  
in the  
Bavarian Julius Maximilian University Würzburg, Germany

Würzburg 2008

Eingereicht am:

Mitglieder der Promotionskommission:

Vorsitzender: Herr Prof. Dr. M. J. Müller

Gutachter: Herr Prof. Dr. E. Kerkhoff

Gutachter: Herr Prof. Dr. G. Krohne

Tag des öffentlichen Promotionskolloquiums:

Doktorurkunde ausgehändigt am:

## **Erklärung**

Hiermit erkläre ich an Eides statt, dass ich die Dissertation „Struktur, Expression und Funktion des neuen KIND-Domänen-Familienproteins very-KIND“ selbständig angefertigt und keine anderen als die von mir angegebenen Quellen und Hilfsmittel benutzt habe.

Ich erkläre außerdem, dass diese Dissertation weder in gleicher oder anderer Form bereits in einem anderen Prüfungsverfahren vorgelegen hat.

Ich habe früher außer den mit dem Zulassungsgesuch urkundlich vorgelegten Graden keine weiteren akademischen Grade erworben oder zu erwerben versucht.

Würzburg, den

Anaid Bedrossian

*Πονούντων καί κινδυνεύόντων τά καλά καί μέγαρα έργα.*

*Great achievements belong to those who spare no pains and dread not risks.*

**Alexander the Great**

*For Ani, Arto and Ohan.*

*In loving memory of my great grandparents.*

## Zusammenfassung

Der Ras-Signaltransduktionsweg wird in Neuronen durch eine große Anzahl verschiedener Signale stimuliert. Hierzu gehören trophische Faktoren, Neurotransmitter und modulatorische Neuropeptide. GDP/GTP-Austauschfaktoren (GEFs) vermitteln die Aktivierung der kleinen Ras-GTPasen, indem sie den Austausch von GDP gegen GTP katalysieren, und hierbei ein Signalnetzwerk ermöglichen. In dieser Arbeit wurde ein neuer gehirnspezifischer Ras-GDP/GTP-Austauschfaktor, very-KIND (VKIND), strukturell und funktionell charakterisiert. VKIND gehört, zusammen mit der Nicht-Rezeptor-Tyrosinphosphatase Typ 13 und dem Aktinnukleator Spir, zu der KIND-Proteinfamilie. Die Kinase Non-catalytic C-lobe Domain (KIND) ist strukturell verwandt mit der C-terminalen katalytischen Domäne (C-Lappen) der p21-aktivierten Proteinkinase (PAK). Der Offene Leserahmen aus 5229 Basenpaare des *VKIND* Gens wurde kloniert. Dieser kodiert für ein Protein aus 1742 Aminosäuren mit einem Molekulargewicht von 191 kD. Die Proteinstruktur des VKINDs ist hoch konserviert und kommt nur in Wirbeltieren und Stachelhäutern vor. Das Vorkommen von zwei KIND-Domänen in der aminoterminalen Region ist für dessen Namensgebung verantwortlich. Die KIND-Domäne fungiert als Protein-Interaktionsmodul ohne bisher bekannte katalytische Eigenschaften. Während die Funktion der KIND1-Domäne noch geklärt werden muss, bindet die KIND2-Domäne das Mikrotubuli-assoziiertes Protein 2 (MAP2). Die zentrale Region des Proteins weist zwei hoch konservierte Cluster mit noch unbekannter Funktion auf, sowie ein Super-Helix-Motiv, *coiled-coil*, welches ein potentiell Protein-Interaktionsmodul darstellt. In der carboxyterminalen Region weist VKIND ein Guaninnukleotid-Austauschfaktor für die Protein-Superfamilie der kleinen Ras GTPasen (RasGEF) auf, welches sich in direkter Nachbarschaft des N-terminalen Strukturmotivs RasGEFN befindet. Das VKIND RasGEF-Modul ist strukturell mit der katalytischen Domäne CDC25 aus *S. cerevisiae* verwandt. Die Aminosäuresequenz der VKIND RasGEF-Domäne weist mit einer Homologie von 23% eine enge Verwandtschaft zur RasGEF-Domäne für RapGTPasen auf. Jedoch unterscheiden sich diese durch zwei zusätzliche Insertionen in der VKIND RasGEF-Domäne. Die Erste aus 24 Aminosäureresten bestehende Insertion ist im N-terminalen Bereich der RasGEF-Domäne zwischen den Helices  $\alpha A$  und  $\alpha B$  des SOS1 RasGEF Moduls lokalisiert, während die Zweite aus elf Aminosäureresten bestehende Insertion im C-terminalen Bereich zwischen den Helices  $\alpha J$  und  $\alpha K$  des SOS1 RasGEF Moduls lokalisiert ist. Die RasGEFN-Domäne spielt eine wichtige Rolle für die strukturelle und katalytische Integrität der GEF-Domäne.

Im Maus-Embryo und in der adulten Maus wird *VKIND* spezifisch im Nervensystem exprimiert. Während der Embryogenese findet eine starke *VKIND*-Expression in dem murinen Neuralrohr, dem Telencephalon, dem Retinal-Ganglion und dem Rhombencephalon statt. Für die adulte Maus ist dagegen eine starke Expression ausschließlich in der Purkinje- und der Körner-Zellschicht des Cerebellums charakteristisch.

Studien der subzellulären Verteilung und Zeitraffer-Video-Analysen zeigten die graduelle Akkumulation des VKIND Proteins in freibeweglichen zytoplasmatischen Partikeln. Diese zirkulären Partikeln wuchsen hierbei bis zu einer Größe von 2  $\mu\text{m}$  an und bewegten sich mit einer Geschwindigkeit von maximal 12  $\mu\text{m}/\text{min}$ . Dies deutet auf eine mögliche Rolle des VKINDs bei dem vesikulären Transport hin.

In dieser Arbeit konnte gezeigt werden, dass die VKIND KIND1/KIND2-Region durch die p38 MAP-Kinase phosphoryliert wird. Vor kurzem wurde von anderen Gruppen ein p38-induziertes Neuritenwachstum als Antwort auf einen hypermotischen Schock untersucht. Im Zusammenhang mit dem inhibitorischen Effekt des VKINDs auf das Neuritenwachstum könnte dies zur weiteren Aufklärung des komplexen Ras-Signalweges und der neuronalen Physiologie beitragen.

## Abstract

In neurons the Ras signaling pathway is activated by a large number of various stimuli, including trophic factors, neurotransmitters and modulatory peptides. Guanine nucleotide exchange factors (GEFs) mediate the activation of Ras GTPases, by catalyzing the exchange of GDP for GTP, and facilitate signaling networks crosstalk. In this work, very-KIND (VKIND), a new brain specific RasGEF was structurally and functionally characterized. VKIND belongs to the KIND protein family along with the non-receptor tyrosine phosphatases type 13 and Spir actin nucleation factors. The kinase non-catalytic C-lobe domain (KIND) is similar to the C-terminal protein kinase catalytic fold (C-lobe) of the p21-activated kinase (PAK). The open reading frame (ORF) of the *VKIND* gene of 5229 base pairs was cloned. The *VKIND* ORF translates into a protein of 1742 amino acids residues with a size of 191 kD. The VKIND protein structure is highly conserved among species and at present the protein is found only in Vertebratae and Echinodermatae. The arrangement of two KIND domains at its amino-terminal region, KIND1 and KIND2, is depicted in its name. The KIND module functions as a molecular interaction structure that is deprived of any enzymatic activity. While the precise occupation of the KIND1 domain remains elusive, the KIND2 domain binds to the microtubules-associated protein 2 (MAP2). The protein central portion features two clusters of high conservation of yet unknown function as well as a coiled-coil motif with a putative multiple protein-protein interaction activity. At the carboxy-terminal region VKIND features a guanine nucleotide exchange factor for Ras-like small GTPases (RasGEF) with a structural RasGEFN motif attached at its N-terminal site. The VKIND RasGEF motif is structurally related to the yeast catalytic domain CDC25. The closest relation of the VKIND RasGEF domain with an average sequence identity of 23% is assigned to the RasGEF domains of exchange factors specific for Rap GTPases with two unique insertions: the first one of 24 amino acids in the N-terminal end of the domain (between helices  $\alpha A$  and  $\alpha B$  of the SOS1 RasGEF module) and the second one of 11 amino acids in the C-terminal part (between, helices  $\alpha J$  and  $\alpha K$  of the Sos1 RasGEF module). The RasGEFN domain plays a critical role in sustaining the structural and catalytical integrity of the guanidine exchange factor.

*VKIND* is specifically and highly expressed in the murine nervous system during embryonic development and adulthood. During embryogenesis *VKIND* expression is present in the murine neural tube, telencephalon, retinal ganglion cells, and rhombencephalon. In the adult murine brain *VKIND* expression is most prominent in the cerebellum, however exclusively restricted to the granular and Purkinje cell layers.

Subcellular distribution studies and time-lapse analysis revealed the gradual accumulation of VKIND into highly motile circular particles which featured estimated maximum velocity of 12  $\mu\text{m}/\text{min}$ . By merging the nascent structures progressively grew to estimated 2  $\mu\text{m}$  in size suggesting a role for VKIND in the vesicular transport process.

Furthermore, the KIND1/KIND2 region of the VKIND protein was found to be phosphorylated by the p38 mitogen-activated protein kinase (MAPK), recently discovered to induce neurite outgrowth in response to hyperosmotic shock. In the light of VKIND negatively controlling neurite outgrowth, further elucidation of the complex Ras pathways may provide rewarding insights in the neuronal physiology.

---

# TABLE OF CONTENTS

	<b>Page</b>
<b>Zusammenfassung</b>	i
<b>Abstract</b>	ii
<b>Table of Contents</b>	iii
<b>Acknowledgments</b>	iv
<b>Chapter I   Introduction</b>	1
<b>Chapter II   Materials</b>	15
<b>Chapter III   Methods</b>	21
<b>Chapter IV   Results</b>	37
<b>Chapter V   Discussion</b>	66
<b>Appendix I   <i>mVKIND</i> Sequence</b>	74
<b>Appendix II   Clone Charts</b>	78
<b>Appendix III   List of Abbreviations</b>	85
<b>Appendix IV   List of Publications</b>	89
<b>Appendix V   Vita</b>	90
<b>Bibliography</b>	91



## Acknowledgments

I am pleased to have the opportunity to express my sincere thanks to numerous people who have contributed to this thesis in any way and made this work possible, on a scientific and personal level:

My thesis supervisor, Prof. Dr. Eugen Kerkhoff, for giving me the opportunity to pursue my Ph.D. thesis in his lab, for his constant kind support and valuable inputs, for introducing me to fluorescent microscopy and for letting me attend interesting conferences.

Prof. Dr. Georg Krohne, for generously accepting to co-refer this work and for being part of my thesis jury.

Dr. Antje Berken, for welcoming me twice in her research group at the MPI Dortmund and for introducing me to the fluorescence-based techniques for *in vitro* analysis of GEF activity, for her valuable guidance throughout this time and for the excellent working atmosphere.

Dr. Susanne Hilgert, for being such a nice and supportive lab colleague and friend, for the motivating discussions, for her permanent helpful inputs throughout our late and long ‘brainstorming’ sessions and the careful proofreading of some chapters.

Felix Stark, for his permanent reliable help whenever scientific or computer ‘urgencies’ occurred in the lab and for our enlightening ‘fresh air’ breaks, for the careful proofreading of some chapters and for being a great friend.

Johanna Borawski and Cornelia Leberfinger (I had the pleasure to work with her just for two years), for caring about the order in our lab, their unfailing support, advice, smile and everyday good mood.

Nikola Staykov, for his helpful scientific advice and the precious support with the Vector NTI software, for our extended stimulating discussions and for being a wonderful friend.

Eleonor Göbel, for being such a dear friend, for her constantly open door, unstinting encouragement and helpful advice.

Alexander Kananis, for being such a close and very old friend, for his permanent support and for helping me out with the other great Alexander.

Dr. Ralph Schreck, for his kind support and for providing me with tons of software.

Dr. Eike Jauch and Martin Beusch (*Martinius*) for their constructive inputs, valuable discussions and support.

Last but not least, my parents, for their precious and unconditional high-speed help from the other side of the planet, whenever needed. Also, my beloved brother and best friend, Ohan, for ceaselessly encouraging me and being ‘there’ all across nine time zones. And, for courageously digging up the ‘red pills’!

Thank you all!

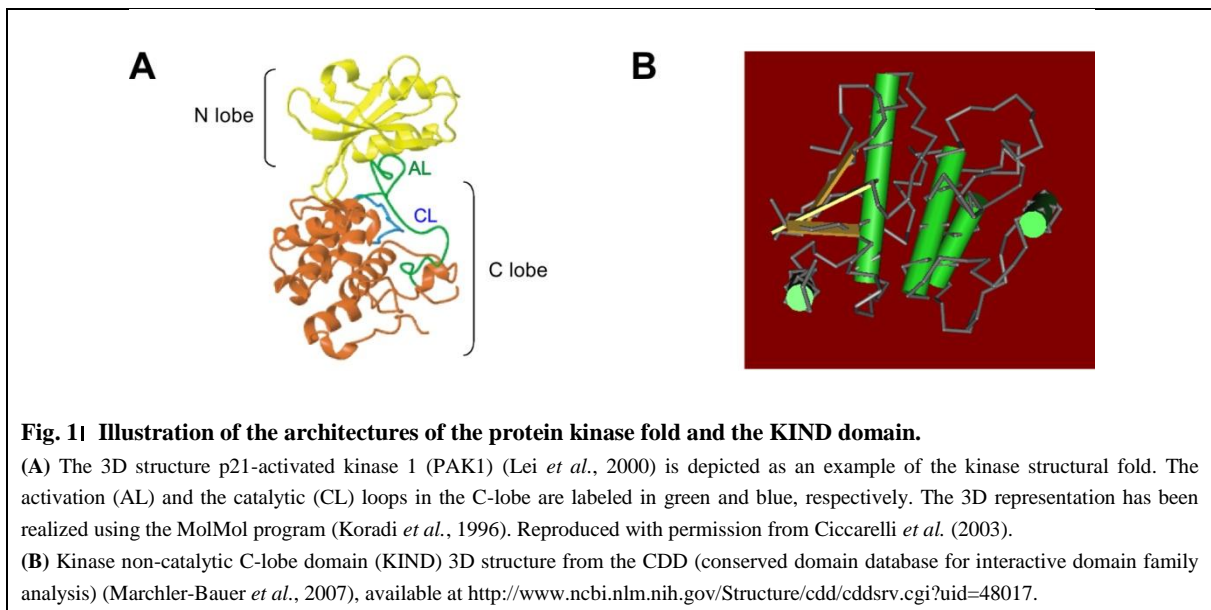
## Chapter I | Introduction

	<b>Page</b>
<b>1.1</b>   The kinase non-catalytic C-lobe domain (KIND)	2
<b>1.2</b>   The guanine nucleotide-binding proteins	6
<b>1.2.1</b>   The Ras superfamily	7
<b>1.2.2</b>   Structure and regulation of Ras GTPases	7
<b>1.2.3</b>   Lipid modification and membrane targeting	8
<b>1.2.4</b>   The RasGEFs' engagement: driving out the nucleotide	8
<b>1.2.5</b>   The GEFs' structural basis for activation skills	10
<b>1.2.6</b>   Rigid regulation of GEFs	10
<b>1.2.7</b>   Ras effectors and signaling cascades	12

## 1.1 | The kinase non-catalytic C-lobe domain (KIND)

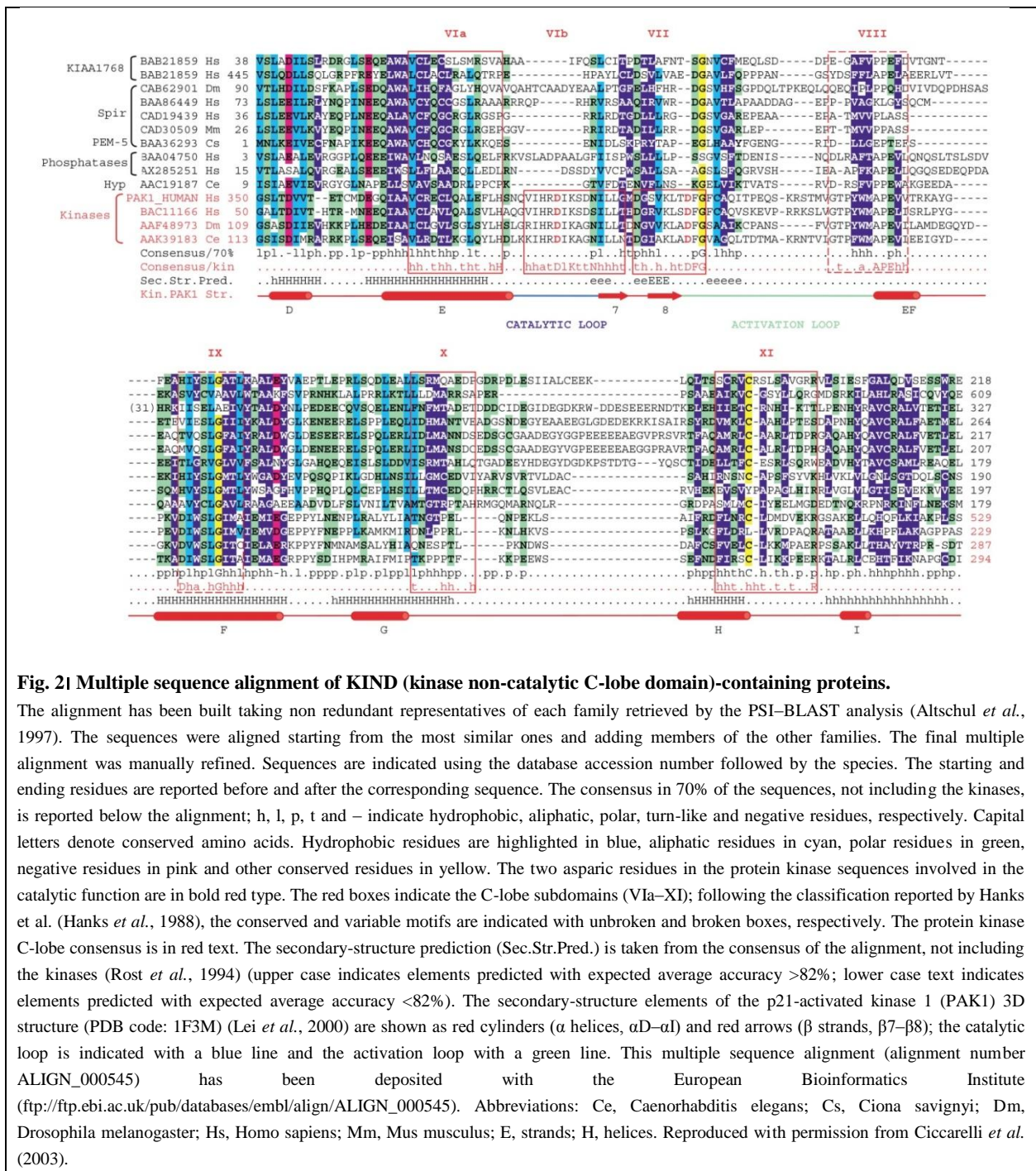
The novel KIND domain was discovered in a sequence analysis of the Spir N-terminal region (Ciccarelli *et al.*, 2003). The *Drosophila melanogaster* p150Spir has been first identified as an important regulator of the actin cytoskeleton, since Spir proteins contain a cluster of four acting binding WH2 (Wiskott-Aldrich homology region 2) domains (Otto *et al.*, 2000; Wellington *et al.*, 1999; Symons *et al.*, 1996). Spir is highly conserved between species and represents a third class of actin nucleation factors along with Arp 2/3 and formin family proteins (Quinlan *et al.*, 2005). Additionally, p150Spir was discovered to be the prime phosphorylation target of the Jun N-terminal kinase (Otto *et al.*, 2000) that is involved in vesicle transport processes (Kerkhoff *et al.*, 2001). In a PSI-BLAST search (Altschul *et al.*, 1997) the first 350 residues of *Dm* p150Spir were found to match ~200 residues of two regions of the to that point still uncharacterized human protein KIAA1768 (BAB21859, presently designated very-KIND, Mees *et al.*, 2005) (Ciccarelli *et al.*, 2003). Residues 30-220 of the very-KIND (VKIND) protein matched consequently various catalytic domains of protein kinases, with best similarities to the p21-activated kinase (PAK, a serine threonine phosphotransferase) (Ciccarelli *et al.*, 2003).

Protein kinases represent one of the most abundant families in genomes of eukaryotes (Hunter, 1987; Rubin *et al.*, 2000). The highly regulated protein kinases act as phosphotransferases on proteins modifying their activity. Comparative analysis of protein kinase sequences defined the boundaries of the eukaryotic protein kinase catalytic domain, 'a kinase fold', which consists of ~250-300 amino acid residues, revealing 12 conserved subdomains without any large amino-acid insertions and harboring characteristic patterns of conserved residues (Hanks *et al.*, 1988; Hanks, 2003). The function of the kinase domains imparting the catalytic activity comprises: 1) binding and orientation of the ATP (or GTP) phosphate donor complexed with divalent cation (typically  $Mg^{2+}$  or  $Mn^{2+}$ ); 2) binding and orientation of the targeted protein substrate; and 3) transmission of the  $\gamma$ -phosphate from ATP (or GTP) to the acceptor hydroxyl residue (Ser, Thr, or Tyr) (Hanks & Hunter, 1995). Twelve kinase domain residues are described as being invariant or nearly invariant throughout the superfamily and play essential roles in the enzyme function (Hanks & Hunter, 1995). Moreover, the patterns of amino acid residues observed within subdomains VIB, VIII and IX were found to be particularly well conserved among the individual members of the distinct protein kinase families (Hanks & Hunter, 1995). The homologous nature of kinase domains triggers a folding into a similar 3-dimensional structure communicating a phosphotransfer according to a similar mechanism (Hanks & Hunter, 1995). The general topology of a protein kinase catalytic core structure was described at first with the solution of the crystal structure of the mouse cAPK catalytic subunit (Knighton *et al.*, 1991a; Knighton *et al.*, 1991b). The kinase domain structure is bilobal with a deep cleft between the structurally independent lobes (Knighton *et al.*, 1991a). The smaller lobe, including the N-terminal subdomains I-IV, is primarily involved with nucleotide binding and orienting (Hanks & Hunter, 1995). This structure has largely beta sheet architecture, which is an unusual nucleotide binding motif (Hanks & Hunter, 1995). The larger lobe, consisting of the C-terminal subdomains VIA-XI, is mainly involved in substrate binding and catalysis (Hanks & Hunter, 1995). Its predominant content is an  $\alpha$ -helical structure with a single beta sheet at the domain interface (Hanks & Hunter, 1995). The joining linker region between the two lobes consists of the subdomain V residues (Hanks & Hunter, 1995). The deep cleft between the N- and C-lobe is recognized as the site initiating the phosphotransfer (Hanks & Hunter, 1995) (Fig. 1A). The majority of the invariant amino acids in the conserved catalytic structure are clustered at the sites of nucleotide binding and catalysis (Knighton *et al.*, 1991a).

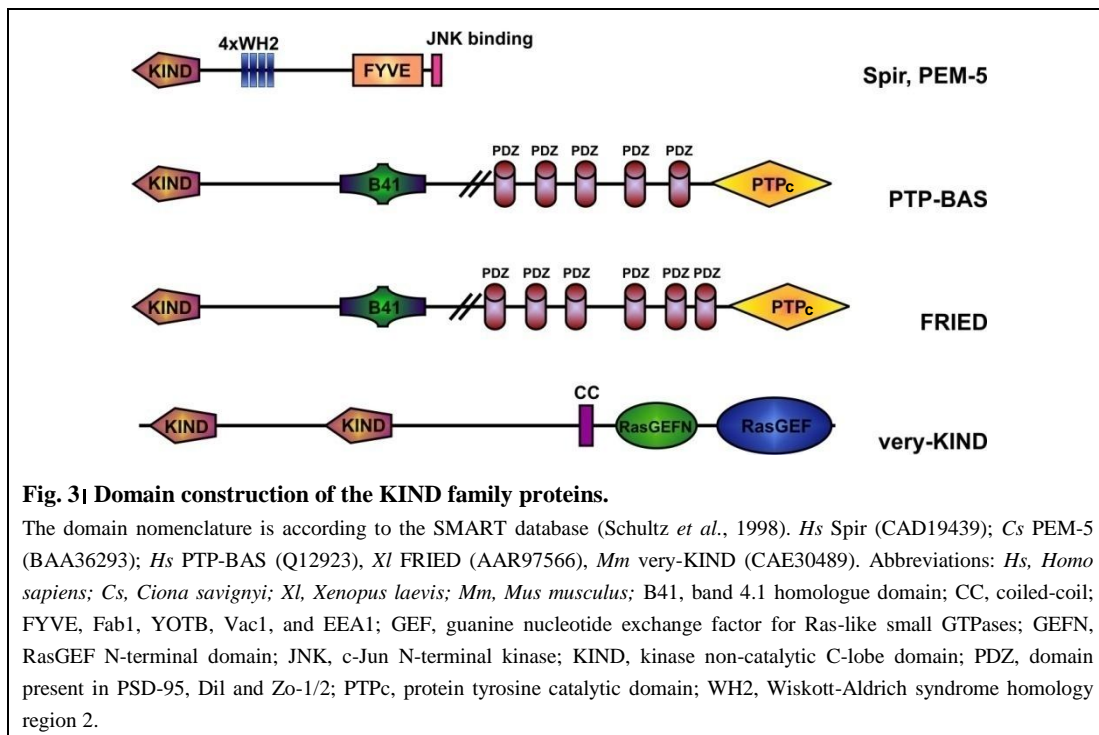


The Spir protein N-terminal sequence matches the entire C-lobe of the protein kinase catalytic core but the N-lobe and the linker region (Ciccarelli *et al.*, 2003) (Fig. 1A). The consensus sequence and the secondary structure prediction are calculated based on the multiple alignment of the shown sequences, excluding the sequence of the protein kinases (Ciccarelli *et al.*, 2003) (Fig. 2). The consensus sequence and the secondary structure prediction line up well to those determined for protein kinases (Ciccarelli *et al.*, 2003) (Fig. 2). Nevertheless, the invariant amino acid residues assigned the catalytic kinase activity in the catalytic loop, Asp<sub>166</sub> and Asn<sub>171</sub> as referenced to cAPK in subdomain VIB, are not found in the N-terminal regions of the aligned proteins (Ciccarelli *et al.*, 2003) (Fig. 2). Moreover, in the activation loop the invariant amino acid Asp<sub>184</sub> (as referenced to cAPK) that is incorporated in the highly conserved DFG triplet in subdomain VII is also missing (Ciccarelli *et al.*, 2003). The significant similarity and the structural context strongly imply that the analyzed regions and the protein kinase C-lobe subunit share a common ancestor. Since structures, however, essential for the enzymatic activity of the protein kinase activity (the N-lobe, along with the deep cleft between the two lobes, and the invariant catalytic residues) are excluded in the analyzed protein regions, the novel domain is supposedly deprived of any catalytic activity (Ciccarelli *et al.*, 2003). Based on the structural resemblance and absence of essential catalytic residues the analyzed new region was named KIND, for kinase non-catalytic C-lobe domain (Ciccarelli *et al.*, 2003) (Fig. 1B and 2).

Additional homologous enzymes and nonenzymes sharing high sequence identity but not sharing any similarity in function have been described (Todd *et al.*, 2002). Functional variations have developed through incremental modifications of the catalytic or substrate binding sites (Todd *et al.*, 2002). It is thought that multifunctional genes subjected to adaptive pressure may undergo gene duplication and divergence to provide for the independent specialization of each function (Todd *et al.*, 2002). Two scenarios for evolution of functional variations are described: the nonenzymes have developed from enzyme precursors, or, conversely, the enzymes originate from noncatalytic ancestors (Todd *et al.*, 2002). The direction of evolution is usually evident from the nature of the superfamily and its members, and by a phylogenetic analysis (Todd *et al.*, 2002). Due to the loss of the N-lobe, linker region and residues that play a functional



catalytic role, the KIND domain appears to be a case of a nonenzyme within a superfamily that otherwise embodies protein kinases. Moreover, the kinase domain is apparently an ancient module, since its ancestor predates the divergence of Bacteria, Archaea and Eukaryotes (Leonard *et al.*, 1998). In contrast, the KIND domain is present only in Metazoa, signifying that it is the ‘odd one out’ in the superfamily. Paired nonenzymes are found to retain a ligand binding capacity though the binding properties of their enzymatic precursors are likely to change (Todd *et al.*, 2002). The PAK1 C-lobe communicates substrate recognition (Knighton *et al.*, 1991a); association of the inhibitory switch (IS) hence blocking the deep cleft with the kinase inhibitor (KI) segment; and rearrangements to the inhibitory conformation of the activation loop, adopting multiple conformations (Lei *et al.*, 2000; Lei *et al.*, 2005). In addition, the same C-lobe surface is an interaction site for the smaller N-lobe and a phosphorylation target (Lei *et al.*, 2000). Conclusively, these data advocate an interaction and/or regulatory potential for the KIND domain.



In fact, recently we reported that the Spir family KIND domain inhibits the actin nucleation by Cappuccino (Capu) family formins (Quinlan *et al.*, 2007) (Fig. 3). The highly conserved eukaryotic formin family is implicated in a wide range of cellular processes, including cytokinesis, cell polarization and embryonic development (Emmons *et al.*, 1995; Zeller *et al.*, 1999). The most highly conserved feature of formins is two contiguous located formin homology domains, FH1 and FH2 (Castrillon & Wasserman, 1994), that are engaged in actin assembly (Evangelista *et al.*, 1997; Pruyne *et al.*, 2002). The *Drosophila* protein Cappuccino is a subclass representative of actin nucleating formins (Higgs, 2005; Quinlan *et al.*, 2007). While competing with actin filaments and microtubules the *Drosophila* and mammalian Spir KIND domain binds the formin homology 2 (FH2) domain of Cappuccino (or its mammalian homologue formin-2) at a ratio of 2:2 (two KIND monomers/one FH2 dimer), displaying an evolutionary conserved interaction (Quinlan *et al.*, 2007). Furthermore, the interaction of the Spir KIND domain with Capu enhances the actin nucleation by Spir. Interestingly, the KIND domains of the protein VKIND (Mees *et al.*, 2005) did not bind the Formin-2 FH2 domain, emphasizing the specificity of the interaction (Quinlan *et al.*, 2007). These data disclose the first interaction and regulatory function properties of the novel KIND domain.

The precise functional role of the KIND domains in the remaining proteins included in the KIND protein family (Fig. 3) is still to be elucidated. Nonetheless, Herrmann *et al.* (2003) reported that a region consisting of the long N-terminal splicing variant of protein tyrosine phosphatase (*Mm* PTP-BL/*Hs* PTP-BAS) harboring the KIND domain associates with the midbody and  $\gamma$ -tubulin at centrosomes during cytokinesis, suggesting a regulatory role (Herrmann *et al.*, 2003). In tightly controlled protein tyrosin phosphatases (*Mm* PTP-BL and *Xl* FRIED, both similar in structure) the KIND module is located at the very N-terminal portion (Herrmann *et al.*, 2003; Itoh *et al.*, 2005) that is in direct vicinity to a FERM (acronym of four point one, Ezrin, Radaxin, and Moesin) domain, by which the phosphatases are directed to the cell cortical area and bind to a number of cell surface receptors as well as the actin cytoskeleton (Chishti *et al.*, 1998; Pearson *et al.*, 2000) (Fig. 3). In addition, FERM binding to 1-phosphatidylinositol-4,5-bisphosphate (PIP<sub>2</sub>) has been described (Hamada *et al.*, 2000). Next to the FERM domain, numerous PDZ domains are positioned (five in *Mm* PTP-BL and six in *Xl* FRIED). PDZ (domain present in PSD-95, Dil and Zo-1/2) domains are able to interact selectively with internal sequences and the C-termini of their target proteins, along with 1-

phosphatidylinositol phosphate (PIP) (Erdmann, 2003). Given the arrangement of the KIND domain in a neighborhood of anchoring and scaffolding domains in the non-receptor subtype protein tyrosine phosphatases, strongly implies its protein-protein interaction potential and can expand the perceptiveness of functional involvement of these PTPs.

An appealing case is the modular structure of the guanidine exchange factor (GEF) VKIND as two homologous KIND domains are arranged in the N-terminal region in a tandem like fashion (Mees *et al.*, 2005). The novel eukaryotic protein bears a name attributed to the dual occurrence of two KIND domains (KIND1 and KIND2) in its structure. Recently, the binding competence of the second KIND domain to the microtubules-associated protein 2 (MAP2) has been shown (Huang *et al.*, 2007). Ortholog genes coding for structural MAP2 are found only in Metazoa and are spliced in several alternative ways (Dehmelt & Halpain, 2005), producing proteins that contain variable number of microtubule-binding repeats near the C-terminus (Lewis *et al.*, 1988; Kalcheva *et al.*, 1995). Each repeat is featuring a conserved KXGS phosphorylation site recognized by the cAMP-dependent protein kinase (PKA) (Ozer & Halpain, 2000) and the microtubule affinity regulating kinase (MARK) (Drewes *et al.*, 1995). MAP2 also interacts directly with F-actin, through an F-actin binding site located inside the domain harboring the microtubule-binding repeats (Roger *et al.*, 2004). Further, each family member has an amino-terminal projection domain of varying size which contains a distinctive PKA regulatory subunit (RII) binding domain (Malmendal *et al.*, 2003) that is anchoring PKA to microtubules (Harada *et al.*, 2002). Mammalian MAP2 is predominantly expressed in neurons (Menezes & Luskin, 1994) and is shown to segregate into nascent dendrites following axonogenesis in developing cortical and hippocampal neuronal cultures (Matus, 1990). Furthermore, MAP2 induces microtubule flexural rigidity (Felgner *et al.*, 1997), microtubule bundles (Lewis *et al.*, 1989; Lewis & Cowan, 1990) and neurites in Neuro-2a neuroblastoma cells; whereas ability of MAP2 to stabilize microtubules is necessary but not sufficient for this effect (Dehmelt *et al.*, 2003). Intriguingly, cytoplasmic JNK phosphorylation of MAP2 in neurons regulates the dendritic complexity and length (Bjorkblom *et al.*, 2005). Linking the neuronally expressed VKIND and MAP2 proteins via the KIND2 interaction domain further elucidates the mechanisms of controlled dendrite outgrowth.

## 1.2 | The guanine nucleotide-binding proteins

The outset of higher organisms required regulation of four essential processes of their origin: cell proliferation, cell differentiation, cell-cell communication and cell movement. The final construction of a spectacular complexity and specificity demands the precise gathering, processing, manipulating and transmission of a staggering amount of information. To ensure information flow specific receptors receive molecular signals and initiate cellular response. The mechanism of long- and short-range signaling involves guanine nucleotide binding proteins (GTP-binding proteins or G proteins) that act as molecular switches. GTP-binding proteins fall into five main superfamilies: 1) heterotrimeric G proteins ( $\alpha$ ,  $\beta$ ,  $\gamma$  subunits) (Marrari *et al.*, 2007); 2) monomeric small 20 to 25-kD Ras-like GTPases (Park & Bi, 2007); 3) translation factors (EF-G, EF-Tu, IF-2, RF-3) (Avarsson, 1995); 4) translocation factors (SRP, SRP-R) (Egea *et al.*, 2005; Bange *et al.*, 2007); and 5) large GTP-binding proteins (Dynamin, GBP, Mx) (Praefcke & McMahon, 2004; Vestal, 2005; Haller *et al.*, 2007).

The Ras superfamily members, Ras GTPases, cycle between an OFF (GDP bound) and an ON (GTP bound) state, as transition into the active state is accelerated by guanine nucleotide exchange factors (GEFs). The VKIND protein studied in the course of this work represents a newly discovered Ras-specific GEF.

### 1.2.1 | The Ras superfamily

In the early 1960s four acute transforming retroviruses were isolated leading by 1983 to the identification of three human transforming genes (H-Ras, K-Ras, N-Ras) (Malumbres & Barbacid, 2003) which in turn became the founding members of the Ras (*Rat sarcoma*) superfamily. In present day over 150 human members build up the Ras superfamily (Ras related) of small guanosine triphosphatases (GTPases), with conserved orthologs present in *Drosophila*, *C. elegans*, *S. cerevisiae*, *S. pombe*, *Dictyostelium* and Plantae (Takai *et al.*, 2001; Colicelli, 2004). This superfamily can be subclassified into five major branches: Ras, Rho, Rab, Ran and Arf on the basis of sequence and functional similarities (monomeric G proteins) (Wennerberg *et al.*, 2005). The Ras family (36 members, e.g. H-Ras, K-Ras, N-Ras, M-Ras, R-Ras, TC21, Rheb, Rad, Gem, Rap1, Rap2, RalA and B) serves as signaling nodes responding to various extracellular stimuli and has critical roles in human oncogenesis (Vojtek & Der, 1998; Repasky *et al.*, 2004; Wennerberg *et al.*, 2005). Nevertheless, several Ras family proteins (Rerg, Noey2 and D-Ras) act rather as tumor suppressors (Colicelli, 2004). Like Ras, the Rho family (*Ras homologues*; 20 members, e.g. RhoA, Rac1, Cdc42, Rnd) regulates signaling networks that mediate actin organization, cell cycle progression and gene expression (Etienne-Manneville & Hall, 2002). Initially described as Rho, Miro proteins appear to form their own subgroup, that instead of modifying the cytoskeleton oversees the integrity of mitochondria (Wennerberg & Der, 2004). The most numerous Rab family (*Ras-like proteins in brain*) of 61 members directs intracellular vesicular transport and protein trafficking along the endocytic and secretory pathways (Zerial & McBride, 2001). The single human Ran protein (*Ras-like nuclear*) defines a distinct subgroup and facilitates directed nucleocytoplasmic transport of RNA as well as proteins (Weis, 2003). Ran GDP/GTP cycling also controls mitotic spindle and nuclear envelope assembly along with DNA replication (Li *et al.*, 2003). The Arf family (*ADP-ribosylation factor*; 27 members, e.g. Arf1-6, Arl1-11, Sar) is involved in regulation of endocytosis, vesicular assembly and transport (Nie *et al.*, 2003; Memon, 2004). Additionally, nine proteins (e.g. SRPRB, RabL2A, RabL3) remain 'unclassified' since neither structural nor functional data relates them to any of the major subfamilies (Wennerberg *et al.*, 2005).

### 1.2.2 | Structure and regulation of Ras GTPases

The groups of Sung-Ho Kim and Fred Wittinghofer provided the first high resolution crystal structures of Ras proteins in the late 1980s (de Vos *et al.*, 1988; Pai *et al.*, 1989) as well as the crystal structure of mutated Ras proteins soon after (Krengel *et al.*, 1990; Tong *et al.*, 1991). A single point mutation causes the functional differences between the normal human H-Ras and its oncogenic allele (Reddy *et al.*, 1982), but almost no structural discrepancies. Transforming alleles encode GTPases with greatly reduced (at least 300-fold) intrinsic enzymatic activity (Gibbs *et al.*, 1984; Trahey & McCormick, 1987). Ras proteins become activated by releasing GDP and binding to GTP which is greatly accelerated by RasGEFs (by several orders of magnitude) (Wolfman & Macara, 1990; Vetter & Wittinghofer, 2001). The intrinsic slow GTPase activity is then highly increased by a GTPases-activating protein (GAP) (Trahey *et al.*, 1988) resulting in hydrolysis of GTP to GDP, inactivation of the Ras protein and signal transduction abolishment. The Ras proteins share a set of conserved GDP/GTP binding motif elements reading: G1, GXXXXGKS/T (phosphate binding site; interacts with the  $\beta$ - and  $\gamma$ -phosphates); G2, T (interacts with a  $Mg^{2+}$  ion); G3, DXXGQ/H/T; G4, T/NKXD (interacts with the nucleotide base); and G5, C/SAK/L/T (Saraste *et al.*, 1990; Bourne *et al.*, 1991). Together these motives assemble an universal 20-kD structural fold for GTP-binding proteins - G domain (Ras residues 5-166) - with a canonical switch mechanism operating the nucleotide binding and hydrolysis (Wittinghofer & Pai, 1991). The G domain architecture is a typical mixed six-stranded  $\beta$  sheet and five  $\alpha$  helices (de Vos *et al.*, 1988). Conformational differences of the two nucleotide-



bound states are usually subtle and correspond primarily to the designated switch I (Ras residues 32-38, L2- $\beta$ 2-region) and switch II (Ras residues 59-67,  $\beta$ 3/ $\alpha$ 2-region) regions (Milburn *et al.*, 1990). In the triphosphate-bound form, two  $\gamma$ -phosphate oxygens interact via hydrogen bonds with the main chain NH groups of the invariant Thr<sub>35</sub> and Gly<sub>60</sub> Ras residues in the switch I and II, respectively (Vetter & Wittinghofer, 2001) (Fig. 4A). The glycine originates from the DXXG motif and the threonine is additionally involved in binding Mg<sup>2+</sup> through its side chain (Vetter & Wittinghofer, 2001) (Fig. 4B). Remarkably, the trigger for the conformational change is presumably universal constituting a loaded spring mechanism which upon  $\gamma$ -phosphate release after GTP hydrolysis relaxes both switch regions into the GDP-specific form (Vetter & Wittinghofer, 2001) (Fig. 4A).

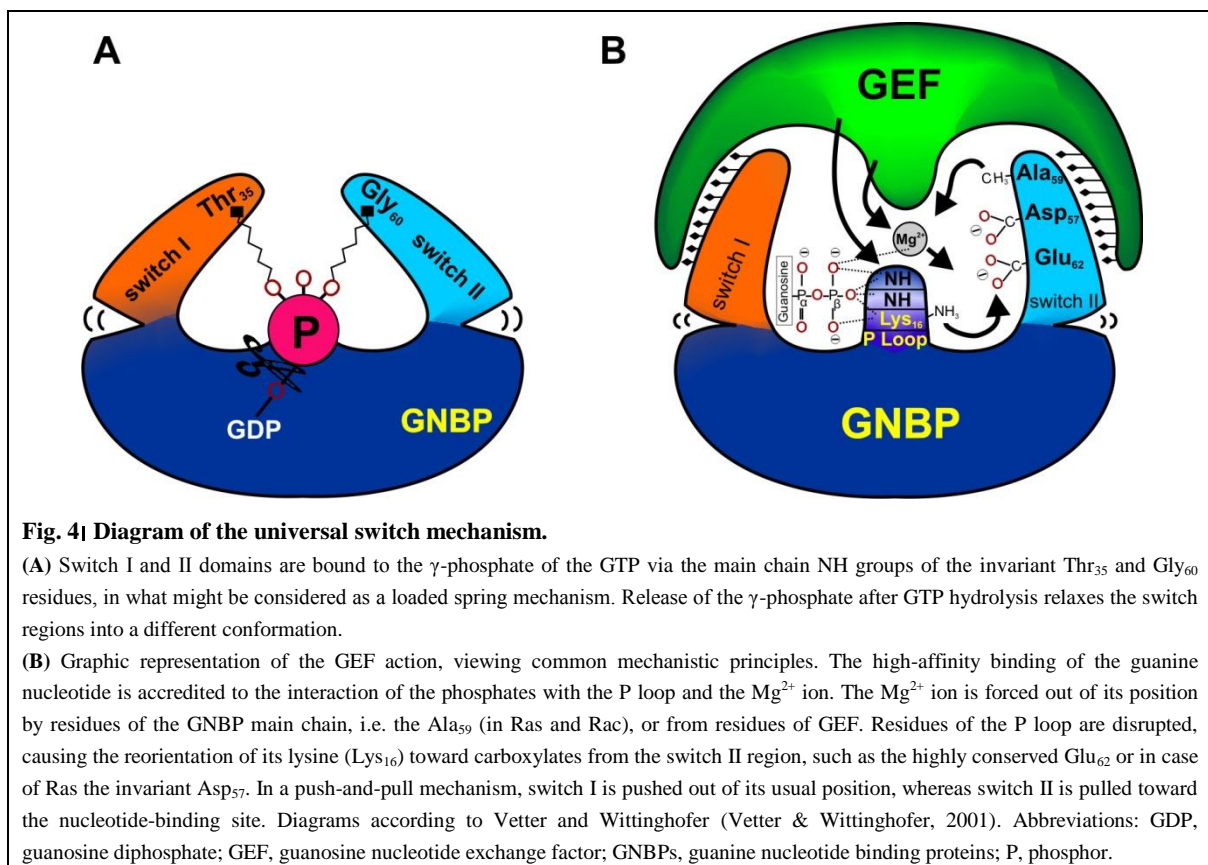
### 1.2.3 | Lipid modification and membrane targeting

In 1980 a key observation revealed the association of retroviral v-Ras proteins with the inner surface of the plasma membrane (Willingham *et al.*, 1980), a crucial biochemical requirement for cellular transformation (Willumsen *et al.*, 1984). The majority of Ras subfamily proteins bear a C-terminal CAAX tetrapeptide (C, cysteine; A, aliphatic; X, any amino acid) sequence (Cox & Der, 2002). The cytoplasmic farnesyltransferase transfers a farnesyl moiety from farnesyl pyrophosphate to the cysteine of all Ras isoforms (Reiss *et al.*, 1990). Subsequently, at the ER the AAX tripeptide is endoproteolytically processed by the endopeptidase Rce1 (Ras and a factor converting enzyme) (Boyartchuk *et al.*, 1997; Kim *et al.*, 1999). The resulting C-terminal isoprenylated cysteine is then methyl esterified (Zhang & Casey, 1996). In addition, for N-Ras a palmitoyl lipid moiety (or two moieties for H-Ras) is attached to cysteines adjacent to the farnesylated cysteine (Lobo *et al.*, 2002; Smotrýs & Linder, 2004). Palmitoylation constitutes a membrane-targeting sequence that dictates the interaction with various membrane compartments and the Ras proteins trafficking to the plasma membrane through the exocytic pathway (Apolloni *et al.*, 2000; Wennerberg *et al.*, 2005). The association of Ras with the plasma membrane has been observed to be stable (Niv *et al.*, 2002). However, the distinct targeting of Ras isoforms to transient cholesterol-dependent assemblies (rafts) laterally segregated on the plasma membrane affects either stimulatory or inhibitory their responsiveness to extracellular signals (Eisenberg & Henis, 2008 and citations therein). ‘Lipid rafts’ are termed to be small cholesterol-enriched assemblies which are complexed with proteins (Hancock, 2006). H-Ras•GDP has higher affinity to rafts, whereas H-Ras•GTP is targeted preferentially to nonrafts (Rotblat *et al.*, 2004). N-Ras•GTP associates with raft-like domains (Roy *et al.*, 2005), while K-Ras interacts mainly with cholesterol-insensitive clusters or microdomains, due to the absence of palmitoyl residues (Prior *et al.*, 2003).

### 1.2.4 | The RasGEFs’ engagement: driving out the nucleotide

The connection between mitogens and Ras was first reported by Kamata and Feramisco as they traced the epidermal growth factor (EGF) to stimulate GTP binding activity of Ras proteins (Kamata & Feramisco, 1984). The signaling pathways started clarifying as growth-factor receptors with tyrosine kinase activity (RTK) essential for transformation were found (Smith *et al.*, 1986). Furthermore, the mammalian adaptor protein, GRB2, was proved to connect activated phosphorylated tyrosine protein kinase receptors through its single SH2 domain to the RasGEF SOS (son of sevenless) through its two SH3 domains (McCormick, 1993) unveiling the mechanism by which external molecules signal through the plasma membrane. SOS on its part facilitates the conversion of Ras•GDP to Ras•GTP enabling Ras•GTP to bind to effector proteins and launch signaling events through them (Milburn *et al.*, 1990). Human SOS1, a large multidomain protein of 1333 residues, contains a central catalytic module (SOS<sup>cat</sup>, residues 550 to 1050), that is sufficient for the

nucleotide exchange activity (Chardin *et al.*, 1993). The SOS<sup>cat</sup> segment includes a core region of significant sequence similarity to CDC25, a Ras-specific GEF from *S. cerevisiae*, named CDC25 domain (residues 750 to 1050) (Broek *et al.*, 1987; Boguski & McCormick, 1993). The canonical recognition sites for SH3 domains (PXXP; P, proline; X, any amino acid) are located in the C-terminal region, whereas the REM (Ras exchanger motif) is upstream of the CDC25 domain, which is responsible for allosterical stabilization of SOS by Ras·GTP (Margarit *et al.*, 2003). Upon binding to RAS·GDP, SOS displaces the switch I and opens the nucleotide binding site by the insertion of a helical hairpin ( $\alpha$ H and  $\alpha$ I) into the Ras active site (Boriack-Sjodin *et al.*, 1998). The  $\alpha$ H helix introduces a hydrophobic side chain (Leu<sub>938</sub>), which blocks Mg<sup>2+</sup> binding, as well as an acidic side chain (Glu<sub>942</sub>), which disturbs the nucleotide  $\alpha$ -phosphate binding site (Boriack-Sjodin *et al.*, 1998). Furthermore, the switch II conformation is distorted by Ala<sub>59</sub>, Gly<sub>60</sub> and Gln<sub>61</sub> of Ras turned inwards the P loop (phosphate binding site), preventing the coordination of magnesium and phosphate (Boriack-Sjodin *et al.*, 1998). Thus the Ras-GEF interaction does not impede the binding sites for the base and ribose of GTP or GDP, allowing nucleotide release and reloading (Boriack-Sjodin *et al.*, 1998).



In general, the common mechanistic principles of a GEF action on the GNBPs (guanine nucleotide binding proteins) is a postulated sequence of fast reversible reaction steps, that lead a binary protein-nucleotide complex through a trimeric GNBPs-nucleotide-GEF complex to a binary stable protein nucleotide free complex (Vetter & Wittinghofer, 2001). In the process the magnesium ion is dislodged; switch I is pushed out of its normal position, while switch II is pulled toward the nucleotide binding site (the so called push-and-pull mechanism); whereas structural disturbance of the P loop is imperative, resulting in a weak affinity of the GNBPs for the nucleotide (Vetter & Wittinghofer, 2001) (Fig. 4B). This series of reactions is reversed when a nucleotide is rebound, predominantly GTP, since its intracellular concentration is 10 times higher than GDP, lowering the affinity of the GNBPs for the GEF (Vetter & Wittinghofer, 2001). As catalysts, GEFs accelerate the formation of the equilibrium between GDP- and GTP-bound forms of the GNBPs

(Lenzen *et al.*, 1998; Klebe *et al.*, 1995). Moreover, the position of the equilibrium is defined by the relative affinities of GDP and GTP to the GNBPs; the cytosolic nucleotide concentration; and the concentration of additional components, such as effectors, which incline the equilibrium toward the GTP-bound form (Vetter & Wittinghofer, 2001).

### 1.2.5 | The GEFs' structural basis for activation skills

Classification of GEFs into families is based on both sequence similarity and cognate small GTP-binding proteins (Cherfils & Chardin, 1999). The majority of GEFs are multidomain proteins comprising catalytic domains of 200-300 residues with one or several contiguous domains, involved in protein-protein or membrane interactions, promoting oligomerization, along with regions with yet unknown function (Cherfils & Chardin, 1999). Within a given subfamily, GEFs are conserved, as RasGEFs (GEFs for Ras proteins) contain a CDC25, Rho-GEFs a DH (dibble-homology), and Arf-GEFs a Sec7 domain, respectively (Vetter & Wittinghofer, 2001). However, in contrast to GNBPs themselves, the catalytic domains of distinct GEF classes are structurally unrelated, as determined by the crystal or NMR structures of representative GEFs of Ran (RCC1), Ras (SOS), various Arf- and Rho-GTPases, as well as of EF-Tu (EF-Ts) (Vetter & Wittinghofer, 2001). Consequently, in spite of GEFs sharing very similar substrates (small GTP-binding proteins), their active sites display a divergence of both shape and sequence, thus a poor evidence of convergent evolution (Cherfils & Chardin, 1999). Unrelated guanine exchange factors, therefore, might have been acquired by diverging GTP-binding proteins, achieving responsiveness to novel types of signals (Cherfils & Chardin, 1999).

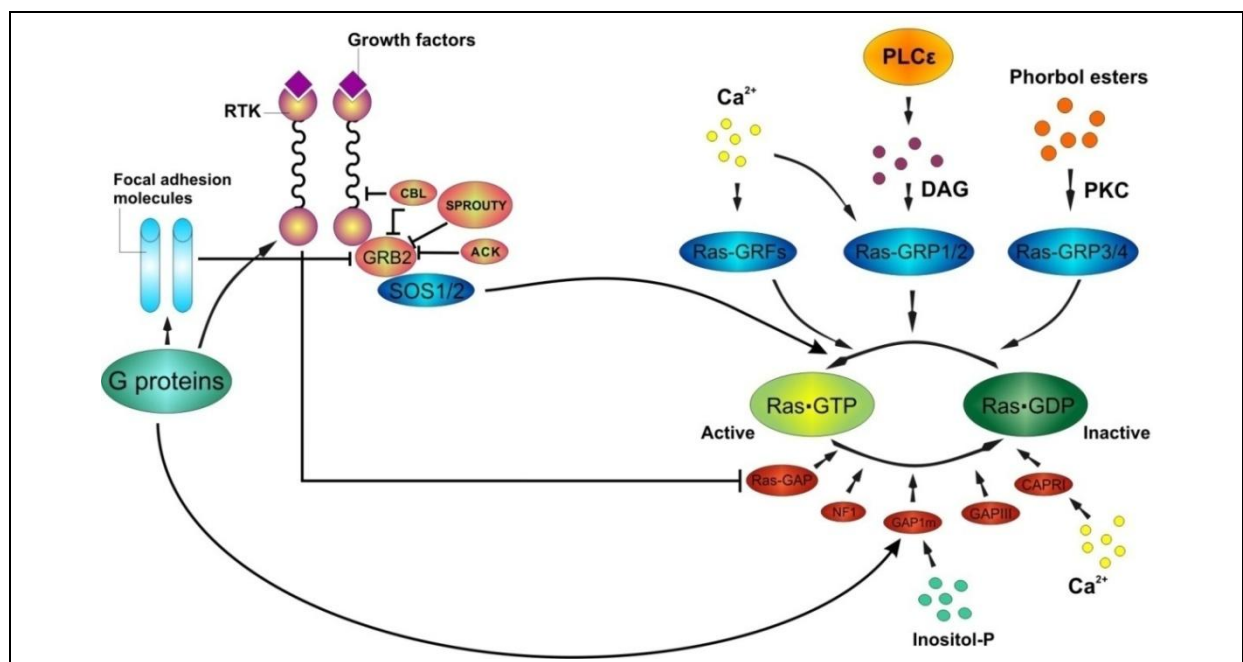
Nevertheless, GEFs usually approach from different angles (Bos *et al.*, 2007). They form extraordinarily large interfaces during complexation with the G proteins, recognizing most notably the switch II regions and in consequence executing an analogous solution to nucleotide expulsion and rebinding (Cherfils & Chardin, 1999) (Fig4B). Intriguingly, exclusive to plants RopGEFs that do not exhibit any homology to animal RhoGEFs, also show common action in perturbing the interaction surface in the P loop and magnesium-binding site (Thomas *et al.*, 2007). Rop (*Rho of plants*) proteins belong to the superfamily of small G proteins (Rho family of Ras-related) and are vital regulators of growth, development and plant responses to various environmental stimuli (Berken *et al.*, 2005).

### 1.2.6 | Rigid regulation of GEFs

In some GEF proteins two different GEFs domains are combined or even GAP domains are introduced (Bos *et al.*, 2007). For example, SOS1 and SOS2 join the DH-PH (dibble homology-pleckstrin homology) domain specific for Rac with the REM and CDC25 domains specific for Ras (Bos *et al.*, 2007). Moreover, GEFs commonly outnumber the G proteins (Garcia-Mata & Burrige, 2007), raising the urge for tight activity regulation. Almost all GEFs are multidomain proteins, harboring lipid or protein interaction domains, allowing controlled localization signaling and scaffolding of protein complexes (Bos *et al.*, 2007). Again, SOS is recruited to the plasma membrane by the GRB2 adaptor protein in a SH2-SH3-domain mediated manner (Aronheim *et al.*, 1994), while the extracellular signal-regulated kinase (ERK) regulates this translocation to a specific cell compartment, since SOS phosphorylation results in its dissociation from GRB2 (negative feedback) (Waters *et al.*, 1995). Scaffolding SOS with GRB2 ensures action on Ras, whereas action on Rac requires the binding of SOS to a complex of Abi1/E3B1, Eps8, and PI3K (Innocenti *et al.*, 2003). However, the same region of SOS mediates the interactions with GRB2 and Abi1/E3B1, which are consequently mutually exclusive (Innocenti *et al.*, 2002). Additional modifications of SOS activity are implemented by allosterical regulation by Ras·GTP, which binds to parts of REM (also named RasGEFN)

and CDC25 and induces a 10-fold increase in the catalytic activity (Margarit *et al.*, 2003). Conversely, this allosteric site is blocked by the DH (RhoGEF) domain, allowing no stimulation of RasGEF activity by Ras•GTP (Sondermann *et al.*, 2004). Further autoinhibition of SOS is displayed by the N-terminal PH domain which is blocking the Rac binding site of the DH domain (Sondermann *et al.*, 2004). In addition, the C-terminal proline-rich region of SOS is playing an inhibitory role decreasing the RasGEF activity (Aronheim *et al.*, 1994).

Besides directed translocation, autoinhibition by flanking N- and C-terminal domains and allosteric feedback modifications, a number of GEFs are regulated by direct binding of second messengers (e.g. cAMP, Ca<sup>2+</sup>, diacylglycerol) and posttranslational modification (Bos *et al.*, 2007). The RapGEFs Epac1 and Epac2 contain cyclic nucleotide-binding (CNB) domains (Bos, 2006) which cover the binding site for Rap (Rehmann *et al.*, 2006). Members of the RasGRP (guanyl nucleotide-releasing protein) family are build up by an N-terminal REM and CDC25 domains adjacent to C-terminal C1 domain as well as a pair of EF-hands (Ebinu *et al.*, 1998). RasGRPs activate Ras and/or Rap *in vivo* in response to increased Ca<sup>2+</sup> and DAG (diacylglycerol) concentrations (Ebinu *et al.*, 1998) (Fig. 5). The conformation of the autoinhibitory region adjacent to the DH domain of the RhoGEF Vav1, with a calponin homology (CH) domain and an acidic (Ac) region presenting conserved tyrosines (Turner & Billadeau, 2002), is altered by a phosphorylation of the Tyr<sub>174</sub> which results in the liberation of the catalytic site (Aghazadeh *et al.*, 2000; Llorca *et al.*, 2005).



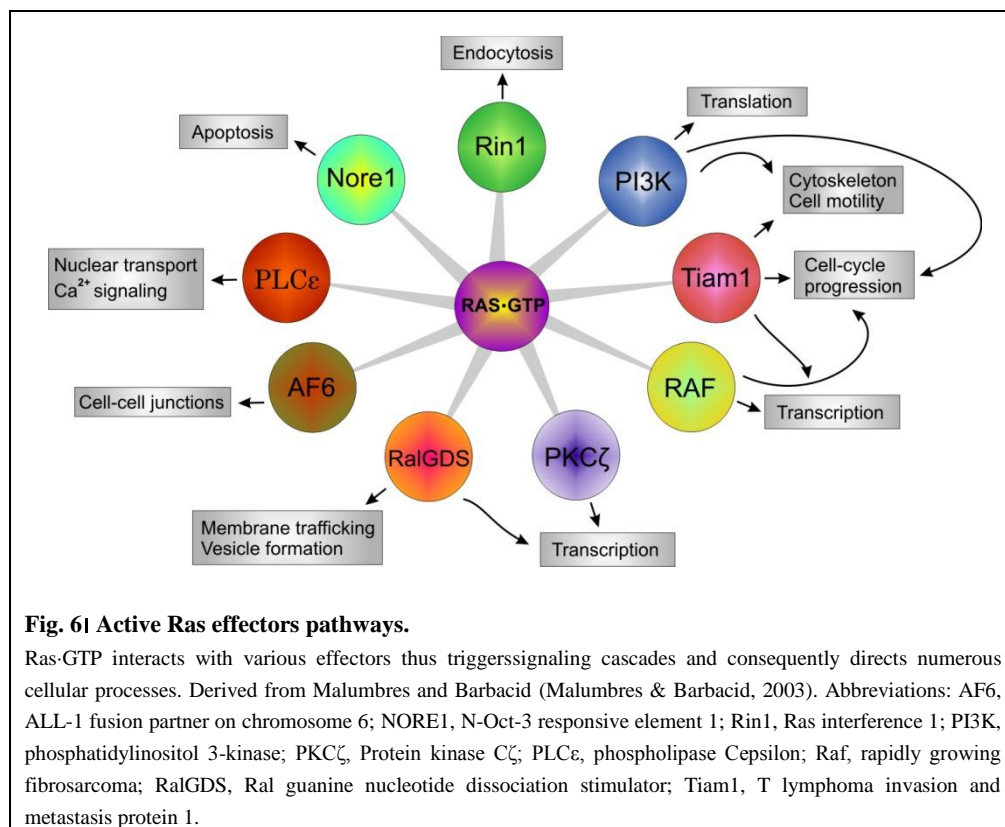
**Fig. 5| Schematic view of the RasGEF/Ras regulation.**

Extracellular signals, mediated by receptor tyrosine kinases (RTKs), adhesion molecules and second messengers stimulate RasGEFs (blue ovals) that activate Ras (green ovals). The SPROUTY and ACK protein families bind to GRB2 and impede the activation of SOS. CBL proteins also act as ubiquitin ligases for RTKs which results in an inactive CRB2. Numerous GAPs (brown ovals) downregulate Ras by catalyzing the GTP hydrolysis. Diagram according to Malumbres and Barbacid (Malumbres & Barbacid, 2003). Abbreviations: ACK, acetate kinase; CBL, Casitas B-lineage lymphoma; DAG, diacylglycerol; GAP, GTPase activating protein; GRB2, growth factor receptor-bound protein 2; Inositol-P, inositol monophosphate; NF1, neurofibromin; PLC $\epsilon$ , phospholipase Cepsilon; PKC, protein kinase C; RasGRP, guanyl nucleotide-releasing protein; Ras, rat sarcoma; SOS, Son of sevenless.

### 1.2.7 | Ras effectors and signaling cascades

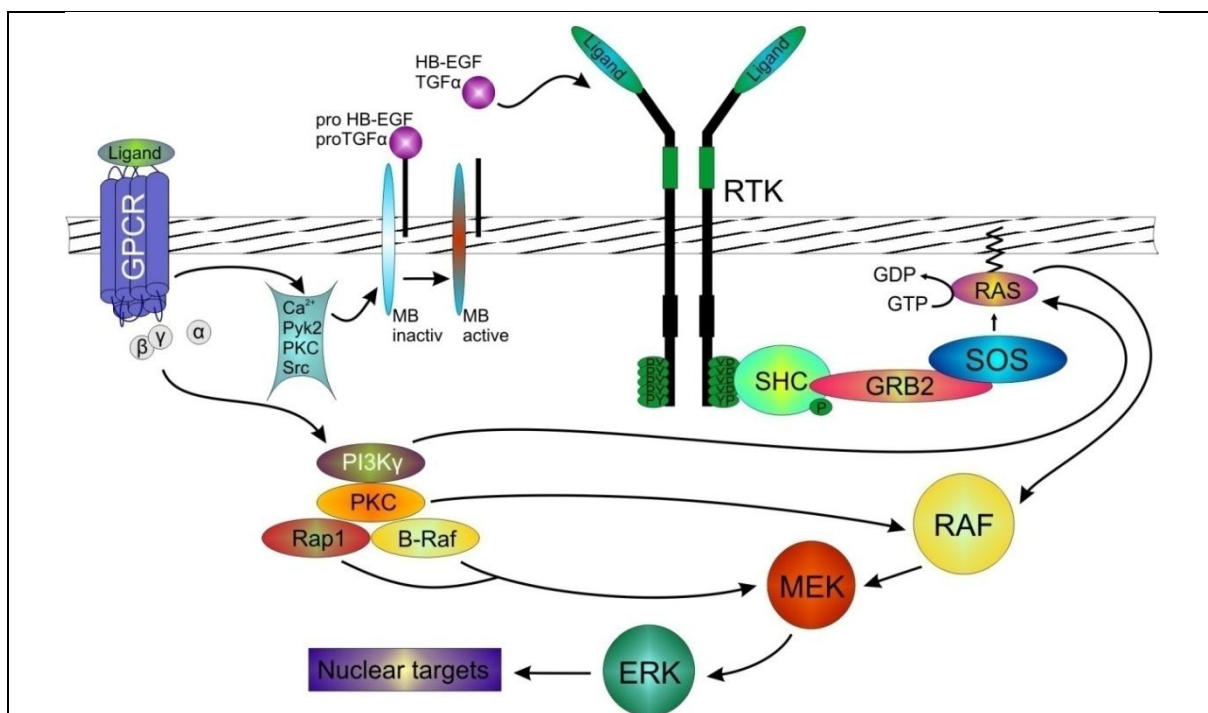
Small G-proteins bind to their downstream effectors and induce conformational changes in functional domains, acting as timed biological molecular switches (biotimers) which determine functioning periods of activation (or inactivation) (Takai *et al.*, 2001) and therefore the signal transduction intervals. Proteins with high affinity to GTP-bound form of GTPases are termed effectors. The Raf kinase (*rapidly growing fibrosarcoma*) (Rapp *et al.*, 1983) was the first discovered mammalian protein with a strong affinity to activated Ras (Ras•GTP) (Moodie *et al.*, 1993).

The growing family of Ras effectors congregates meanwhile more than 10 members (e.g. AF6, Nore1, PI3K, PKC $\zeta$ , PLC $\epsilon$ , RalGDS, Raf, Rin1, Tiam1) (Repasky *et al.*, 2004) (Fig. 6). These are characterized by a common subdomain in their otherwise unrelated protein body, a putative Ras binding domain (RBD) with an uniform ubiquitin fold ( $\beta\beta\alpha\beta\beta\alpha\beta$ ) (Herrmann, 2003). Ras•GTP directly binds to Raf and triggers activation leading to conformational changes, phosphorylation (by the members of the Src kinase family) and hetero-oligomerization (Van Aelst *et al.*, 1993; Marais *et al.*, 1995; Park *et al.*, 1996; Garnett *et al.*, 2005) (Fig. 7). In consequence Raf is localized to the cytoplasmic surface of the plasma membrane (Leevers *et al.*, 1994). In addition, Prohibitin and 14-3-3 proteins complex with Raf and in turn regulate Ras ability of Raf activation (Kyriakis, 2007). A further signal modulating factor, a kinase suppressor of Ras (KSR) has been identified to function downstream of Ras, which upon Ras activation translocates to the plasma membrane, binds to Raf and blocks Ras signaling as well as MEK (mitogen and extracellular regulated kinase) and MAPK (mitogen-activated protein kinase) activation (Therrien *et al.*, 1995; Therrien *et al.*, 1996). Activated mammalian Raf proteins (c-Raf-1, A-Raf, B-Raf) subsequently phosphorylate and activate the soluble MEK (MAP kinase kinase 1 and 2) at the plasma membrane (Dent *et al.*, 1992; Kyriakis *et al.*, 1992) which then phosphorylates and activates the cytosolic MAP kinase (ERK, extracellular signal-regulated kinase) (Crews *et al.*, 1992; Matsuda *et al.*, 1992). As a result the active MAP kinases translocate to the nucleus and induce gene expression (Katz *et al.*, 2007) (Fig. 7).



Ras isoform-specific cellular responses are attributed to distinct post-translational lipid modifications of the isoforms which are set within their divergent C-termini (Rocks *et al.*, 2006). These membrane-anchors ultimately enforce localization to diverse subcellular compartments (Silvius, 2002; Hancock, 2003) as a base for distinctive local Ras signal transmissions that propagate characteristic local cellular responses (Mor & Philips, 2006).

Notably, further spatial separation of protein kinases and phosphatases creates cellular gradients of phosphorylated (active) forms of MEK and ERK, with high-level concentrations in the periplasmic site near the phosphorylation location and low-level ones at a distance from the membrane (Kholodenko, 2003). Several mechanisms, such as endocytosis of phosphorylated MEK, cytoplasmic streaming, recruitment to scaffolds and molecular motors are involved in the transmission of phosphorylation signals further into the cell (Kranenburg *et al.*, 1999; Agutter *et al.*, 1995; Garrington & Johnson, 1999; Verhey & Rapoport, 2001).



**Fig. 71 Diagram of the Ras signaling cascade upon activation of RTKs and G- protein coupled receptors.**

The recruitment of the guanine exchange factor SOS into a close proximity to the membrane anchored Ras triggers the ERK cascade which induces gene expression. Activated GPCRs stimulate ERK cascades either via transactivation of the RTKs that involves distinct cell type dependent mediators (i.e. calcium, Pyk2 and PKC and Src-family kinases), or by parallel pathways engaging PI3K $\gamma$ , PKC, Rap1 and B-Raf. Representation according to Kholodenko (Kholodenko, 2003) as well as Wetzker and Bohmer (Wetzker & Bohmer, 2003). The membrane plane is indicated. Abbreviations: ERK, extracellular signal-regulated kinase; GPCR, G-protein-coupled receptor; GRB2, growth factor receptor-bound protein 2; HB-EGF, heparin-binding EGF; MEK, mitogen and extracellular regulated kinase; MP, metalloproteinase; PKC, protein kinase C; PI3K $\gamma$ , phosphatidylinositol 3-kinase  $\gamma$ ; Pyk2, proline-rich tyrosine kinase 2; Ras, rat sarcoma; Raf, rapidly growing fibrosarcoma; Rap, Ras-related protein; RTK, receptor tyrosine kinase; SHC, Src homologous and collagen-like; SOS, Son of sevenless; TGF $\alpha$ , transforming growth factor- $\alpha$ .

Further major noncanonical Ras effector targets among the Ras signaling pathways are the phosphatidylinositol 3-kinase (PI3K) as well as Ral and Rac guanine nucleotide exchange factors (Ral-GDS and Tiam1) (Rodriguez-Viciano *et al.*, 1994; Feig *et al.*, 1996; Lambert *et al.*, 2002). When active PI3K generates the second messenger PIP<sub>3</sub> (phosphatidylinositol-3,4,5-triphosphate), which recruits PDK1 (phosphatidylinositol-dependent kinase 1) and AKT (also PKB, protein kinase B) to the plasma membrane (Cully *et al.*, 2006). AKT is being activated by PDK1 phosphorylation and is suggested a crucial role in modulating cell death and proliferation (Cully *et al.*, 2006). RalGEFs play a fundamental role in human cell transformation, tumor cell growth and cell survival (Chien & White, 2003; Rangarajan *et al.*, 2004) since

Ralsignaling is found to regulate endo- and exocytosis, actin cytoskeletal organization, cell migration as well as gene expression (Feinstein, 2005). The stimulated Tiam1 (T lymphoma invasion and metastasis protein 1) RacGEF activity in the Ras-Rac cross talk is implicated in Ras-induced skin tumorigenesis (Malliri *et al.*, 2002).

A next family of Ras effectors is represented by the RASSF (Ras association domain family) proteins that function as human tumor suppressors (Tommasi *et al.*, 2002). The Rab5-GEF, Rin1 (Ras interaction/interference), facilitates Ras-regulated endocytosis (Tall *et al.*, 2001). Activation of PLC $\epsilon$  (phospholipase Cepsilon) by PDGF is mediated by Ras, has demonstrated a crucial role of PLC $\epsilon$  in carcinomas progression (Bai *et al.*, 2004). Moreover, AF6 (Afadin) and PKC $\zeta$  (protein kinase C $\zeta$ ) are implied in a variety of cellular processes, such as cell adhesion and transcription, respectively (Toker, 1998; Zhang *et al.*, 2005).

While a large number of Ras effectors performs a plethora of tasks in response to extracellular cell stimuli, some of the divergent signaling pathways conduct significant cross talk, which conclusively converges at a certain level and confers a specific phenotype (Rajalingam *et al.*, 2007). The growth factor signal transduction by Ras alone can dispose most if not all of the different phenotypes in the recipient cell (Rajalingam *et al.*, 2007). Thereby, oncogenic Ras is able to transform cells both *in vitro* and *in vivo* (Barbacid, 1987) and by overstimulation of several pathways contributes to neoplastic processes (Bar-Sagi & Hall, 2000; Downward, 2003).

## Chapter II | Materials

	<b>Page</b>
<b>2.1   Chemicals</b>	16
<b>2.2   Enzymes</b>	18
<b>2.3   Antibodies</b>	18
<b>2.3.1   Primary antibodies</b>	18
<b>2.3.2   Secondary antibodies</b>	18
<b>2.4   Oligodeoxynucleotides</b>	18
<b>2.5   Plasmids</b>	19
<b>2.6   Organisms and eukaryotic cell lines</b>	19
<b>2.6.1   Bacterial strains</b>	19
<b>2.6.2   Eukaryotic cell lines</b>	19
<b>2.6.3   Mice</b>	19
<b>2.7   Analytical kits</b>	20
<b>2.8   Standards</b>	20
<b>2.9   Equipment</b>	20



## 2.1 | Chemicals

Materials	Supplier, Ordering #
( $\alpha$ - <sup>32</sup> P)dCTP (6000 Ci/mmol)	Amersham, Chalfont St. Giles (UK)
2-Propanol	Merck, Darmstadt
DABCO (1,4-Diazabicyclo (2,2,2) Octane)	Sigma, Munich, D27802
3 MM-Paper	Schleicher & Schuell, Dassel
3AT:3Amino1,2,4-triazol	Sigma, Munich
6-well-plate	Greiner, 657 160
Acetic acid	AppliChem, Darmstadt
Acetone	Merck, Darmstadt
Acrylamide/Bisacrylamide 19:1 and 37.5:1	Bio-Rad, Munich, 1610120 and 1610125
Adenine	Sigma, Munich, A9126
Agar select	Sigma, Munich, A5054
Agarose Ultra pure	Life Technology, Belgium, 15510-027
Ammonium acetate	Merck, Darmstadt
Ammonium persulfate	Sigma, Munich, A3678
Ampicillin Sodium crystalline	Sigma, Munich, A9518
AraC/HCL	Sigma, Munich, C6645
ATP	Sigma, Munich
Bacto Tryptone	Life Technology, Belgium
Bacto-Agar	Difco Laboratories, Detroit (USA)
Bacto-Peptone	Difco Laboratories, Detroit (USA)
Bandage	Drugstore, Würzburg
Basal Medium Eagle (BME)	Sigma, Munich, B 1522
Benzamidin	Sigma, Munich
Boric acid	Sigma, Munich, B0252
Bottle Top Filter 0,22 $\mu$ m	Nalge Nunc International, Wiesbaden
Bovine Serum Albumin (BSA)	Sigma, Munich, A 9418
Bromphenol Blue	Sigma, Munich
BSA powder	Sigma, Munich, A4503
Calcium chloride	Sigma, Munich
Cell culture dishes	Sarstedt, Nümbrecht-Rommelsdorf
Cell culture flasks	Sarstedt, Nümbrecht-Rommelsdorf
Chloramphenicol	Sigma, Munich, C0378
Chloroform	Merck, Darmstadt
Coomassie Blue G	Sigma, Munich
Cytosine $\beta$ -D-arabinofuranoside hydrochloride (AraC)	Sigma, Munich, C6645
D(+)-Glucose Monohydrate	Merck, Darmstadt

Diethylpyrocarbonate (DEPC)	Sigma, Munich, D5758
Dimethylformamide (DMF)	Sigma, Munich
Dimethylsulfoxide (DMSO)	Sigma, Munich, D2650
Dithiothreitol (DTT)	Sigma, Munich
DNA labeling kit	Roche, Penzberg
dNTPs	peQLab, Erlangen
Dried milk powder	Nestlé
Dulbecco's Modified Eagle Medium (DMEM)	Life Technology, Belgium, 31330-038
Duralon-UV-Membranes	Stratagene, 420114
ECL-hyperfilm	Amersham, Chalfont St. Giles (UK)
EDTA	Sigma, Munich, E5134
Eppendorf combitips	Eppendorf, Hamburg
Eppendorf tubes	Eppendorf, Hamburg
Ethanol, abs.	AppliChem, Darmstadt
Ethidium bromide	Life Technology, Belgium
Fetal calf serum (FCS)	PAN Systems, Nürnberg
Formaldehyde	Sigma, Munich, F1635
Gentamycin sulfate	Sigma, Munich, G 1264
Glutathione Sepharose® 4B	Amersham, Chalfont St. Giles (UK), 17075601
Glycerol	Sigma, Munich
Glycine	Merck, Darmstadt
Greiner tubes	Greiner, Frickenhausen
HEPES	Sigma, Munich
Hoechst Stain Solution	Sigma, H 6024
Hydrochloric acid	Merck, Darmstadt
Hyperfilm™ MP	Amersham, Chalfont St. Giles (UK), RPN3103K
Imidazole	Sigma, Munich, I 0125
Immersion oil	Leica, 11513859
IPTG	Sigma, Munich, I6758
IPTG	Sigma, Munich
Kanamycin	Sigma, Munich, K1377
LB Broth Base	Sigma, Munich, L3022
L-glutamine	Sigma, Munich, G1251
Lipofectamine™	Invitrogen, Karlsruhe, 18324012
Lithium acetate	Sigma, Munich
Magnesium acetate	Sigma, Munich
Magnesium chloride	Merck, Munich, M2670
Magnesium sulfate	Sigma, Munich
Methanol	Rühl AG
MOPS acid	Sigma, Munich, M3183

Moviol 4-88	Calbiochem-Novabiochem, 475904
NAP-10 columns	Amersham, Chalfont St. Giles (UK), 17085401
Oregon Green -conjugated Phalloidin	Molecular Probes, O-7466
Parafilm® M	Brand GmbH, Wertheim
PBS Dulbecco's (10x)	Molecular Probes, 14200083
PBS Dulbecco's (1x)	Molecular Probes, 14190169
PCR-Tubes 0,2ml	Eppendorf, 0030 124.332
PCR-Tubes 0,5ml	Eppendorf, 0030 124.502
Pepstatin	Sigma, Munich
peqGOLD RNAPure™	peQLab, Erlangen
Phenol Red	Sigma, P 5530
Phenol:Chloroform: Iso-amylalkohol	AppliChem, Darmstadt
Phenylalanine	Sigma, Munich
Pipes	Sigma, Munich, P6757
PMSF	Sigma, Munich
Poly Screen PVDF transfer membrane	NEN™ Life Science Products, Cologne
Poly-L-Lysine	Sigma, Munich, P 2636
Ponceau S	Sigma, Munich
Potassium acetate	Merck, Darmstadt
Potassium chloride	Sigma, Munich, P4504
Potassium hydrogen phosphate	Merck, Darmstadt
Potassium hydroxide	Merck, Darmstadt
Protein G-Agarose	Boehringer, 1 243 233
Protran Nitrocellulose transfer membrane	Schleicher & Schell, Dassel
QuickHyb	Stratagene, 201220
Random Prime L. Kit	Roche, 1004760
Rhodamine-conjugated Phalloidin	Molecular Probes, R-415
Salmon sperm DNA	Stratagene, 201190
SDS ultra pure	Sigma, Munich, L4390
Sodium acetate	Sigma, Munich
Sodium chloride	Sigma, Munich, S3014
Sodium dehydrogenate phosphate	Merck, Darmstadt
Sodium fluoride	Sigma, Munich
Sodium hydrogen carbonate	Sigma, Munich
Sodium hydroxide	Sigma, Munich
Sodium pyrophosphate	Sigma, Munich
Sterile filter Millex-GS	Millipore, Schwalbach
TEMED	Sigma, Munich, T9281

Tris Base	Sigma, Munich, T1503
Triton X-100	Sigma, Munich
Trizole	Life Technology, Belgium
Trypsin	Sigma, Munich, T 9935
Trypsin Inhibitor	Sigma, Munich, T6522
Trypsin-EDTA	Life Technology, Belgium
Tween 20	Sigma, Munich, P1379
Tyrosine	Sigma, Munich
Uracil	Sigma, Munich
Urea	Molecular Probes, 15505027
Water	Sigma, W 3500
Whatman round filter	Whatman, Maidstone (USA)
Xylencyanole blue	Sigma, Munich
Yeast extract	Life Technology, Belgium
β-Mercaptoethanol	Sigma, Munich

## 2.2 | Enzymes

Enzyme	Supplier, Ordering #
Calf Intestinal Phosphatase (CIP)	NEB, M0290 S
DNase	Sigma, D 5025
Endonucleases	NEB and MBI-Fermentas
Klenow Fragment	Roche, 1008404
Pfu DNA-Polymerase	Promega, M 774B
Pfx DNA-Polymerase	Invitrogen, 12344-024
RNase A	Roche, 109169
T4 DNA ligase	NEB, M0202
Taq DNA-Polymerase	peQLab, 01-1030

## 2.3 | Antibodies

### 2.3.1 | Primary antibodies

Antibody / Antigen	Species	Dilution for stain	Dilution for WB	Supplier, Ordering #
Anti-GST / anti-GST	goat monoclonal	—	1:10000	Amersham, 27-4577-01
Anti-mVKIND / anti- <i>mVKIND</i>	rabbit polyclonal	1:1000	1:300	immunoGlobe
Living colors A.v. / anti-EGFP	rabbit monoclonal	—	1:100	Clontech, 8367-1
Myc 9E10 / anti-Myc	mouse polyclonal	1:28.6	1:200	Santa Cruz, sc-40

### 2.3.2 | Secondary antibodies

Antibody	Species	Dilution for stain	Dilution for WB	Supplier, Ordering #
Anti-goat horseradish-peroxidase linked	sheep polyclonal	—	1:5000	Amersham, NA933
Anti-mouse horseradish-peroxidase linked	sheep polyclonal	—	1:4000	Amersham, NA9310
FITC-conjugated anti-mouse	donkey polyclonal	1:250	—	Dianova, 715-095-151
TRITC-conjugated anti-mouse	goat polyclonal	1:250	—	Dianova, 715-025-151
TRITC-conjugated anti-rabbit	donkey polyclonal	1:250	—	Dianova, 711-025-152

## 2.4 | Oligodeoxynucleotides

All oligonucleotides were acquired from *MWG BIOTECH* of standard HPSF quality, diluted in  $\text{MPH}_2\text{O}$  to 10 pmol/ $\mu\text{l}$  and stored at  $-20^\circ\text{C}$ . For detailed information see Appendix II.

Primer	Sequence
5'-mVK-in situ	5' cg <u>GGATCC</u> GCC GCC ATG GAG CAG AAG CTG ATC TCC GAG GAG GAC CTG CAG GCC ATG GAC CCA GCC TCC 3' *
3'-mVK-in situ	5' gc <u>TCTAGA</u> C CAG GGA GTA GAT GTG AGC CTC 3' *
5'-mVK	5' gc <u>GGA TCC</u> GAG AAG GGT CCT TAC TTC TTG 3' *
3'-mVK	5' cg <u>GAA TTC</u> CTA CTG GAA TGT GGC CTT CAT 3' *

\* Underlined nucleotide bases mark endonuclease restriction sites.

## 2.5 | Plasmids

Plasmid	Description	Marker	Supplier
pBACe3.6	pUC-derived cloning plasmid used for preparing BAC libraries	Chloramphenicol	—
pBluescript II	high copy number ColE1-based phagemid cloning vector	Ampicillin	Stratagene
pcDNA3	mammalian CMV promoter driven high-level constitutive expression vector	Ampicillin	Molecular Probes
pcDNA3.1(V5-HiS)TOPO	pcDNA3-derived mammalian constitutive expression vector	Ampicillin	Invitrogen
pEGFP-C1	mammalian CMV promoter driven EGFP C-terminally fusion protein expression, optimized to mammalian codon usage	Kanamycin	Clontech
pGEX-6P-1	vector for high-level expression of C-terminally GST-tagged proteins in bacteria	Ampicillin	Pharmacia
pSport1	cloning pUC-derived phagemid cloning vector	Ampicillin	Invitrogen

## 2.6 | Organisms and cell lines

### 2.6.1 | Bacterial strains

Strains	Description	Supplier/Reference
E. coli Dh5 $\alpha$	F <sup>-</sup> , $\phi$ 80dlacZ $\Delta$ M15, $\Delta$ (lacZYA-argF)U169, <i>deoR</i> , <i>recA1</i> , <i>endA1</i> , <i>hsdR17</i> (rK <sup>-</sup> , mK <sup>+</sup> ), <i>phoA</i> , <i>supE44</i> , $\lambda^-$ , <i>thi-1</i> , <i>gyrA96</i> , <i>relA1</i>	Gibco BRL/ Hanahan, 1983
Rosetta	F <i>ompT hsdS<sub>B</sub></i> (r <sub>B</sub> <sup>-</sup> m <sub>B</sub> <sup>-</sup> ) <i>gal dcm</i> pRARE <sup>2</sup> (Cam <sup>r</sup> )	Novagen, #70953-3/Kane, 1995

### 2.6.2 | Eukaryotic cell lines

Line	Description	Reference
primary cells	murine granular cells	primary cerebellar mouse cells
HeLa	human cervical epithelial carcinoma cell line	MSZ stock
NIH 3T3	continuous immortalized mouse embryo fibroblast cell line	America Type Culture Collection (ATCC) CRL-1711

### 2.6.3 | Mice

Organism	Description	Reference
C57BL/6	mouse inbred strain, substrain 6 separated prior to 1937	Little, 1921
CD1	albino outbred mouse strain	Charles River, 1959

## 2.7 | Analytical kits

Analytical kits	Supplier, Ordering #
ECL Western Blotting Detection	Amersham, RPN 2106
NucleoTrap® Gel Extract Kit	Macherey Nagel, 636018
One Step RT-PCR Kit	Qiagen, 10212
pcDNA3.1(V5- HiS)TOPO TA Expression Kit	Invitrogen, K4900-01
pegGOLD dNTP Set	peQLab, 20-2010
Plasmid Giga Kit	Qiagen, 10191
Plasmid Maxi Kit	Qiagen, 12163
QIAquick PCR purification Kit	Qiagen, 28106
RNA Isolation Kit	Stratagene, 200345

## 2.8 | Standards

Standards	Supplier, Ordering #
1 kb ladder for DNA	Invitrogen, 15615-024
Kaleidoscope prestained standards	Bio-Rad, 1610324
Precision Plus Protein dual color standards	Bio-Rad, 1610374
Pre-stained Molecular Weight Standard Mixture for protein	Amersham, RPN 800

## 2.9 | Equipment

Apparatus	Supplier	Apparatus	Supplier
3100 Avant Sequencer	Applied Biosciences	Fluorescent Microscope	Leica DMIRBE
Agarose electrophoresis gel chamber	Stratagene	Freezer	Liebherr, Nunc
Autoclave	Webeco	Ice maker	Scotsman
Blotting chamber	Hoefer	Incubator	Heraeus, Memmert
Cell freezing container	Nalgene	Photometer	Hitachi
Centrifuges	Eppendorf, Sorvall, Heraeus	Pipettes	Eppendorf, Abimed
Computer	Apple	Precision balance	Sartorius
Contrast microscope	Fluovort FS, Leitz	Shaker	Bellco Biotechnology
Counting chamber	Neubauer (improved)	Sterile bench	Heraeus
Digital camera	Hamamatsu C4742-95	Thermocycler	Eppendorf, Perkin Elmer
Digital chemical balance	Sartorius	UV crosslinker	Stratagene
Film processor	Kodak		

## Chapter III | Methods

	<b>Page</b>
<b><u>3.1   Molecular Biological Methods</u></b>	23
<b>3.1.1   Separation of nucleic acids by gel electrophoresis</b>	23
3.1.1.1   Agarose gel electrophoresis	23
3.1.1.2   Northern blot	23
<b>3.1.2   Isolation of nucleic acids from aqueous solutions</b>	24
3.1.2.1   Alcohol precipitation	24
3.1.2.2   Isolation of plasmid DNA	24
3.1.2.3   Isolation of total RNA	25
3.1.2.4   Gel DNA recovery	25
3.1.2.5   Quantification of nucleic acids by spectrophotometry	25
<b>3.1.3   Amplification of DNA by polymerase chain reaction</b>	25
3.1.3.1   PCR	25
3.1.3.2   Primer design	26
3.1.3.3   Reverse transcription polymerase chain reaction	27
3.1.3.4   Colony PCR	27
<b>3.1.4   DNA Cloning</b>	27
3.1.4.1   Generating a DNA insert	27
3.1.4.2   Generating recombinant plasmid DNA	28
3.1.4.3   Noncohesive ends cloning	28
3.1.4.4   Deletion mutagenesis	29
3.1.4.5   Ligation	29
3.1.4.6   Transformation and culturing of E. coli Dh5 $\alpha$ bacterial cells	29
3.1.4.7   Sequencing	30
<b><u>3.2   Protein Chemical Methods</u></b>	30
<b>3.2.1   Electrophoretic separation of proteins</b>	30
3.2.1.1   SDS-PAGE	30
3.2.1.2   Electroblotting and immunodetection	31
<b>3.2.2   Recombinant protein expression in prokaryotes</b>	31
<b>3.2.3   Glutathione based affinity chromatography</b>	32
<b>3.2.4   Buffer exchange</b>	32
<b><u>3.3   Cell Biological Methods</u></b>	32
<b>3.3.1   Cell culture</b>	32
3.3.1.1   NIH 3T3 and HeLa cells maintenance and passaging	32
3.3.1.2   Preparation of murine granule cells	33
3.3.1.3   Cell density	34
<b>3.3.2   Transfection</b>	34

---

<b>3.3.2.1</b>   Transfection with Lipofectamine	34
<b>3.3.2.2</b>   Transfection with calcium-phosphate coprecipitation	34
<b>3.3.3</b>   Immunocytochemistry	35
<b>3.3.4</b>   Time-lapse video live cell analysis	35

## **3.1 | Molecular Biological Methods**

### **3.1.1 | Separation of nucleic acids by gel electrophoresis**

#### **3.1.1.1 | Agarose gel electrophoresis**

Agarose gel electrophoresis is a technique used to separate DNA fragments based on their size. DNA is negatively charged in solution and is forced to migrate through an agarose gel to the positive pole by an electric field. Migration rate is inversely proportional to the logarithm of the number of base pairs. Longer molecules move more slowly due to their entrapment in the gel matrix. Gel agarose concentration is chosen to be appropriate for the size of DNA fragments. Concentration of 0.7%-agarose gels shows good resolution of large DNA molecules (up to 12 kb), whereas 2%-agarose gels are suitable for smaller molecules (down to 0.2 kb). DNA can be visualized by illumination by UV light based on the incorporation of fluorescent dye (ethidium bromide) into the DNA helix. If the DNA was to be used for further cloning procedures only brief exposure to UV light was performed to minimize the risk of DNA damage. The agarose (% (w/v) = gel concentration) was dissolved by boiling in 0.5x TBE buffer (microwave). After cooling to 60°C ethidium bromide was added to a final concentration of 5 µg/ml. DNA-loading buffer was added to the DNA samples. Gels were run usually at 100 volts for 30-60 min. The agarose gel areas containing the DNA fragments of interest were excised and DNA was recovered from the gel by employing NucleoTrap® Gel Extract Kit (*Macherey Nagel*, →2.7).

<b>10x TBE buffer</b>		<b>DNA-loading buffer</b>	
Tris-Base, pH 8.3	0.89 M	Tris-Base, pH 7.4	9 mM
EDTA	25 mM	EDTA	0.45 mM
Boric acid	0.89 M	Glycerin	46% (v/v)
		SDS	0.2% (w/v)
		Bromphenol blue	0.05% (w/v)

#### **3.1.1.2 | Northern blot**

Northern blot is a method used to study gene expression. Isolated and purified total RNA from organs of an adult C57BL/6 mouse (→2.6.3) was separated by gel electrophoresis and transferred onto a Duralon UV membrane (*Stratagene*) by capillary action with a high salt solution. The following hybridization step allowed the detection of RNA with a radioactive labeled probe complementary for the RNA fragment in question. The specifically bound probe was visualized by autoradiography. For the gel, 1 g agarose was dissolved in 73.4 ml DEPC treated  $\text{MPH}_2\text{O}$  by boiling (microwave). Solution was cooled to 50°C, next, 16.6 ml 37% formaldehyde solution and 10 ml 10x formaldehyde gel running buffer (FGRB) were added. The gel was poured into the gel chamber under the chemical hood. The gel was pre-run for 5 min at RT and 5 V/cm. 30 µg RNA were dissolved in 10 µl DEPC treated  $\text{MPH}_2\text{O}$ . RNA sample buffer was added to a final volume of 20 µl and samples were incubated at 65°C for 15 min. Next, samples were chilled on ice, centrifuged for 5 s and complemented with 3 µl of a 1 µg/µl ethidium bromide stock solution. The gel was pre-run for 5 min at RT and 5 V/cm. Samples were loaded onto the gel and electrophoresis was carried out until the bromphenol blue line migrated approximately 8 cm. The gel was then soaked in 0.05 N NaOH for 20 min and subsequently rinsed in DEPC treated  $\text{MPH}_2\text{O}$  and further soaked in 20x SSC (3 M NaCl, 0.3 M Na-citrate) for 45 min. The gel containing the RNA of interest was blotted onto the Duralon membrane (*Stratagene*) by capillary force in 20x SSC for 6-18 h. Membrane was then briefly washed in 2x SSC and



placed under a UV crosslinker (*Stratagene*) with default settings. 1000 bp DNA probes were labeled with ( $\alpha$ - $^{32}$ P)dCTP by DNA random primed labeling kit (*Roche*) following the manufacturer's instructions. The radioactively labeled DNA fragment was hybridized employing QuickHyb solution (*Stratagene*). The QuickHyb solution was incubated for 20 min at 42°C. The roller oven was pre-heated to 65°C. The Duralon membrane containing the RNA and a grid filter were briefly dipped in DEPC treated  $_{MP}H_2O$ . The membrane was rolled onto the grid and placed into the roller bottle. 15 ml pre-warmed QuickHyb solution was added and the air bubbles were removed with a pipet. The blot was pre-hybridized for 30 min at 65°C. 0.6 ml QuickHyb solution and 30 ng ( $\alpha$ - $^{32}$ P)dCTP labeled double stranded DNA were briefly boiled, complemented with 1000  $\mu$ g salmon sperm DNA and added onto the membrane. Thereafter, hybridization was performed for 4 h at 65°C in a roller oven. The membrane was then washed twice with 2x SSC/0.1% SDS solution for 15 min at RT. A further washing step was exercised twice with 0.1x SSC/0.1% SDS solution for 15 min at 60°C. Finally, autoradiograms were prepared.

10x FGRB		RNA sample buffer	
NaOAc	20,7 mM	37% formaldehyde solution	18.9% (v/v)
EDTA	2.6 mM	formamide	66% (v/v)
MOPS	50 mM	10x FGRB	9.4% (v/v)
	ad 500 ml DEPC treated $_{MP}H_2O$	0.5 % bromphenol blue solution	5.7% (v/v)
	adjust to pH 7.0 with 2N NaOH		Store at -20°
20X SSC			
NaCl	3 M		
NaCitrate	341 mM		
	add 1000 ml $_{MP}H_2O$		
	adjust pH to 7.0 with 1M HCl		

### 3.1.2 | Isolation of nucleic acids from aqueous solutions

#### 3.1.2.1 | Alcohol precipitation

Ethanol precipitation is a rapid technique to concentrate DNA. A DNA precipitate is allowed to form in ethanol in the presence of moderate concentration of monovalent cations (0.1 volumes of 3M NaOAc). Initial precipitation was done with 2 to 2.5 volumes of ice cold absolute EtOH for 20 min at low temperature (-20°C). DNA was recovered by centrifugation at 15000 g for 20 min at RT. Next, the precipitate was redissolved in ice cold 70% ethanol, followed by a brief centrifugation eliminating the residual salt. After drying the pellet was resuspended in an appropriate buffer or  $_{MP}H_2O$ . Isopropanol can be used instead of ethanol. One volume isopropanol was added to the aqueous solution. Precipitation was achieved by mixing and incubation for 10 min at RT. DNA precipitate was collected by centrifugation at 15000 g for 10 min at RT. Isopropanol and salt were removed by subsequent wash with ice cold 70% ethanol.

#### 3.1.2.2 | Isolation of plasmid DNA

Isolation of plasmid DNA from bacterial cells was carried out by using *Qiagen* Plasmid Maxi Kit and *Qiagen* Plasmid Giga Kit following the manufacturer's instructions ( $\rightarrow$ 2.7).

### 3.1.2.3 | Isolation of total RNA

To isolate total RNA, 50-100 mg tissue was homogenized in 1 ml *peqGOLD* RNAPure™ using an UltraThurrax homogenizer. If a cell monolayer was treated, the supernatant was removed and cells were washed with PBS. 1 ml *peqGOLD* RNAPure™ (*peQLab*) was applied to 10 cm<sup>2</sup> and cells were gently resuspended by pipeting. Subsequently, samples were incubated for 5 min at RT. 0.2 ml chloroform (per 1ml *peqGOLD* RNAPure™) were added, samples were vortexed thoroughly for 15 s and incubated for 3-10 min at RT. Following centrifugation at 12000 g for 5 min at RT the upper aqueous phase was separated (containing the RNA) and was mixed with 0.5 ml isopropanol in a fresh tube. After incubation for 5-15 min at RT, RNA was precipitated by centrifugation at 12000 g for 10 min at 4°C. The supernatant was discarded and pellet was washed twice with 1 ml 75% ethanol (12000 g, 10 min, 4°C) and briefly air-dried. Finally the pellet was dissolved in DEPC treated <sub>MP</sub>H<sub>2</sub>O by pipeting, photometrically examined (→3.1.2.5) and stored at -80°C.

### 3.1.2.4 | Gel DNA recovery

Following gel electrophoresis analysis DNA fragments of interest were excised and recovered from the gel by using the NucleoTrap® Gel Extract Kit (*Macherey Nagel*, →2.7) following the manufacturer's instructions.

### 3.1.2.5 | Quantification of nucleic acids by spectrophotometry

ssDNA, dsDNA and RNA absorb light in ultraviolet range, most strongly in 254-260 nm range. The measurement at 260 nm allows a calculation of the dsDNA concentration. An OD<sub>260</sub> of 1 corresponds to approximately 50 µg/ml of dsDNA. The ratio between measurements at 260 nm and 280 nm provides an estimate of the purity of the samples. Proteins absorb light at 280 nm.

Formulas:

$$C \text{ (double stranded DNA)} = \text{OD}_{260} \times \text{factor of dilution} \times 50 \text{ } [\mu\text{g/ml}]$$

$$C \text{ (RNA and oligos)} = \text{OD}_{260} \times \text{factor of dilution} \times 40 \text{ } [\mu\text{g/ml}]$$

1 µl DNA (or RNA) sample was dissolved in <sub>MP</sub>H<sub>2</sub>O (1:100) and photometrically examined (*Hitachi*). Nucleic acid concentration was calculated employing the formulas described above.

## 3.1.3 | Amplification of DNA by polymerase chain reaction

### 3.1.3.1 | PCR

The polymerase chain reaction (PCR) is a powerful technique for oligonucleotide primer directed enzymatic amplification of a specific DNA sequence of interest. The PCR product is obtained from the DNA template *in vitro* applying a heat-stable DNA polymerase. An automated thermal cycler puts the reaction through 30 or more cycles of denaturation of dsDNA, annealing of primers and polymerization. Denaturation separates the complementary strands and was carried out at 92 °C. Annealing temperature was calculated based on the primer sequence ( $T_m$ ). Primers are single-stranded oligonucleotides complementary to the flanking areas of the targeted segment which serve as a starting point for DNA replication. During polymerization the enzyme catalyzes the synthesis of a new strand DNA. The optimal temperature varies according to the polymerase species. PCR products were visualized on an agarose gel (→3.1.1.1).

Taq PCR components	( $\mu$ l)	Pfu PCR components	( $\mu$ l)	Pfx PCR components	( $\mu$ l)
Taq Pol buffer 10x	5	Pfu Pol buffer 10x	10	Pfx Pol buffer 10x	5
MgCl <sub>2</sub> (25 mM)	3	Plasmid DNA (~200 ng/ $\mu$ l)	1	Plasmid DNA (~200 ng/ $\mu$ l)	1
Plasmid DNA (~200 ng/ $\mu$ l)	1	5'-Primer (10 pmol/ $\mu$ l)	2	5'-Primer (10 pmol/ $\mu$ l)	3
5'-Primer (10 pmol/ $\mu$ l)	2	3'-Primer (10 pmol/ $\mu$ l)	2	3'-Primer (10 pmol/ $\mu$ l)	3
3'-Primer (10 pmol/ $\mu$ l)	2	dNTPs (25 mM)	1	Pfx Pol (2.5 U/ $\mu$ l)	1
dNTPs (10 mM)	1	Pfu Pol (3 U/ $\mu$ l)	1	M <sub>P</sub> H <sub>2</sub> O	ad 50
Taq (3 U/ $\mu$ l)	0.4	M <sub>P</sub> H <sub>2</sub> O	ad 100		
M <sub>P</sub> H <sub>2</sub> O	ad 50				

**Standard 1-step PCR Program**

#	Step	Temperature	Time	Cycle (s)
hot start				
1	Denaturing	92°C	2 min	1
2	Denaturing	92°C	0.25 min	30
	Annealing	T <sub>mR</sub>	0.25 min	
	Elongation	72°C	1 min*/kb	
3	Completion	72°C	10 min	1
4	Storage	15°C	hold	

**Standard 2-step PCR Program**

#	Step	Temperature	Time	Cycle(s)
hot start				
1	Denaturation	92°C	2 min	1
2	Denaturation	92°C	0.25 min	2
	Annealing	T <sub>mR</sub>	0.25 min	
	Elongation	72°C	1 min*/kb	
3	Denaturation	92°C	0.25 min	30
	Annealing	T <sub>mR</sub>	0.25 min	
	Elongation	72°C	1 min*/kb	
4	Completion	72°C	10 min	1
5	Storage	15°C	hold	

\*1 min per 1000 bp of DNA sequence of interest was calculated for the duration of the elongation step based on the average processivity of the specific polymerase.

Taq Pol → 1 min/kb DNA sequence

Pfu Pol → 2 min/kb DNA sequence

Pfx Pol → 1 min/kb DNA sequence, operates at 68°C

The basic melting temperature T<sub>m</sub> of the primers was calculated with the formula:

$T_m = 2 \times (aA + bT) + 4 \times (cG + dG)$  [ °C], where *a*, *b*, *c*, and *d* are the numbers of bases A, T, G and C in the primer sequence, respectively.

$T_{mR} = T_m - 5$  (or 4) [ °C], without taking into consideration the restriction endonuclease recognition site sequence (additional to the gene specific sequence)

$T_{mR} = T_m - 5$  (or 4) [ °C], calculating the entire primer, including the introduced endonuclease recognition site

**3.1.3.2 | Primer design**

Primers were designed to be 21 base pairs in length with a melting temperature preferentially over 60°C. The minimum GC content was 50%. In case a restriction site was added to the primer 5'- or 3'-site additional bases were constructed to support the recognition by endonucleases. The primers terminate in one or more G or C bases at the 3'-end. All primers were synthesized by *MWG BIOTECH* of standard HPSF quality.

### 3.1.3.3 | Reverse transcription polymerase chain reaction

Reverse transcription polymerase chain reaction (RT-PCR) is the most sensitive technique for mRNA detection and quantification currently available. RT-PCR engages two sequential steps. First, single-stranded RNA is reverse transcribed into complementary DNA (cDNA) by using total cellular RNA, a reverse transcriptase enzyme, a primer, dNTPs and an RNase inhibitor. Three types of primers can be used for a RT-Reaction: oligo (dT) primers, random primers and gene specific primers. And second, the resulting cDNA is used as template for PCR amplification of a gene of interest. RT-PCR can be carried out as one-step RT-PCR in which all reaction components are mixed in one tube. Throughout the course of this work RT-PCR was performed using the *Qiagen OneStep RT-PCR Kit* (→2.7) with gene specific primers.

RT-PCR components		( $\mu$ l)	RT-PCR Program				
Qiagen buffer 5x		10	#	Step	Temperature	Time	Cycle (s)
RNA (~200 ng/ $\mu$ l)		1	1	Reverse Transcriptase	50°C	30 min	1
5'-Primer (10 pmol/ $\mu$ l)		3		HotStarTaq activation	95°C	15 min	1
3'-Primer (10 pmol/ $\mu$ l)		3	2	Denaturing	92°C	0.25 min	30
dNTPs (0.4 $\mu$ M)		2		Annealing	$T_m$	0.25 min	
Enzyme Mix		2		Elongation	72°C	1 min*/kb	
$M_{\text{P}}H_2O$		ad 50	3	Completion	72°C	10 min	1
			4	Storage	15°C	hold	

### 3.1.3.4 | Colony PCR

Colony PCR is a rapid method for screening for positive bacteria clones on a plate subsequent to DNA cloning (→3.1.4). Gene specific primers of the desired sequence were used for a Taq-PCR reaction mix (→3.1.3.1). The reaction mix was aliquoted to 10 PCR tubes on ice. Single isolated bacteria colonies from a LB-plate were picked with an autoclaved toothpick into the PCR-tubes containing the mix. The tested colonies were transferred to a fresh LB-plate for further usage. Cell lysis was achieved by an additional initialization heating step at 95°C for 3 min in the thermocycler (*Eppendorf*) prior to the standard PCR-program (→3.1.3.1). PCR-products were analyzed by agarose gel electrophoresis (→3.1.1.1). Cultures for positives clones were prepared for plasmid DNA isolation (→3.1.2.2).

## 3.1.4 | DNA Cloning

DNA cloning is a technique for DNA fragments reproduction. A vector is required to carry the DNA fragment of interest into a host cell. All cloning vectors used in the course of this work were plasmids. Plasmids are small circular molecules of double stranded DNA derived from natural plasmids that occur in bacterial cells. A DNA fragment can be inserted into a plasmid if both, the circular plasmid and the source of DNA, have recognition sites for the same restriction endonuclease. The plasmid and the foreign DNA are cut by a restriction endonuclease producing intermediates with sticky and complementary ends. The new plasmid can be introduced into bacterial cells and produce many copies of the inserted DNA.

### 3.1.4.1 | Generating a DNA insert

DNA inserts were generated by PCR (→3.1.3.1) or by releasing DNA fragments out of plasmids. PCR products were separated on an agarose gel and purified (→3.1.1.1). Subsequential incubation with restriction endonucleases produced blunt ends or single-stranded overhangs (cohesive ends also called sticky

ends) complementary to those in the vector. Primers were designed to provide a restriction site at each end of the PCR product (→3.1.3.2). In other cases the PCR products contained the cleavage site. Accurate digestion was verified by agarose gel electrophoresis, followed by purification of the digested products (→3.1.1.1).

Preparative restriction double digestion	( $\mu$ l)	U
PCR cDNA product (~500 ng)	20	
10x reaction buffer	3	
restriction endonuclease I	variable	10-20
restriction endonuclease II	variable	10-20
$\text{MPH}_2\text{O}$	ad 30	

The temperature of incubation, the choice of reaction buffer as well as the amount of units applied were dependent on the restriction endonuclease's requirements. Duration of incubation was in most cases minimum 2 h. In case double digestion was not suitable, the cDNA was subjected to cleavage by one enzyme at a time, followed by gel electrophoresis and extraction (→3.1.1.1).

### 3.1.4.2 | Generating recombinant plasmid DNA

Plasmid DNA was cleaved by corresponding restriction endonucleases which produced cohesive ends complementary to the insert DNA. After verification of a successful plasmid linearization and vector fragment integrity by gel electrophoresis (→3.1.1.1), the vector was purified using the NucleoTrap® Gel Extract Kit (*Macherey Nagel*, →2.7).

Preparative restriction double digestion	( $\mu$ l)	U
plasmid DNA (~1 $\mu$ g)	variable	
buffer 10x	3	
restriction endonuclease I	variable	5-10
restriction endonuclease II	variable	5-10
$\text{MPH}_2\text{O}$	ad 30	

The temperature of incubation and the choice of reaction buffer, as well as the amount of units applied were dependent on the restriction endonuclease's requirements. Duration of the incubation was 0.5-1 h. In case a double digestion was not suitable DNA was subjected to cleavage by one enzyme at a time, followed by a gel electrophoresis and extraction (→3.1.1.1).

### 3.1.4.3 | Noncohesive ends cloning

If not having compatible restriction sites for a cloning procedure at hand, a blunt (noncohesive end) cloning was performed. Also, provided a restriction endonuclease generated noncohesive ends upon restriction of an insert, a blunt end cloning was carried out. The insert and vector termini were both blunted by using *E. coli* DNA polymerase I large fragment (Klenow fragment, *Roche*) according to the manufacturer's instructions. Klenow has 5'-3' polymerase and 3'-5' exonuclease, but not 5'-3' exonuclease activities. Next, the vector was dephosphorylated by using the calf intestinal phosphatase (CIP) to decrease the background of non-recombinants that arise from self-ligation. CIP was also employed according to the manufacturer's

instructions. Gel purification of the vector was performed to reduce the frequency of aberrant clones (→3.1.1.1).

#### 3.1.4.4 | Deletion mutagenesis

Specific deletions were introduced into cloned DNA using completely overlapping sense and antisense primers containing the mutation of interest. Mutagenic primers lacking the DNA sequences designated for deletion were employed for PCR amplification using pSport1-mVKINDfl construct as template and the Pfx DNA Polymerase (*Invitrogen*), according to the manufacturer's conditions. Primers were extended for 10 min at 68°C during which the desired mutations were incorporated and subsequently amplified. The PCR products obtained were two different linear DNA fragments, the parental template and the mutated DNA. Parental template DNA was subjected to degradation by DpnI digestion (30 U/50 µl PCR sample, for 1 h at 37°C). Subsequently, DpnI endonuclease was heat inactivated for 15 min at 65°C. Mutant DNA was circularized by blunt end ligation, achieved by transforming competent *E. coli* Dh5α bacterial cells with DpnI-treated PCR sample (→3.1.4.5). Clones were tested by colony PCR (→3.1.3.4).

#### 3.1.4.5 | Ligation

Ligation is the process of joining linear DNA fragments together with a covalent bond. A phosphodiester bond between the 3'-hydroxyl termini and the 5'-phosphate is catalyzed by the T4 DNA ligase. The enzyme originates from the T4 bacteriophage and ligates DNA fragments having blunt and sticky ends annealed together. The optimal incubation temperature for T4 DNA ligase is 16°C. Following generation and purification of insert (→3.1.4.1) and vector (→3.1.4.2) DNA fragments, the fragments were eluted (→3.1.1.1) together in 1x T4 ligase buffer and supplemented with T4 DNA ligase (*NEB*). To maximize the yield, a ligation reaction was set in an estimated vector:insert molar ratio of 3:1. Following over night incubation at 16°C, the total reaction was used for transformation of competent cells (→3.1.4.6).

Ligation	(µl)	U
DNA fragments	19	
T4 DNA ligase	1	400 U/µl
final volume	20	

#### 3.1.4.6 | Transformation and culturing of *E. coli* Dh5α bacterial cells

Transformation of bacterial cells is achieved by an uptake of plasmid DNA. The procedure involves heat shocking and ice shocking alternately. Cells, which efficiently accept extra DNA, are known as competent cells. Competent cells are prepared by treatment with CaCl<sub>2</sub> (Morrison, 1977). Plasmids holding an origin of replication recognized by the host cell DNA polymerase are being replicated along with the endogenous DNA. Moreover, plasmids expressing antibiotic resistance provide a way of identifying and isolating cells that have successfully incorporated the desired plasmid. 20 µl of a ligation reaction (→3.1.4.5) were added to 200 µl competent bacterial cells (*E. coli* Dh5α) previously thawed on ice, gently mixed and incubated on ice for further 40 min. Cells were heat shocked for 90 s at 42°C and chilled on ice for 2 min. 1 ml LB was added and the cells were incubated under shaking for 30-60 min at 37°C. Cells were collected by centrifugation at 3500 rpm for 3 min at RT. Supernatant was discarded and the cell pellet was dissolved in 150 µl LB. Next, 50 µl and 100 µl were plated out on LB agar plates containing the appropriate antibiotic as selection marker and plates were incubated overnight at 37°C. Colonies of transformants were inoculated for

further investigation (→3.1.3.4) or plates were stored for several weeks at 4°C. For bacterial culture and subsequent plasmid purification, designated transformed *E. coli* Dh5 $\alpha$  clones were shaken over night in LB broth supplemented with either 100  $\mu$ g/ml ampicillin or 100  $\mu$ g/ml kanamycin at 37°C. Later cells were pelleted and plasmid DNA was isolated employing the Plasmid Maxi Kit (*Qiagen*, →2.7).

### 3.1.4.7 | Sequencing

Throughout the course of this work, DNA was sequenced by automated sequencing using the 3100 Avant Sequencer (*Applied Biosystems*), employing the Big Dye Terminator VII Cycle Sequencing Kit (*Applied Biosystems*).

## 3.2 | Protein Chemical Methods

### 3.2.1 | Electrophoretic separation of proteins

Polyacrylamide gel electrophoresis (PAGE) is applied to separate protein mixtures based on their migration in solution in response to an electric field. The sample is run in a support matrix which separates the molecules by size and provides a record of the electrophoretic run. Proteins are amphoteric compounds, therefore their net charge is determined by the pH of the solution. The net charge is independent of its size, i.e. the charge is carried per unit mass. Under denaturing conditions the anionic detergent sodium dodecyl sulfate (SDS) disrupts the secondary and tertiary structure and binds to proteins quite specifically in a mass ratio of 1.4:1. Therefore SDS confers a negative charge to the polypeptides in proportion to their length (equal charge per unit length). 2-mercaptoethanol reduces disulphide bridges in proteins. During denaturing SDS-PAGE separation is achieved by polypeptide migration determined not by its intrinsic electrical charge, but by its molecular weight.

#### 3.2.1.1 | SDS-PAGE

Throughout the course of this work protein samples were subjected to SDS-PAGE using a discontinuous buffer system providing a good resolution. In a discontinuous system a non-restrictive large pore gel, called stacking gel, is layered on top of a separating gel, called a resolving gel. Each gel was made with a different buffer along with the tank buffer being different from the gel buffers. Prior to loading, protein samples were added 1x SDS-loading buffer and boiled for 5 min at 100°C. Protein sizes were analyzed using the pre-stained Protein Ladder (*Amersham, Bio-Rad*) as molecular mass marker. Electrophoresis was performed at 36 mA at RT until the BPB (bromphenol blue) dye reached the bottom of the gel.

	Resolving gel			Stacking gel	
	6%	10%	12%		
Acrylamide: Bisacrylamide (37.5:1)	5.85 ml	9.3 ml	11.16 ml	Acrylamide: Bisacrylamide (19:1)	2.25ml
3M Tris-HCl, pH 9	3.8 ml	3.8 ml	3.8 ml	1M Tris-HCl, pH 6.8	1.25 ml
$\text{mP}\text{H}_2\text{O}$	19.15 ml	15.7 ml	13.84 ml	$\text{mP}\text{H}_2\text{O}$	6.25 ml
20% SDS	150 $\mu$ l	150 $\mu$ l	150 $\mu$ l	20% SDS	50 $\mu$ l
TEMED	30 $\mu$ l	30 $\mu$ l	30 $\mu$ l	TEMED	15 $\mu$ l
10% APS	150 $\mu$ l	150 $\mu$ l	150 $\mu$ l	10% APS	100 $\mu$ l

10x Electrophoresis buffer		1x SDS-loading buffer	
Glycine	190 mM	Tris-HCl, pH 6.8	60 mM
Tris base	25 mM	Glycerin	10% (v/v)
SDS	0.1% (w/v)	SDS	3% (w/v)
	pH 8,6	$\beta$ -Mercaptoethanol	5% (v/v)
		Bromphenol blue	0.005%

### 3.2.1.2 | Electroblothing and immunodetection

Proteins were transferred efficiently from a polyacrylamide gel ( $\rightarrow$ 3.2.1.1) to a nitrocellulose membrane by electroblotting (western blot) using a *Sigma* blotting tank. The transfer was carried out for 1.5 to 2 h at 150 mA at RT in western transfer buffer. Protein transfer was verified by staining the nitrocellulose membrane with Ponceau S solution (*Sigma*). Nitrocellulose membrane was incubated in staining solution for 1 min at RT. Rinsing with  $\text{MPH}_2\text{O}$  for 5 min at RT with shaking reveals the protein distribution on the nitrocellulose membrane. Thereafter the membrane was destained twice with PBS-Tween (PBST) buffer for 15 min at RT with shaking until staining faded away completely. For immunodetection the nitrocellulose membrane was blocked over night in blocking buffer at 4°C. After blocking the membrane was incubated in blocking buffer containing the corresponding primary antibody ( $\rightarrow$ 2.3.1) for 3 h at RT. Subsequently, the membrane was washed 3 times with PBST for 10 min at RT with shaking. Next, the membrane was incubated in PBST:blocking buffer 3:1 (v/v) containing the secondary HRP-linked antibody ( $\rightarrow$ 2.3.2) for 45 min at RT followed by a second washing as described above. Finally, the exceed liquid was removed and the antibody coupled peroxidase was detected with an ECL reagent kit (enhanced chemoluminescence, *Amersham*) ( $\rightarrow$ 2.7). Signals were detected by autoradiography using an ECL-hyperfilm (*Amersham*).

Western transfer buffer		Panceau S	
Glycine	190 mM	Panceau S	0.2% (w/v)
Tris base	25 mM	Trichloroacetic acid	3% (w/v)
Methanol	20% (v/v)		

PBS-Tween		Blocking buffer	
Tween 20	0.05% (v/v)	dried milk powder	5-10% (w/v)
PBS, pH 7.4	1x	PBS-Tween	1x

### 3.2.2 | Recombinant protein expression in prokaryotes

*E. coli* strain Rosetta (*Novagen*,  $\rightarrow$ 2.6.1) was transformed with the recombinant protein expression vector pGEX-6P-1, coding for N-terminally GST-fused proteins. The bacterial culture was grown in LB broth supplemented with 100  $\mu\text{g/ml}$  ampicillin and 34  $\mu\text{g/ml}$  chloramphenicol. The Rosetta strain contains a pRARE plasmid ( $\text{cam}^r$ ) coding for tRNAs of the rarely used codons Arg, Ile, Gly, Leu and Pro, enabling high protein expression yields (Novy *et al.*, 2001). The recombinant protein transcription driven by a *lacZ* promotor was then induced with isopropyl- $\beta$ -D-thiogalactopyranoside (IPTG). Initially, the recombinant host was grown over night to saturation in LB with shaking (180 rpm) at 37°C. Next, 5 l of LB broth were inoculated with the primary culture (10:1) and incubated with shaking (180 rpm) at 37°C to  $A_{600}$  of 0.6. Recombinant expression was then induced by 1 mM IPTG (to 0.1 mM) and cells were cultured over night



with shaking (120 rpm) at 21°C. Finally, cells were pelleted (*Beckmann GSA*, 10000 g, 10 min, 4°C), subsequently washed once with PBS and if required stored at -20°C.

### 3.2.3 | Glutathione based affinity chromatography

Glutathione-S-transferase (GST) from *Schistosoma japonicum* is used as tag for proteins for expression and purification applications. GST is a 26 kD protein which binds to glutathione with high affinity and specificity. Recombinant proteins fused to GST can then be selectively purified based on its high affinity for immobilized glutathione (glutathione sepharose). Sepharose is a bead form of agarose. The binding occurs under nondenaturing conditions since GST loses its ability to bind glutathione sepharose when denatured. The cDNA of interest was cloned into pGEX-6P-1 and expressed as described in 3.2.2. In the course of this work purification was performed using the *Amersham Pharmacia* Glutathione Sepharose 4b resin according to the manufacturer's batch purification protocol. To reduce protein degradation, the entire purification process was performed on ice. Recombinant host cells (Rosetta) were resuspended in TBST buffer and disrupted by sonification (6 x 15 s at 50%, and 1 x 20 s at 100%). Cell debris was cleared by centrifugation at 10000 g (*Sorvall SS34*) for 30 min at 4°C. The cleared lysate was incubated with Glutathione Sepharose 4b (*Amersham Pharmacia*) (250 µl bead volume/10 ml cleared lysate), earlier washed 3x with TBST, for 2 h at 4°C under rotation. After 3 cycles of washing with 800 µl TBST bound protein was released from the slurry with 1000 µl elution buffer (2x 500 µl). Fractions were collected, stored at -20°C. Aliquots of the fractions were analyzed by SDS-Page (→3.2.1.1).

TBST		Elution Buffer	
Tris-HCl, pH 7.4	10 mM	Tris-HCl, pH 8.0	500 mM
NaCl	150 mM	reduced glutathione	10 mM
Tween 20	0.1% (v/v)		

### 3.2.4 | Buffer exchange

To extract the protein in question from a previously used buffer, protein samples were applied to Nap-10 columns (*Amersham*). Prior to application, columns were equilibrated with 15 ml of the desired buffer (glycerin free). Subsequently, proteins were eluted into 1 ml desired buffer.

## 3.3 | Cell Biological Methods

### 3.3.1 | Cell culture

#### 3.3.1.1 | NIH 3T3 and HeLa cells maintenance and passaging

The mouse fibroblasts NIH 3T3 and human cervix carcinoma HeLa eukaryotic cells were grown in T75 flasks in DMEM (Dulbecco's Modified Eagle Medium, *Life Technology*) in the presence of 10% FCS, penicillin (100 U/ml), streptomycin (100 U/ml) and L-Glutamine (200 mM). Cells were cultured in a humidified incubator at 37°C with 5% CO<sub>2</sub> (*Heraeus*). In the course of this work NIH 3T3 and HeLa cell lines were passaged every 3 days upon reaching 80-90% confluence. Cells were washed with 5 ml PBS, thereafter 1 ml of Trypsin-EDTA (*Life Technology*) was added to detach the cells from the flask. Next, 4 ml DMEM were added and cells were brought into suspension. 1 ml cell suspension was presented to 9 ml DMEM in a fresh sterile T75 flask (*Sarstedt*).

### 3.3.1.2 | Preparation of murine granule cells

To extract murine granule cells, seven mouse cerebella were dissected from C57BL/6 mice (→2.6.3) at postnatal day 5 and the meninges were removed. Tissues were incubated in few drops of 37°C pre-heated solution 1, triturated with a sterile scalpel in the hood and washed in 10 ml of solution 1 (centrifugation at 1200 rpm, *Heraeus*, for 3 min at RT). Supernatant was aspirated, 7 ml 37°C pre-heated solution 2 were added and tissues were incubated in a sterile 100 mm dish for 13 min at 37°C with 5% CO<sub>2</sub> with occasional shaking. Following neutralization, achieved by 7 ml 37°C pre-heated solution 4, cells were pelleted by centrifugation at 1200 rpm for 3 min at RT. The supernatant was again aspirated and tissues were triturated in 2 ml 37°C pre-heated solution 3 by 25 strokes with a sterile pasteur pipet. After allowing to sediment for 10 min, the supernatant was transferred to a fresh sterile 15 ml tube containing 3 ml 37°C pre-heated solution 5. 2 ml of 37°C pre-heated solution 3 were added to the sediment and it was dissociated with a pasteur pipet for a second time. Following afresh sedimentation period of 10 min, the supernatants were consolidated in the 15 ml tube and centrifuged at 1200 rpm for 10 min at RT. In the meanwhile the poly-lysine solution was removed from the petri dishes and let to air-dry in the hood. The supernatant was discarded and cells were incubated in complete medium. Cerebellar granule cells were counted and seeded in 60 mm poly-lysine coated dishes at a density of 5x 10<sup>6</sup> and incubated at 37°C with 5% CO<sub>2</sub>. For a cytostatic treatment of glial cells, 10 µl Ara-c/HCl were added on the following day. RNA of 5x 10<sup>6</sup> granule cells was isolated at 0, 24, 48 and 96 h post preparation (→3.1.2.3).

Krebs-Ringer 10x		Solution 1	
NaCl	1.2 M	Krebs-Ringer buffer 1x	
KCl	50 mM	BSA	0.3% (w/v)
KH <sub>2</sub> PO <sub>4</sub>	12 mM	MgSO <sub>4</sub>	1,24 mM
NaHCO <sub>3</sub>	0.25 M		
D-Glucose	0.14 M		
Phenol red	a pinch		
	filter and store at - 20°		

Solution 2		Solution 3	
Solution 1		Krebs-Ringer buffer 1x	
Trypsin	0,025% (w/v)	DNase	0,008% (w/v)
		Trypsin inhibitor	0,052% (w/v)
		MgSO <sub>4</sub>	2,79 mM

Solution 4		Solution 5		Complete medium	
Solution 1	6,2% (v/v)	Krebs-Ringer buffer 1x		BME 1x	
Solution 3	93,75% (v/v)	MgSO <sub>4</sub>	2,48 mM	FCS	10% (v/v)
		CaCl <sub>2</sub>	13,1 µM	KCl	20 mM
				Gentamycin sulphate 1x	

### 3.3.1.3 | Cell density

To determine cell concentration of cultured cells, cells were resuspended and loaded onto a Fuchs-Rosenthal (*Neubauer*) counting chamber. On a phase contrast microscope (Fluovert FS, *Leitz*) particle count was performed in the middle corner square, consisting of 25 smaller squares.

Cell number was calculated as follows:

$$C(\text{cell}) = \text{counted cells} \times \text{dilution} \times 5000 \text{ [cells/ml]}$$

### 3.3.2 | Transfection

Transfection is the process of introducing nucleic acids into cells by non-viral methods, such as liposomes and calcium phosphate precipitation techniques.

#### 3.3.2.1 | Transfection with Lipofectamine

Eukaryotic cells were transfected with a liposome transfection method (Lipofectamine, *Invitrogen*). Synthetic cationic lipids are used to deliver nucleic acid into cells presumably through endocytosis. Cationic lipids at physiological pH build a unilamellar liposomal structure with a positive surface charge which associates with the negatively charged DNA. Thus a compaction of the nucleic acid in a liposome/nucleic acid complex is facilitated. Following association with the negatively charged cell membrane, the complex enters the cell and appears in endosomes. Later the exogenous DNA is relocated to the nucleus.

One day prior to transfection cells were seeded in a 6-well plate at a cell density of  $1 \times 10^5$ . Complexes were prepared by adding high quality DNA ( $\mu\text{g}$ ) to transfection reagent ( $\mu\text{l}$ ) at a ratio of 1:6. Transfection was performed according to the manufacturer's conditions for 4-5 h at  $37^\circ\text{C}$  with 5%  $\text{CO}_2$  (humidified incubator). Serum and antibiotics were not present during transfection.

#### 3.3.2.2 | Transfection with calcium-phosphate coprecipitation

Mixing DNA and calcium phosphate, and adding the mixture in a controlled manner to a buffered saline/phosphate solution generates a DNA-calcium phosphate coprecipitate. Coprecipitate particles form slowly at RT. Following dispersion onto cultured cells the coprecipitate adheres to the cell surface and is taken up by cells presumably via endocytosis or phagocytosis. Cells were plated in a 6-well plate (at  $\text{Ø}$  35 mm) at a density of  $1 \times 10^5$ . 3-4 h prior to transfection cells were provided with fresh growth medium. In a tube A 9  $\mu\text{l}$   $\text{CaCl}_2$  (2M) was mixed with 5  $\mu\text{g}$  DNA to a total volume of 75  $\mu\text{l}$ . Solution A was added drop wise to solution B, holding 75  $\mu\text{l}$  HBS (2x), until solution A was completely depleted. A fine precipitate was allowed to form for 30 min at RT. Subsequently, the precipitate was distributed drop wise onto the cells in a well of a 35 mm well dish. Transfection was performed overnight at  $37^\circ\text{C}$  with 5%  $\text{CO}_2$  in a humidified incubator (*Heraeus*).

2x HBS	
NaCl	1.6 g
KCl	0.074 g
$\text{Na}_2\text{HPO}_4 \cdot 2\text{H}_2\text{O}$	0.027 g
Glucose	0.2 g
HEPES	1 g
$\text{MPH}_2\text{O}$	ad 100 ml, adjust to pH 7.05 with NaOH

### 3.3.3 | Immunocytochemistry

Immunocytochemistry is a powerful technique for recognizing the location of endogenous or exogenously expressed proteins in cultured cells. It involves a first antibody which targets directly the antigen. In a subsequent step, a second antibody (anti IgG) with an attached fluorescent dye (fluorochrome) interacts with the first antibody, which improves the visualization. The procedure is carried out in fixed permeabilized cells on a cover slip. For immunological staining cells were seeded on glass cover slips ( $\varnothing$  10 mm) in a 6-well plate and transfected with the nucleic acid of interest by Lipofectamine (as described in 3.3.2). 24 h post transfection cells were washed 3x with PBS and fixed with 600  $\mu$ l 3.7% paraformaldehyde (PFA) in PBS for 20 min at 4°C. Following 3x washing with PBS, cells were permeabilized with 600  $\mu$ l 0.2% Triton X-100 in PBS for 3.5 min at RT and washed again 3x with PBS. For immunodetection, fixed cells were incubated in 50  $\mu$ l 1% FCS/PBS (v/v) blocking solution in the presence of a suitable primary antibody for 1 h at RT and then washed 3x with PBS. A second incubation in the presence of either TRITC-conjugated (red) or FITC-conjugated (green) secondary antibodies (dilution 1:250 in 50  $\mu$ l 1% FCS/PBS) along with either Oregon Green phalloidin or rhodamine phalloidin (dilution 1:20), respectively, was performed for 1 h at RT with exclusion of light. Fixed cells were washed 3x with PBS and rinsed in  $\text{MPH}_2\text{O}$ . A drop of Moviol was placed on a microscope slide and the cover slip was gently positioned on top, allowing Moviol to spread beneath the cover slip and cover the cells. Moviol functions as a mounting medium with DABCO operating as a fluorescence stabilizer. Slides were air-dried overnight at RT with exclusion of light. Immunostains were stored at 4°C and examined on a fluorescent microscope.

GFP-fusion proteins were detected by autofluorescence and filamentous actin by staining with conjugated phalloidin (1:20, *Molecular Probes*). Anti-mVKIND rabbit polyclonal antibody (anti-mVKIND serum/0.1%  $\text{NaN}_3$  (v/v), 1:1000, *immunoGlobe*,  $\rightarrow$ 2.3.1) was employed for immunodetection of the mouse VKIND protein. Myc-tagged proteins were detected with anti-Myc 9E10 (1  $\mu$ g/ml, *Santa Cruz*,  $\rightarrow$ 2.3.1). TRITC-conjugated goat anti-mouse antibody (1:250, *Dianova*,  $\rightarrow$ 2.3.2) and FITC-conjugated donkey anti-mouse antibody (1:250, *Dianova*,  $\rightarrow$ 2.3.2) were used as secondary antibodies. Cells were analyzed on a *Leica* DMIRBE fluorescence microscope (100x oil objective) and documented with a monochrome digital camera (*Hamamatsu*). Digital pictures were processed using *Openlab* software (*Improvision*).

Moviol	
Glycol	20 ml
Moviol	15 g
0,2 M Tris-HCl pH 8,5	100 ml
DABCO	3.5 g

### 3.3.4 | Time-lapse video live cell analysis

Transfected NIH 3T3 cells transiently expressing EGFP-fused exogenous proteins were seeded on glass cover slips ( $\varnothing$  25 mm) in DMEM (Dulbecco's Modified Eagle Medium, *Life Technology*) in the presence of 10% FCS, penicillin (100 U/ml), streptomycin (100 U/ml) and L-Glutamine (200 mM). Upon visual evidence of high levels transient expression the cover slip was clamped in a cover slip chamber. Cells were overlaid with 37°C warm growth medium and immediately transferred to a fluorescent microscope (*Leica*) while being incubated at 37°C. Cells positive for EGFP fluorescence were selected and focused at 100x/1.30 oil objective. Subsequently, a time-lapse fluorescent monitoring was initiated with images captured every 30 s employing a digital camera (*Hamamatsu*). Images (1024x1022 pixels) were optimized and light

intensities were color-coded with *Openlab* imaging software (*Improvision*). Quick Time videos (.mov format) were generated using time series pictures.

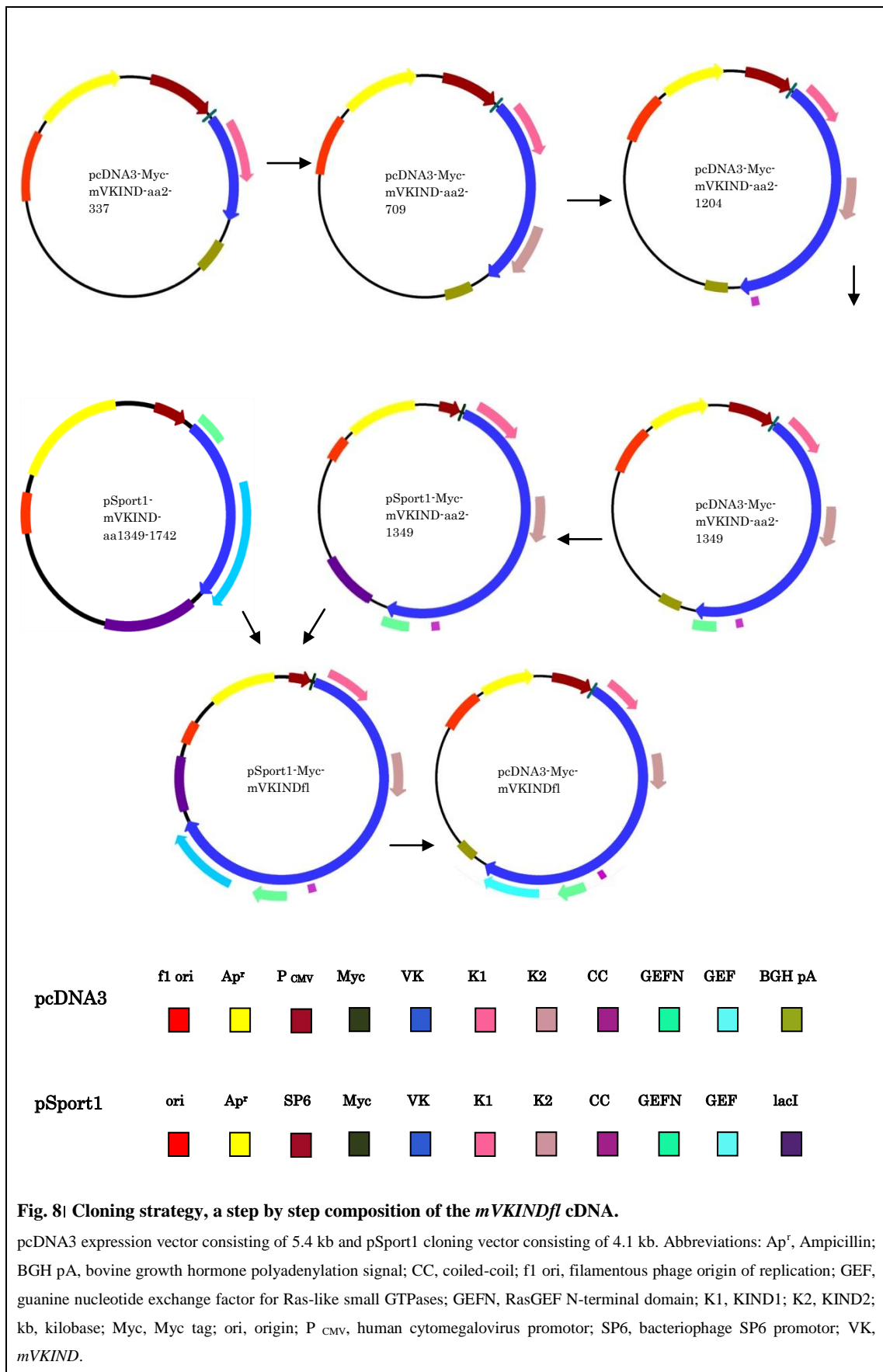
## Chapter IV | Results

	<b>Page</b>
<b>4.1</b>   Cloning	38
<b>4.2</b>   VKIND structural analysis	40
<b>4.3</b>   Phylogenic analysis	41
<b>4.4</b>   The VKIND RasGEF domain	43
<b>4.5</b>   The murine VKIND protein	44
<b>4.6</b>   Expression analysis	44
<b>4.7</b>   Developmental time course of <i>VKIND</i> expression in mouse embryo	45
<b>4.8</b>   <i>VKIND</i> gene expression in postnatal mouse brain	47
<b>4.9</b>   Transient expression analysis	48
<b>4.9.1</b>   EGFP fusion protein expression	48
<b>4.9.2</b>   Transient expression of C-terminally truncated mVKIND mutants coding for KIND1 domain and KIND1/KIND2 domains	50
<b>4.9.3</b>   Transient expression of C-terminally truncated mVKIND mutants coding for Myc-mVKIND-aa2-1204, Myc-mVKIND-aa2-1234 and Myc-mVKIND-aa2-1349	51
<b>4.9.4</b>   Transient expression of N-terminally truncated mVKIND mutants coding for Myc- mVKIND-aa456- 1742, Myc-mVKIND-614-1742 and Myc-mVKIND-aa2-1451-1742	53
<b>4.9.5</b>   Transient expression mVKIND deletion mutants coding for Myc-mVKIND- $\Delta$ aa880-1235, Myc-mVKIND- $\Delta$ aa880-948 and Myc-mVKIND- $\Delta$ aa1059-1235	55
<b>4.9.6</b>   Transient expression of mVKIND deletion mutants coding for Myc-mVKIND- $\Delta$ aa1238-1364	57
<b>4.9.7</b>   Transient expression of mVKINDfl	58
<b>4.9.8</b>   Summary of the transient expression of mVKINDfl and mVKIND truncation mutants	59
<b>4.10</b>   Live cell imaging of EGFP-mVKINDfl transfected cells	60
<b>4.11</b>   mVKIND antibody	62
<b>4.12</b>   Murine VKIND protein phosphorylation by the p38 MAPK	64

The new protein module kinase non-catalytic C-lobe domain (KIND) was originally identified as a conserved domain represented in the N-terminal region of the Spir family actin organizers (Otto *et al.*, 2000; Ciccarelli *et al.*, 2003). Moreover, data base searches identified the KIND domain in a second distinct protein family represented by the non-receptor tyrosine phosphatase type 13 (PTP type 13, PTP-Bas, PTP-BL) (Erdmann, 2003) and an additional protein sequence deduced from a human expressed sequence tag (EST) KIAA1768. In the course of this work a new representative of the KIND family, very-KIND (VKIND) (ortholog of the human EST clone KIAA1768), was cloned and characterized.

## 4.1 | Cloning

In order to characterize the mouse ortholog of the human KIAA1768 EST clone (accession: NP\_689856) the third member of the KIND family was cloned. Due to its two KIND domains it was designated *very-KIND* (*VKIND*). An open reading frame of 5229 base pairs (with a translational stop codon) (accession: AJ580324) was deduced from sequenced cDNA fragments, in analogy to the mouse KIAA1768 clone (accession: AK046817) and the partial sequence of a mouse gene which was predicted by automated computational analysis (accession: XM\_133920). A cDNA fragment encompassing the complete coding region was generated by cloning six RT-PCR fragments, employing cerebellum RNA of an adult C57BL/6 mouse as template (→3.1.3.3, accession: AJ580324). The endonuclease single restrictions sites within the *mVKIND*'s coding sequence XhoI (base 1008), BstXI (base 2072), NheI (base 3174), XbaI (base 4044) were incorporated in the cloning process. The complete mouse *VKIND* cDNA (*mVKINDfl*) was assembled in the pSport1 cloning vector (Fig. 8) and inserted into the pcDNA3 expression vector at restriction sites HindIII (formerly blunted) and EcoRI (Tab. 1). The sequence was confirmed by DNA sequence analysis (→3.1.4.7). The vector pcDNA3 induces a high level mammalian expression from the CMV promoter. A Myc-epitope tag (amino acids 410-419 of c-Myc) was fused in frame to the amino-terminus (second codon) to allow efficient detection. The Myc tag as well as the HindIII restriction site was introduced in the forward primer 5'-mKISN-XbaI/HindIII+Myc (→App. II). The expression of the *mVKIND* directed by the CMV promoter of the pcDNA3 vector was verified by SDS-PAGE and immunoblotting, employing the Myc 9E10 antibody (→3.2.1.1, 3.2.1.2). The employed cloning strategy is presented in Fig. 8.





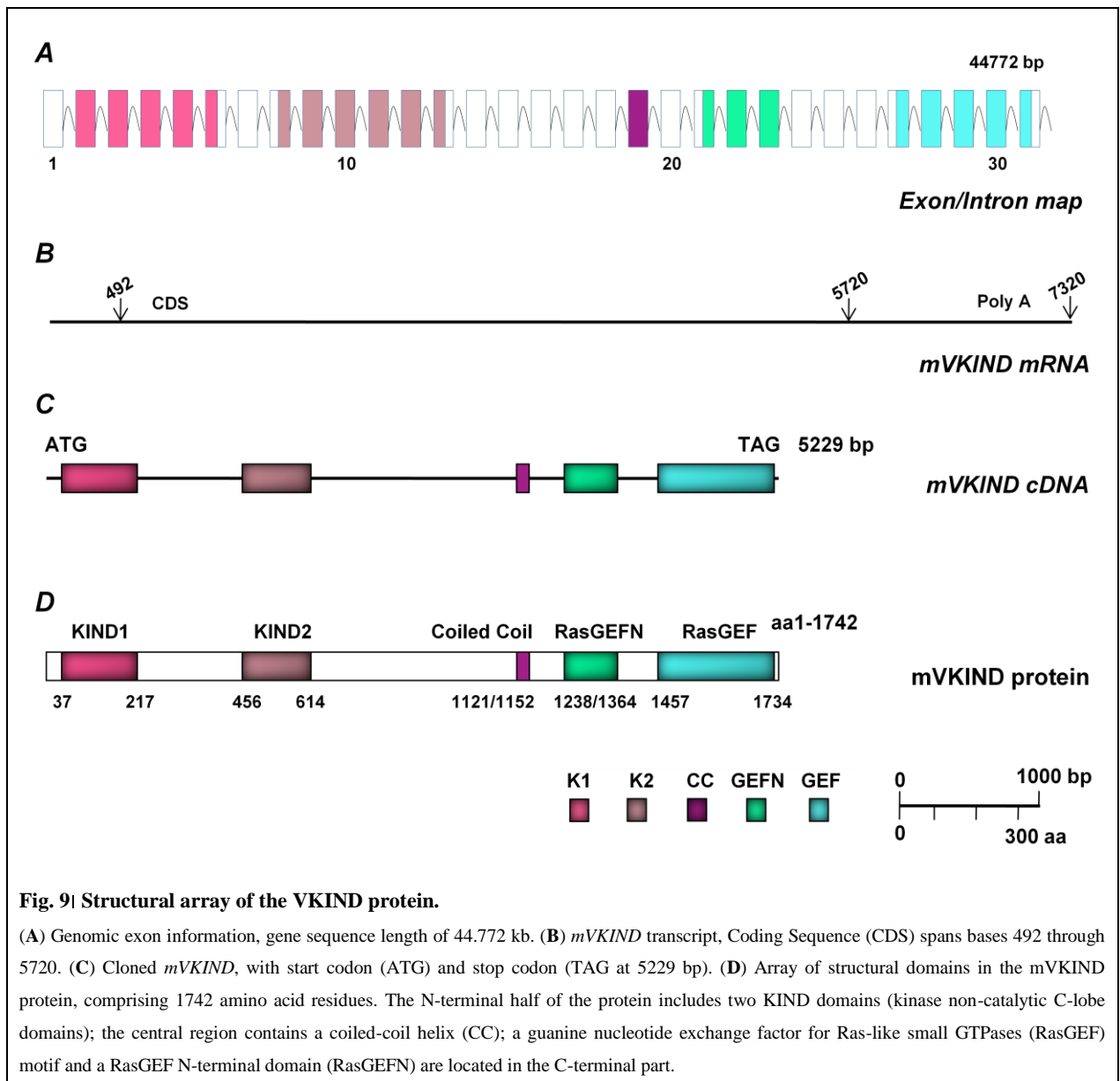
Tab.11 provides data about the DNA constructs employed in the cloning of the *mVKINDfl* cDNA, including the deduced protein sequence, the primers, and the restriction sites used to insert the cDNAs into the pcDNA3 expression vector and the pSport1 cloning vector, respectively.

**Tab. 1| Overview of the *mVKIND* cloning constructs. Detailed construct records are illustrated in Appendix II**

Construct	Coding Sequence	≡ Protein Sequence of Insert	Primer	Restriction Site 5'/3'
pcDNA3-Myc-mVKIND-aa2-337	4-1013 bp	aa2-337	5'-mKISN-XbaI/HindIII+Myc 3'-mKISN-afterXhoI	HindIII/BamHI
pcDNA3-Myc-mVKIND-aa2-709	4-2129 bp	aa2-709	5'-mVKIND-beforeXhoI 3'-mVKIND-afterBstXI+BamHI	HindIII/BamHI
pcDNA3-Myc-mVKIND-aa2-1204	4-3614 bp	aa2-1204	5'-mVKIND-beforeBstXI 3'-mVKIND-3-rev+KpnI	HindIII/XhoI (blunt)
pcDNA3-Myc-mVKIND-aa2-1349	4-4049 bp	aa2-1349	5'-vKIND-beforeNheI 3'-vKIND-afterXbaI	NheI/XbaI
pSport-Myc-mVKIND-aa2-1349	4-4049 bp	aa2-1349	—	HindIII/XbaI
pSport-mVKIND-aa1349-1742	4044-5229 bp	aa1349-1742	5'-vKIND-beforeXbaI 3'-vKIND-Ende+EcoRI	XbaI/EcoRI
pSport1-Myc-mVKINDfl	4-5229 bp	aa2-1742	—	HindIII/EcoRI
pcDNA3-Myc-mVKINDfl	4-5229 bp	aa2-1742	—	HindIII (blunt)/EcoRI

## 4.2 | VKIND structural analysis

The murine *VKIND* gene is located on the mouse chromosome 7 at location 139,746,507-139,791,278 (transcript ID: ENSMUST00000084468) and contains 31 exons. The corresponding exon-intron gene map is pictured in Fig. 9A. The mRNA comprising the mVKIND protein counts 7320 base pairs and has a C-terminal polyA site (accession: NM\_177261) (Fig. 9B). An open reading frame of 5229 base pairs translates into 1742 amino acids residues (Fig. 9C, D). Since the sequence of the novel protein mVKIND was yet not characterized, it was submitted to an analysis with the *Simple Modular Architecture Research Tool* (SMART) for identification and annotation of protein domains (Schultz *et al.*, 1998) (<http://smart.embl-heidelberg.de>). SMART revealed two non-catalytic C-lobe domains (KIND) in the amino-terminus and a guanine nucleotide exchange factor for Ras-like small GTPases (RasGEF) in the carboxy-terminus, with a structural motif attached at its N-terminal (RasGEFN). Furthermore, *COILS* (version 2.2), a program that compares sequences to a database of known parallel two-stranded coiled-coils and derives a similarity score (Lupas *et al.*, 1991) ([http://www.ch.embnet.org/software/COILS\\_form.html](http://www.ch.embnet.org/software/COILS_form.html)) calculated a coiled-coil in the central portion of mVKIND (Fig. 9D). Amino acid residues 1123 through 1151 were assigned a probability of forming coiled-coils greater than 99%, whereas residues 1121, 1122 and 1152 were assigned a probability greater than 90%.

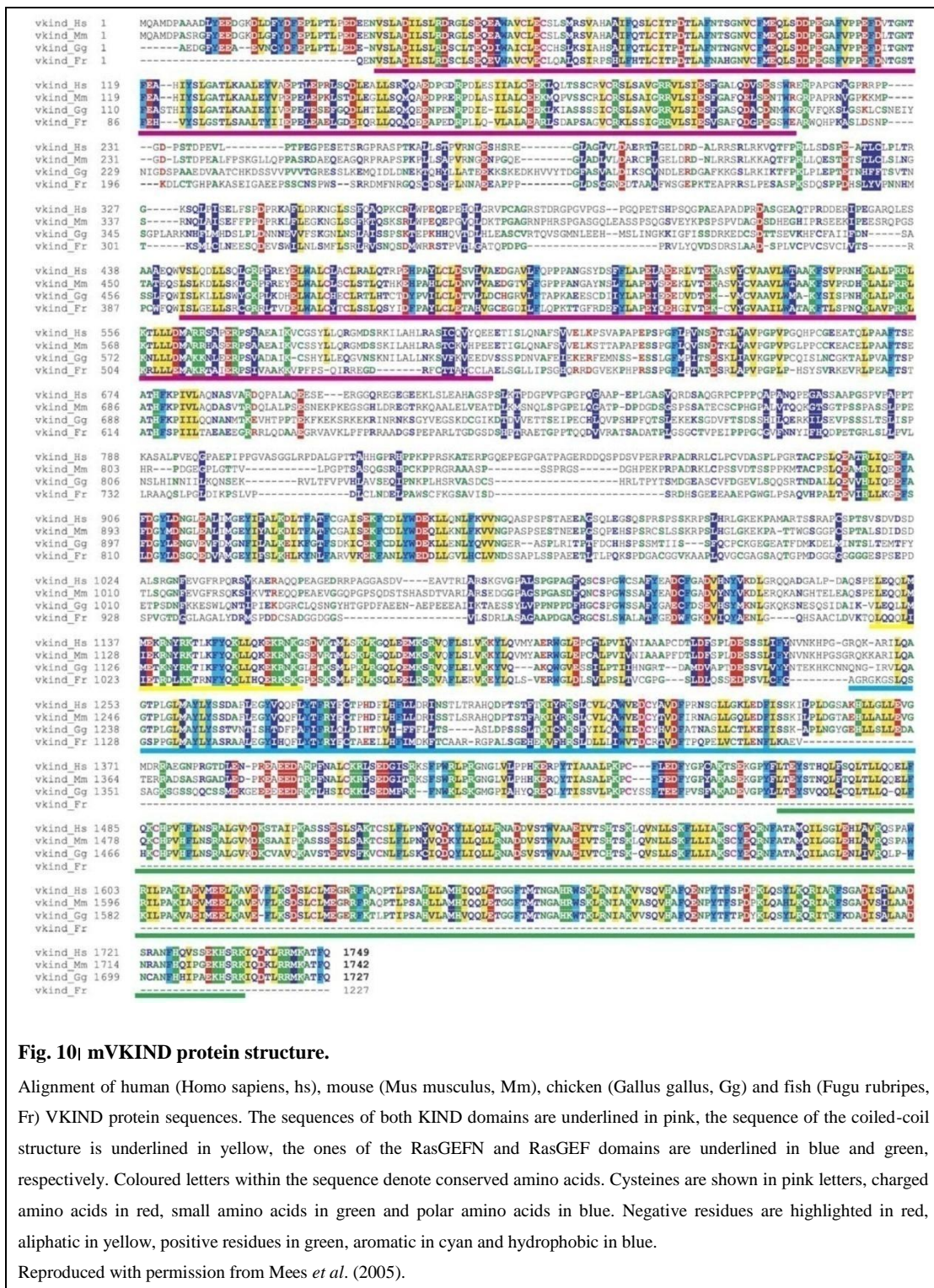


**Fig. 9 | Structural array of the VKIND protein.**

(A) Genomic exon information, gene sequence length of 44.772 kb. (B) *mVKIND* transcript, Coding Sequence (CDS) spans bases 492 through 5720. (C) Cloned *mVKIND*, with start codon (ATG) and stop codon (TAG at 5229 bp). (D) Array of structural domains in the *mVKIND* protein, comprising 1742 amino acid residues. The N-terminal half of the protein includes two KIND domains (kinase non-catalytic C-lobe domains); the central region contains a coiled-coil helix (CC); a guanine nucleotide exchange factor for Ras-like small GTPases (RasGEF) motif and a RasGEF N-terminal domain (RasGEFN) are located in the C-terminal part.

### 4.3 | Phylogenetic analysis

The mouse VKIND protein was a novel protein without established function and activity. To analyze putative orthologs, the *mVKIND* sequence was used as template for a tBLASTn homology search (Altschul *et al.*, 1997) (<http://www.ncbi.nlm.nih.gov/blast/Blast.cgi>) within the completed fully sequenced genome databases of *R. norvegicus* (RGSC build 3.4), *G. gallus* (WASHUC build 2), *F. rubripes* (Fugu build 3.0), *D. rerio* (Zv6 build 2.1), *S. purpuratus* (BCM Spur 2.1), *C. elegans* (WS build 144) and *D. melanogaster* (BGDP build 5.1). Putative orthologs were found in Vertebratae and Echinodermatae, but not in Nematodae and Insectae. Next, a BLAST search was conducted at NCBI in EST non-mouse non-human database implying the mouse sequence as a query. The search yielded EST evidence in *X. laevis*, *X. tropicalis*, *O. mykiss*, *D. rerio*, *P. marinus*, *P. lividus*, *G. gallus*, *T. guttata*, *R. norvegicus*, *B. taurus* and *M. fascicularis*.



**Fig. 10| mVKIND protein structure.**

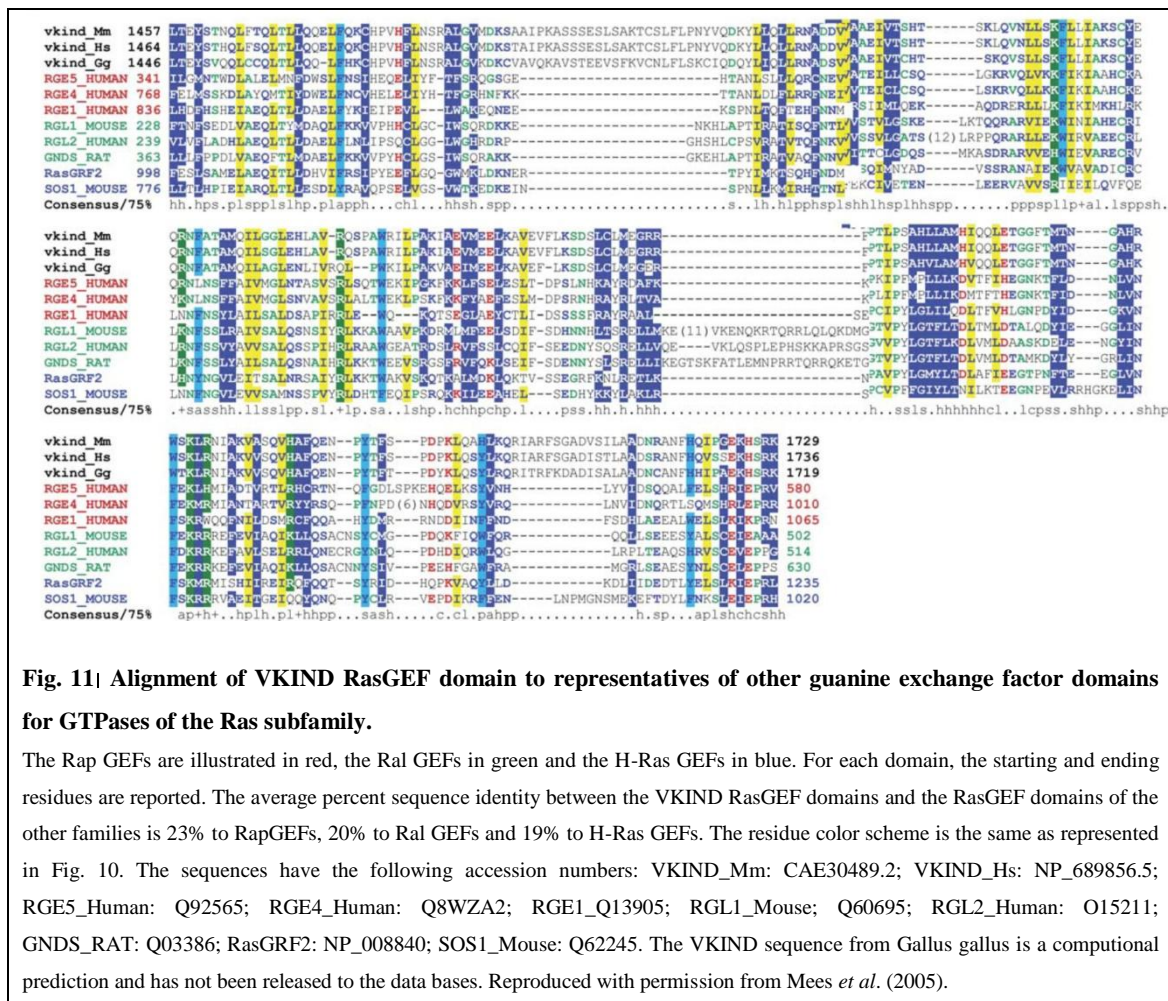
Alignment of human (Homo sapiens, hs), mouse (Mus musculus, Mm), chicken (Gallus gallus, Gg) and fish (Fugu rubripes, Fr) VKIND protein sequences. The sequences of both KIND domains are underlined in pink, the sequence of the coiled-coil structure is underlined in yellow, the ones of the RasGEFN and RasGEF domains are underlined in blue and green, respectively. Coloured letters within the sequence denote conserved amino acids. Cysteines are shown in pink letters, charged amino acids in red, small amino acids in green and polar amino acids in blue. Negative residues are highlighted in red, aliphatic in yellow, positive residues in green, aromatic in cyan and hydrophobic in blue.

Reproduced with permission from Mees *et al.* (2005).

A sequence alignment of the human, mouse, chicken and fugu protein showed a high conservation within the predicted two KIND domains, the coiled-coil region, the RasGEFN and the RasGEF domains (Fig. 10). The alignment also reveals two clusters of high conservation in-between the second KIND and the RasGEFN domains of yet unknown functional and structural identities (aa-880-962 and aa1071-1115).

### 4.4 | The VKIND RasGEF domain

The Ras superfamily of small GTPases includes over 150 proteins (Colicelli, 2004). The five major subfamilies (Ras, Rho, Rab, Ran and Arf) are involved in cancer, cell cycle, regulation, differentiation, vesicle trafficking, nuclear transport, control of cell morphology and chemotaxis. While Ras superfamily proteins are structurally highly conserved, the GEF proteins which mediate the GDP-GTP exchange of small GTPases are distinct for each subfamily. The catalytic domain of exchange factors specific for Ras subfamily GTPases is homologous to the yeast RasGEF CDC25 (Broek *et al.*, 1987). To investigate the specificity of the novel RasGEF domain, its sequence was aligned to representatives of other GEF domains for Ras subfamily GTPases, such as RapGEFs, RalGEFs and the H-RasGEFs. The alignment demonstrates



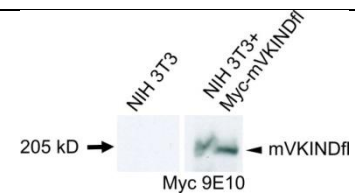
that the VKIND RasGEF domain is a CDC25 like domain closest related to the RasGEF domains of exchange factors specific for Rap GTPases, such as the Epac, MR-GEF and RA-GEF (Fig. 11). The average sequence identity between the Rap specific RasGEF domains and the VKIND catalytic domain is 23%. Furthermore, the alignment revealed that the VKIND enzymatic domain has a unique structure. It features two insertions, first one of 24 amino acids in the N-terminal end of the domain (between helices  $\alpha$ A and  $\alpha$ B of the SOS1 RasGEF module) and the second one of 11 amino acids in the C-terminal part (between helices  $\alpha$ J and  $\alpha$ K of the Sos1 RasGEF module) (Boriack-Sjodin *et al.*, 1998).

#### 4.5 | The murine VKIND protein

The murine VKIND protein consists of 1742 amino acids (Fig. 9D) with a calculated size of 191,204 Dalton (Da). To confirm accurate expression of the cloned Myc-epitope tagged full length mVKIND, the pcDNA3-Myc-mVKINDfl construct was transiently expressed in NIH 3T3 mouse fibroblasts for 48 h (→3.3.2.1). Total cell lysates were examined by SDS-polyacrylamide gel electrophoresis and subsequent electroblotting (→3.2.1.1). Next, an immunodetection using a c-Myc antibody 9E10 (→3.2.1.2, 2.3.1) was performed. The transiently expressed mVKINDfl protein migrates with an apparent molecular weight of 205 kD (Fig. 12) which is in good agreement with the predicted size.

**Fig. 12| *In vivo* expression of the mVKIND protein.**

NIH 3T3 cells were lipofected with pcDNA3-Myc-VKINDfl expression plasmid. Total protein lysates were analysed by immunoblot using anti-Myc antibodies. mVKINDfl migrates with an apparent molecular weight of approximately 205 kD. Abbreviations: kD, kilo Dalton; Myc, Myc tag; mVKINDfl, murine very-KIND full length.



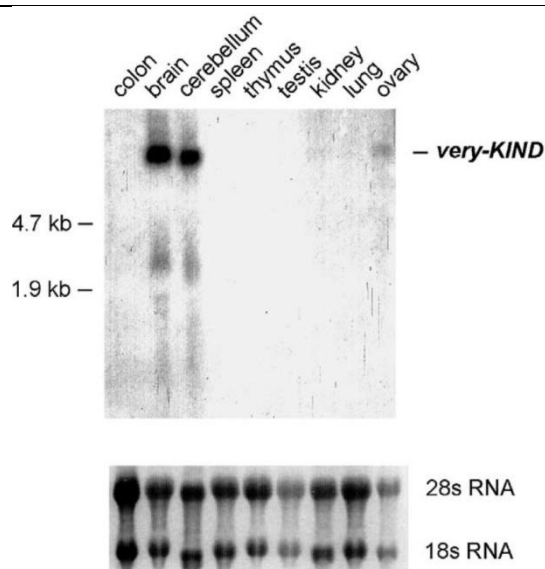
#### 4.6 | Expression analysis

The versatile complexity of Ras-subfamily functions is associated with a multitude of activating stimuli and the spatial and temporal segregation of the signaling pathways (Mitin *et al.*, 2005; Rocks *et al.*, 2006). To investigate the spatial expression of the VKIND gene in mammals a Northern blot analysis was performed. The appearance of *mVKIND* mRNA was investigated in various tissues of an adult C57BL/6 mouse (→2.6.3), such as colon, brain, cerebellum, spleen, thymus, testis, kidney, lung and ovary (Fig. 13). An ( $\alpha^{32}\text{P}$ )dCTP labeled 1 kb *mVKIND* cDNA probe (encoding amino acids 2-335) was applied (→3.1.1.2).

The northern hybridization revealed a highly restricted gene expression pattern at which strong expression was only found in the brain, along with a very faint staining in the RNA isolated from ovary. The mouse VKIND mRNA migrates on the formaldehyde agarose gel much slower than the ribosomal RNA 28s subunit (4.7 kb). Its estimated size is 7-8 kb which is concordant with the published data (accession: NM\_177261) (Fig. 9B).

**Fig. 13| *mVKIND* mRNA expression.**

The expression of the *mVKIND* gene in different tissues of an adult murine was analyzed by Northern hybridization. Total RNA preparations of the indicated tissues were separated on a formaldehyde-agarose gel and blotted onto a Duralon UV membrane. The *mVKIND* mRNA was detected with an ( $\alpha^{32}\text{P}$ )dCTP labelled murine VKIND cDNA fragment encoding amino acids 2-335. The size of the ribosomal RNAs 4.7 and 1.9 kb (4.7, 1.9 kb) are indicated. The migration of the VKIND mRNA is marked (*very-KIND*). As a loading control the ethidium bromide stained 28 and 18 s ribosomal RNAs are shown. Reproduced with permission from Mees *et al.* (2005).



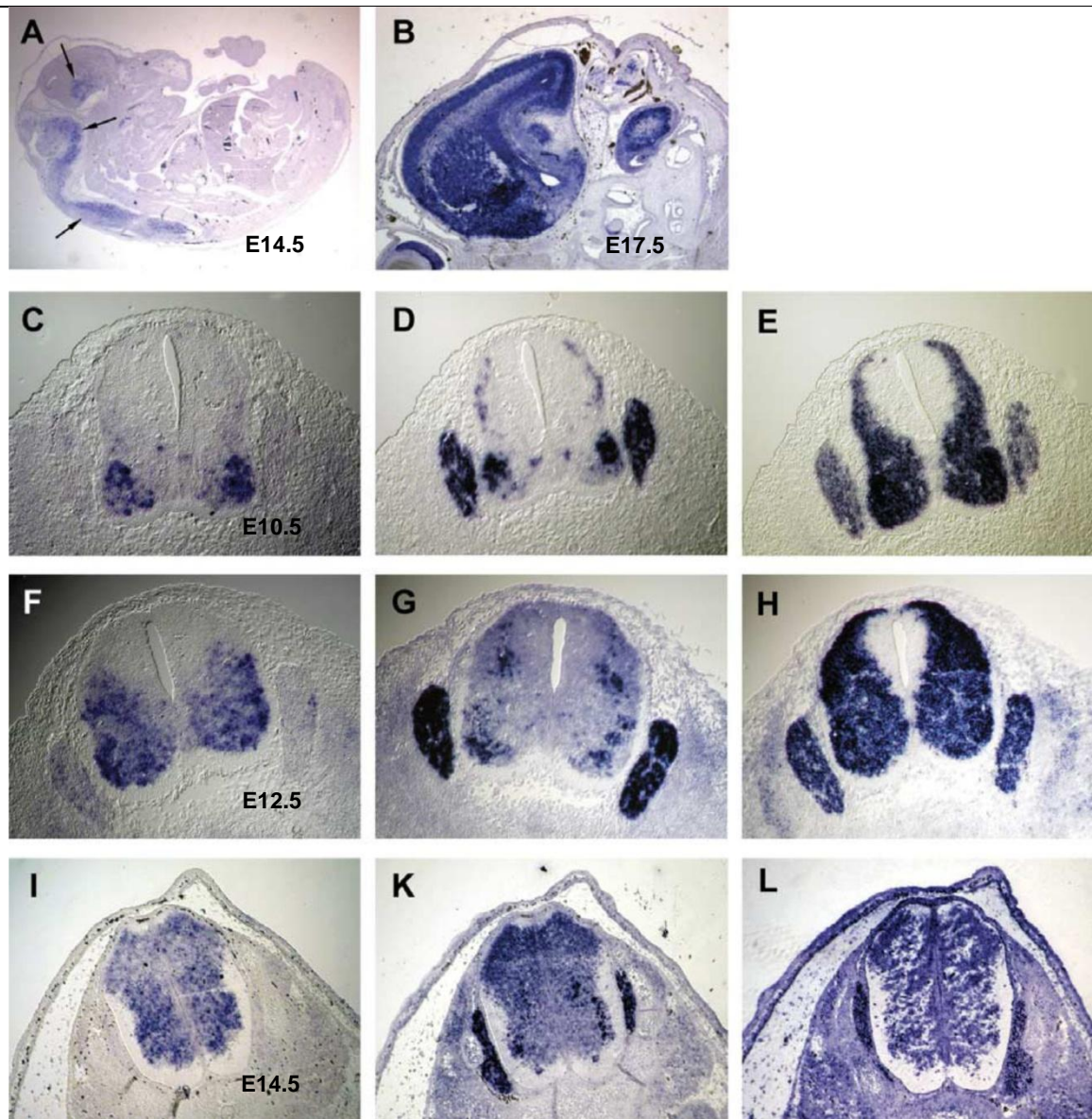
#### 4.7 | Developmental time course of *VKIND* expression in mouse embryo

Gene expression is being temporally and spatially regulated during mouse development (Zhao *et al.*, 2002). To study the developmental time course of *mVKIND* expression, sagittal and transverse sections of perfused CD1 mouse embryo tissue were subjected to RNA *in situ* hybridizations. Paraffin sections were hybridized with a digoxigenin-labeled antisense riboprobes for *mVKIND* (codon 2-126, accession: AJ580324.2), mouse *islet1* (codon 129-349, accession: AJ32765.1) and mouse *doublecortin* (codon 124-360, accession: NM\_010025.2) generated from plasmid templates as described previously (Leimeister *et al.*, 1998). cDNA fragments were amplified by RT-PCR (→3.1.3.3) from cerebellum total RNA of a C56BL/6 mouse (*VKIND*) and total RNA of a day 14.5 mouse embryo (*islet1*, *doublecortin*). Next, they were inserted into the pcDNA3 vector using restriction sites BamHI/XbaI (for *mVKIND*), and BamHI/EcoRI (for *islet1* and *doublecortin*) (Tab. 2). The developing brain and the neural tube are found to be strongly stained. At E14.5 a high *VKIND* expression is detected in the mid- and hindbrain, whereas the expression in the forebrain is only weak. During development a shift of the main expression towards the telencephalon is observed at E17.5 (Fig. 14A, B). The neural tube exhibits *VKIND* expression in the ventro-lateral part at E10.5 (Fig. 14C) as well as in the dorsal part during later development (Fig. 14C, F, I). At E10.5 the expression pattern in the neural tube partially coincides with *islet1*, a post mitotic motoneurons marker within the neural tube (Fig. 14D) (Appel *et al.*, 1995), and *doublecortin*, an early post mitotic migrating neurons marker (Fig. 14E) (Hannan *et al.*, 1999). In contrast, *VKIND* is not detectable in the developing DRG (dorsal root ganglia) cells at E10.5 (Fig. 14C), while *islet1* demonstrates a strong staining intensity (Fig. 14D). Still, at E12.5 few cells in the DRG stain positive for *VKIND* (Fig. 14F). At E14.5 the entire neural tube except for the marginal layer shows strong staining, but only in a speckled pattern (Fig. 14I).

**Tab. 2| Overview of the *in situ* plasmid templates. Detailed construct records are illustrated in Appendix II**

Construct	Coding Sequence	≡ Protein Sequence of Insert	Primer	Restriction Site 5'/3'
pcDNA3-Doublecortin	370-1082 bp	aa124-360	BamHI-m-Doublecortin-CT-5' m-Doublecortin-CT-EcoRI-3'	BamHI/EcoRI
pcDNA3-Islet1	385-1050 bp	aa129-350	BamHI-m-Islet1-CT-5' m-Islet1-CT-EcoRI-3'	BamHI/EcoRI

In the developing eye at E17.5 the expression of *VKIND* mRNA (Fig. 15A) overlaps widely with the expression of *islet1*, a vertebrate ganglion cell layer marker (Fig. 15B), and *doublecortin* (Fig. 15C). At earlier stages of development and in post natal mice no staining for *VKIND* mRNA could be observed.

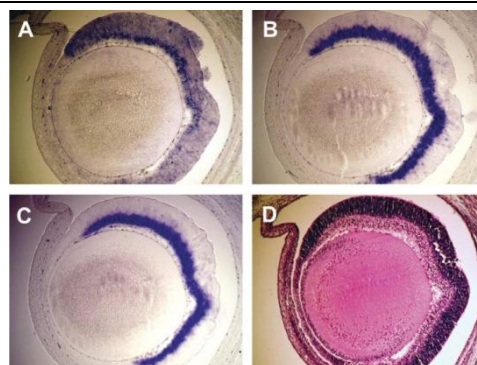


**Fig. 14| Expression pattern of *VKIND* in the mouse embryo.**

(A) At E14.5 *VKIND* is detected mainly in the mid- and hind-brain and in the neural tube (marked by arrows). (B) At E17.5 the expression in the neural tube is maintained. Moreover, additional high expression in the telencephalon is observed. (C) In the neural tube *VKIND* expression is exhibited by E10.5 at the ventral edge and (F, E12.5; I, E14.5) spread out dorsally at later stages. Comparative studies show the expression of the neuronal markers (D, G, K) *islet1* and (E, H, L) *doublecortin*. Reproduced with permission from Mees *et al.* (2005).

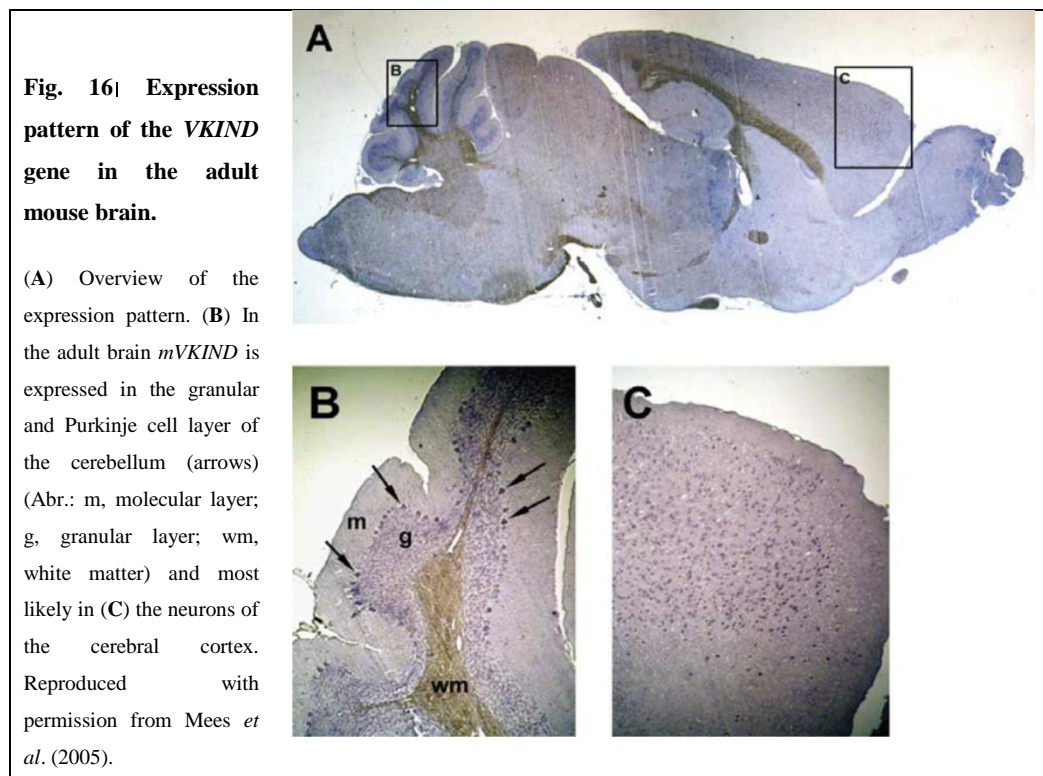
**Fig. 15| Expression of the *VKIND* gene in the mouse embryonic eye.**

At E17.5 in the predominantly (A) *VKIND* stains the future neuronal cell layers similar to (B) *islet1* and (C) *doublecortin*. Layers are defined according to (D) Haematoxylin–Eosin (HE) staining. Reproduced with permission from Mees *et al.* (2005).



#### 4.8 | *VKIND* gene expression in postnatal mouse brain

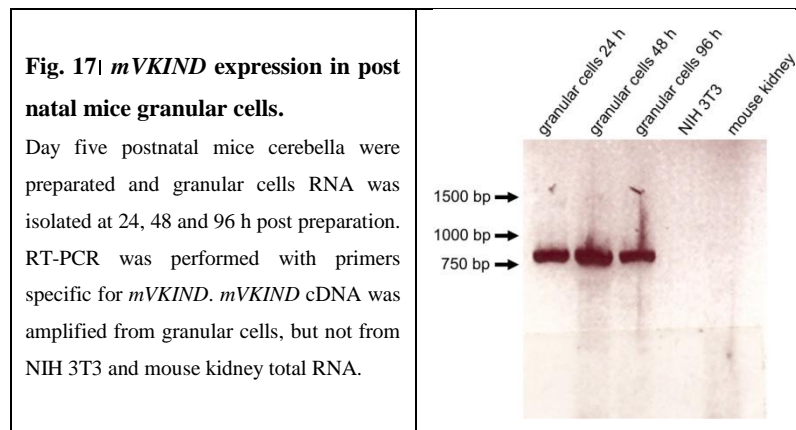
Since the developing brain presents a strong staining for *mVKIND* mRNA, *in situ* hybridizations for *mVKIND* were performed in adult CD1 mouse perfused brain tissue. Paraffin sections were hybridized with a digoxigenin-labeled antisense riboprobe for *mVKIND* (codon 2-126, accession: AJ580324.2) generated from a plasmid template as described previously (Leimeister *et al.*, 1998). For the construction of the plasmid template, a cDNA fragment (codon 2-126, accession: AJ580324.2) was amplified by RT-PCR (→3.1.3.3) from cerebellum RNA of a C56BL/6 mouse and inserted into the pcDNA3 vector using restriction sites BamHI and XbaI. The following primers were used: 5'-mVK-in situ and 3'-mVK-in situ (→2.4). In the adult mouse brain *VKIND* expression is most prominent in the cerebellum, however exclusively restricted to the granular and Purkinje cell layer (Fig. 16A, B). The branching white matter of the cerebellum and the molecular layer display no staining. Large cells throughout most of the cerebral cortex are stained positive for *mVKIND* mRNA in a punctuate pattern (Fig. 16C).



Pursuing an establishment of primary murine cerebellar cell culture and a prospect of further *VKIND* study, seven five days old C57BL/6 mice were sacrificed and cerebellar tissue was prepared. Granular cells were cultured in complete medium in 60 mm poly-lysine coated dishes at 37°C with 5% CO<sub>2</sub> (incubator). Glial cells were cytostatically suppressed with Ara-c/HCL (→3.3.1.2). RNA of 5x 10<sup>6</sup> granule cells was isolated at 24, 48 and 96 h post preparation. RT-PCR was performed employing 0.1 µg RNA isolated from granular, NIH 3T3 and mouse kidney cells as single-stranded RNA template (→3.1.2.3). The employed *mVKIND* gene specific primers were: 5'-mVK and 3'-mVK (→2.4). Primers were amplifying 880 base pairs *mVKIND* gene segment. Generated cDNA fragments were examined by agarose gel electrophoresis (→3.1.1.1).



cDNA fragments of a precise length were synthesized from granular cells RNA (at 24, 48 and 96 h). Furthermore, no cDNA was transcribed from NIH 3T3 and mouse kidney cells RNA (Fig. 17), showing that the *mVKIND* gene is specially expressed in the granular cells.



## 4.9 | Transient expression analysis

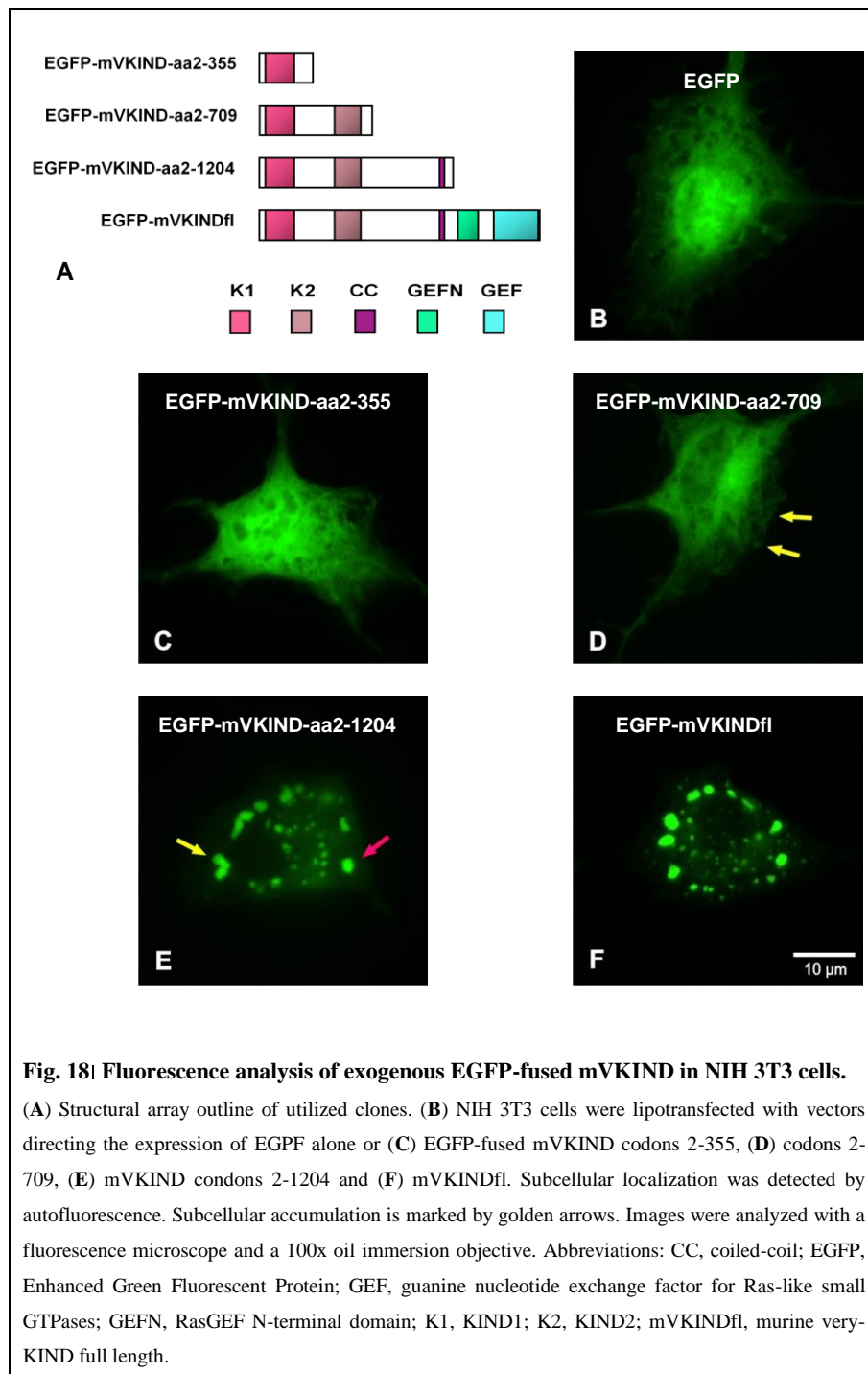
The VKIND protein harbors five structural domains with an unresolved function and activity. To monitor the protein expression, putative interactions as well as the cellular localization of the novel KIND family member in eukaryotic cells, mouse NIH 3T3 fibroblast cells were transfected with mammalian expression vectors carrying the *mVKIND* cDNA.

### 4.9.1 | EGFP fusion protein expression

To explore the subcellular distribution of the novel RasGEF protein and gain insights of its function, high level constitutive expression plasmids were constructed, fusing distinct truncated mVKIND mutants to the enhanced green fluorescent protein (EGFP). In this manner, a direct detection of fusion proteins by EGFP fluorescence is possible. Tab. 3 provides information about the EGFP-tagged constructs: the length of the incorporated protein sequence, the primers, and the restriction sites used to insert the cDNAs into the pEGFP-C1 expression vector. NIH 3T3 cells were transiently transfected with pEGFP-C1-mVKIND-aa2-355, pEGFP-C1-mVKIND-aa2-709, pEGFP-C1-mVKIND-aa2-1204 and pEGFP-C1-mVKINDfl (→3.3.2.1, 1 µg DNA each). 24 h post-transfection cells were fixed and subjected to visual fluorescent microscopy analysis (→3.3.3). All constructs were expressed at high amounts. Fig. 18A shows a schematic outline of the utilized clones. The cellular distribution of the negative control (non fused EGFP) is illustrated in Fig. 18B. EGFP-mVKIND-aa2-355 (Fig. 18C) is evenly spread in the cell cytoplasm and in the nucleus.

**Tab. 3| Overview of the EGFP-tagged constructs. Detailed construct records are illustrated in Appendix II**

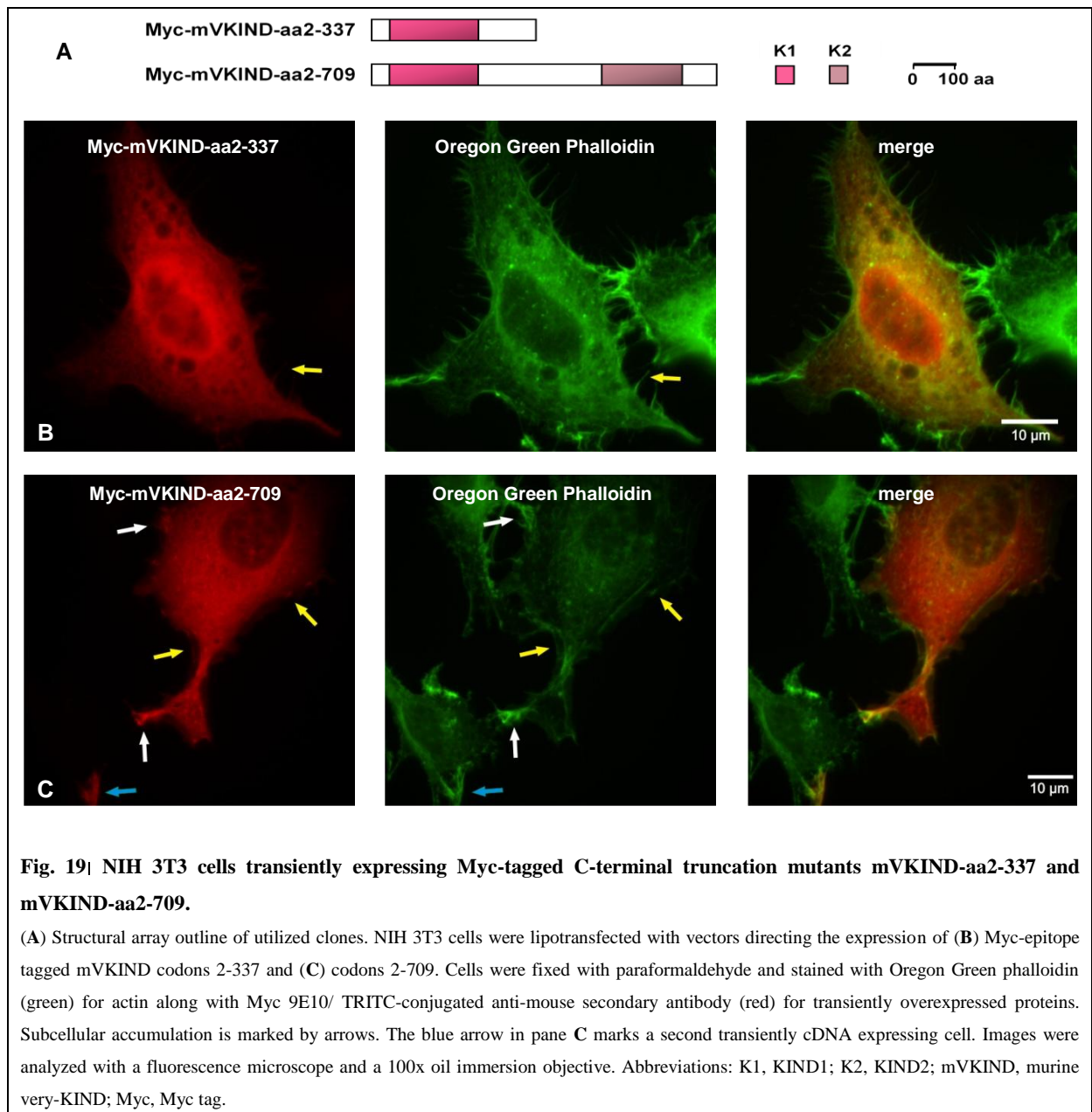
Construct	Coding Sequence	≡ Protein Sequence of Insert	Primer	Restriction Site 5'/3'
pEGFP-C1-mVKIND-aa2-355	4-1066 bp	aa2-355	5'-fr.I+BglII 3'-fr.I-afterXhoI+EcoRI	BglII/EcoRI
pEGFP-C1-mVKIND-aa2-709	4-2129 bp	aa2-709	5'-mVKIND-beforeXhoI 3'-mVKIND-afterBstXI+BamHI	XhoI/BamHI
pEGFP-C1-mVKIND-aa2-1204	4-1364 bp	aa2-1204	—	BamHI/XbaI
pEGFP-C1-mVKINDfl	4-1742 bp	aa2-1742	—	SacI/KpnI



EGFP-mVKIND-aa2-709 displays additionally a very slight perinuclear and lamellipodial accumulation (Fig. 18D). Interestingly EGFP-mVKIND-aa2-1204 induced the development of large circular structures (Fig. 18E). The incorporation of expressed protein into these entities is observed to be forceful. The fraction of expressed protein which is excluded from those structures and remains in the cytosol is negligible. No protein is detectable at the cell periphery. EGFP-mVKINDfl expression pattern resembles very much the one of EGFP-mVKIND-aa2-1204 (Fig. 18F).

#### 4.9.2 | Transient expression of C-terminally truncated mVKIND mutants coding for KIND1 domain and KIND1/KIND2 domains

The KIND module has been identified as an interaction domain (Ciccarelli *et al.*, 2003; Huang *et al.*, 2007). To study the localization of the KIND1 and KIND2 domains and to confirm the expression patterns of the EGFP-fused clones (Fig. 18C and D), coding for the KIND1 domain and KIND1/KIND2 domains, respectively, their Myc-tagged equivalents (Tab. 1) were transfected into NIH 3T3 cells (→3.3.2.1, 1 µg DNA each).



24 h post-transfection cells were fixed and stained with a primary antibody directed against the Myc tag epitope (9E10), located at the N-terminus of the fusion proteins, followed by a TRITC-conjugated anti-mouse secondary antibody to expose the exogenous proteins. F-actin was visualized with 2',7'-difluorofluorescein (Oregon Green 488 dye)-conjugated phalloidin and subjected to fluorescent analysis

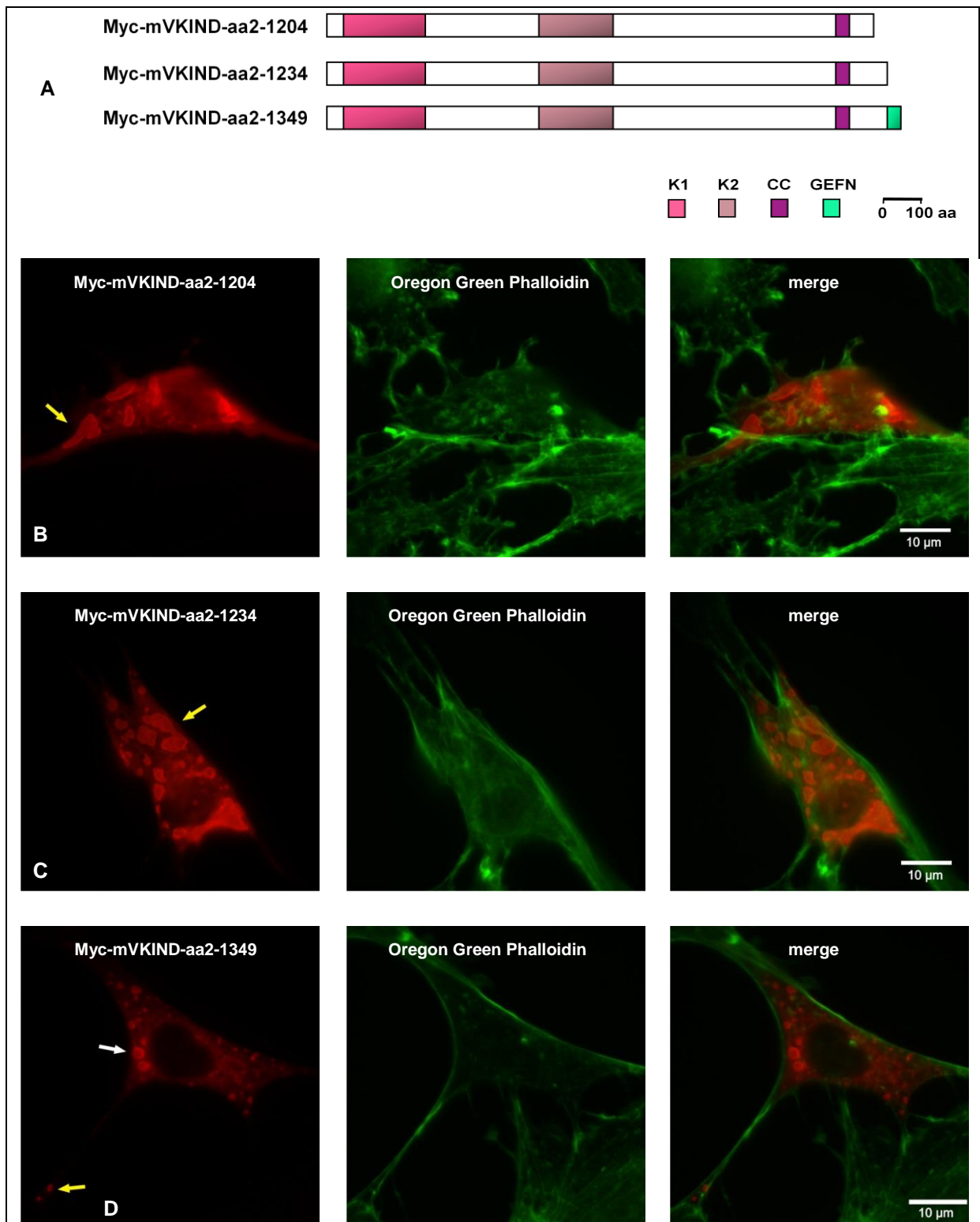
(→3.3.3). Both constructs were expressed at high amounts. Fig. 19A pictures a schematic outline of the utilized clones. Myc-mVKIND-aa2-337, harboring the KIND1 domain, is detected in the cytosol, faintly accumulated in the perinuclear region (Fig. 19B). Myc-mVKIND-aa2-337 is also spotted in actin based cell surface protrusions (golden arrow). Myc-mVKIND-aa2-709, coding for both KIND domains, is observed mostly in the cell cytoplasm and is also enriched along actin bundles at the cell edges (Fig. 19C, golden arrows). Increased staining is found at cell-cell contact interfaces (red arrow). These findings are in good agreement with the data provided by the distribution analysis of the counterpart EGFP-fusion proteins (→ 4.8.1).

#### 4.9.3 | Transient expression of C-terminally truncated mVKIND mutants coding for Myc-mVKIND-aa2-1204, Myc-mVKIND-aa2-1234 and Myc-mVKIND-aa2-1349

To investigate putative targeting properties of the protein region adjacent to the KIND1 and KIND2 domains of the mouse VKIND protein, the Myc-tagged mVKIND-aa2-1204, mVKIND-aa2-1234 and mVKIND-aa2-1349 C-terminally truncated mutants (Tab. 1 and 4) were expressed into NIH 3T3 cells (→3.3.2.1). 24 h post-transfection cells were fixed and treated with a primary antibody directed against the Myc tag epitope (9E10), located at the N-term of the fusion proteins, followed by a TRITC-conjugated anti-mouse secondary antibody to visualize the exogenous proteins. F-actin was stained with 2',7'-difluorofluorescein (Oregon Green 488 dye)-conjugated phalloidin and subjected to fluorescent analysis (→3.3.3). Fig. 20A pictures a schematic outline of the transfected clones. Both Myc-tagged mVKIND-aa2-1204 and mVKIND-aa2-1349 mutants were expressed at high amounts, whereas the mVKIND-aa2-1234 expression was observed only in few cells. Myc-mVKIND-aa2-1204 is harboring both KIND domains, the adjacent region and the coiled-coil and its expression pattern (Fig. 20B) is in agreement with the expression pattern of its EGFP-tagged equivalent (Fig. 18E). This truncated mutant formed structures in the cytosol, with estimated width of up to 7.7  $\mu\text{m}$  and length of up to 8.8  $\mu\text{m}$  (golden arrow). Myc-mVKIND-aa2-1234 was observed to be difficult to express, nevertheless it also formed closed structures of estimated dimension of up to 10  $\mu\text{m}$  width and 5.5  $\mu\text{m}$  length (golden arrow) (Fig. 20C). Myc-mVKIND-aa2-1349, encompassing both KIND domains, the coiled-coil and a portion of the GEFN motif, exhibited a high expression and is viewed in roundish entities in the cytosol, with an estimated diameter of 3  $\mu\text{m}$  (Fig. 20D, red arrow). The golden arrow points the distribution of the mouse VKIND mutant in the NIH 3T3 cell extension. All three truncation mutants are excluded from the nucleus and the cell membrane.

**Tab. 4| Overview of the pcDNA3-mVKIND-aa2-1234 construct. Detailed construct records are illustrated in Appendix II**

Construct	Coding Sequence	≡ Protein sequence of Insert	Primer	Restriction Site 5'/3'
pcDNA3-mVKIND-aa2-1234	4-3702 bp	aa2-1234	5'-mKISNXbaI/HindIII-Myc 3'-ab3682bp+EcoRI	HindIII/EcoRI



**Fig. 20** NIH 3T3 cells transiently expressing Myc-tagged C-terminal truncation mutants mVKIND-aa2-1204, mVKIND-aa2-1234 and mVKIND-aa2-1349.

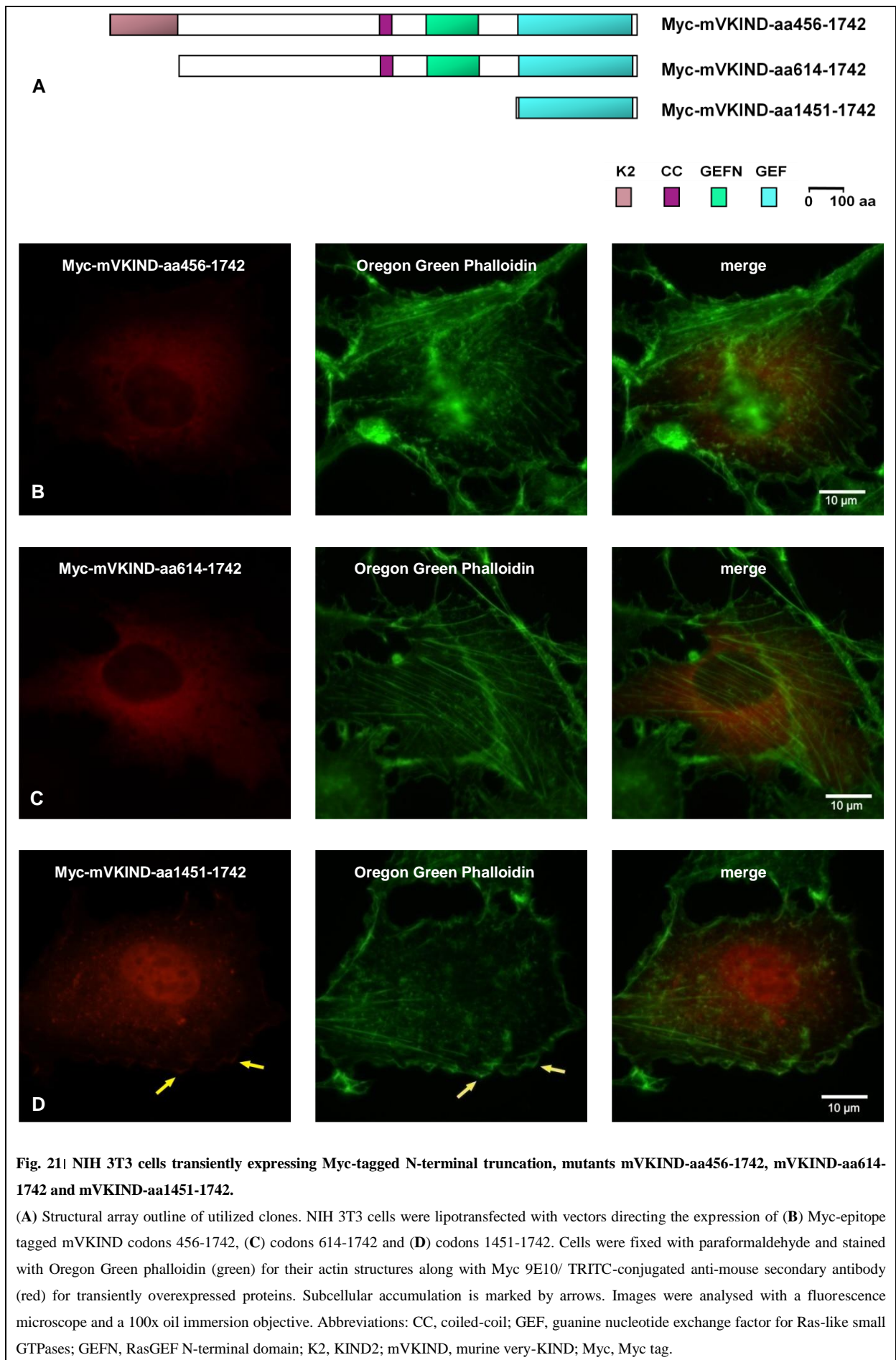
(A) Structural array outline of utilized clones. NIH 3T3 cells were lipotransfected with vectors directing the expression of (B) Myc-epitope tagged mVKIND codons 2-1204, (C) codons 2-1234 and (D) codons 2-1349. Cells were fixed with paraformaldehyde and stained with Oregon Green phalloidin (green) for actin structures along with Myc 9E10/ TRITC-conjugated anti-mouse secondary antibody (red) for transiently overexpressed proteins. Subcellular accumulation is marked by arrows. Images were analysed with a fluorescence microscope and a 100x oil immersion objective. Abbreviations: CC, coiled-coil; GEFN, RasGEF N-terminal domain; K1, KIND1; K2, KIND2; mVKIND, murine very-KIND; Myc, Myc tag.

#### 4.9.4 | Transient expression of N-terminally truncated mVKIND mutants coding for Myc- mVKIND-aa456- 1742, Myc-mVKIND-614-1742 and Myc-mVKIND-aa2-1451-1742

To further explore the function of the KIND1 and the KIND2 domains of the mVKIND protein, N-terminal truncation mutants were constructed, depleted of either one or both KIND domains (Myc-mVKIND-aa456-1742 and Myc-mVKIND-aa614-1742, respectively). To analyze the distribution of the guanine nucleotide exchange factor domain, an N-terminal truncation mutant was created, encompassing the cDNA of the RasGEF module only (Myc- mVKIND-aa2-1451-1742) (Tab. 5). NIH 3T3 cells were transfected with these constructs (→3.3.2.1) and fixed 24 h later. An immunostain was performed using a primary antibody directed against the Myc tag epitope (9E10), located at the N-term of the fusion proteins and a TRITC-conjugated anti-mouse secondary antibody to identify exogenous proteins. F-actin was stained with 2',7'-difluorofluorescein (Oregon Green 488 dye)-conjugated phalloidin and fluorescent images were taken (→3.3.3). Fig. 21A pictures a schematic outline of the transfected clones. Both Myc-tagged mVKIND-aa456-1742 and mVKIND-aa614-1742 mutants were observed only in few cells and were expressed at low amounts, whereas the Myc-mVKIND-aa1451-1742 mutant displayed high expression. Myc-mVKIND-aa456-1742 harbors the KIND2 domain, its adjacent region as well as the RasGEFN and RasGEF domains. It is expressed predominantly and evenly in the cell cytoplasm (Fig. 21B), alike the Myc-mVKIND-aa614-1742 mutant which is depleted of the KIND2 domain (Fig. 21C). Myc-mVKIND-aa1451-1742 is detected throughout the cytosol and in the nucleus (Fig. 21D). It is also detected in bundles of actin in the cell membrane (golden arrows).

**Tab. 5| Overview of the N-terminally truncated constructs coding for Myc-mVKIND-aa456-1742, Myc-mVKIND-614-1742 and Myc-mVKINDaa-1451-1742. Detailed construct records are illustrated in Appendix II**

Construct	Coding Sequence	≡ Protein Sequence of Insert	Primer	Restriction Site 5'/3'
pcDNA3-Myc-mVKIND-aa456-1742	1366-5229 bp	aa456-1742	5' KpnI+Myc-ab1366 3'-vKIND-Ende+EcoRI	KpnI/EcoRI
pcDNA3-Myc-mVKIND-aa614-1742	1840-5229 bp	aa614-1742	5' KpnI+Myc-ab1840 3'-vKIND-Ende+EcoRI	KpnI/EcoRI
pcDNA3-Myc-mVKIND-aa1451-1742	4351-5229 bp	aa1451-1742	5'-Ras-GEF-BamHI+Myc 3'-Ras-GEF-EcoRI	BamHI/EcoRI



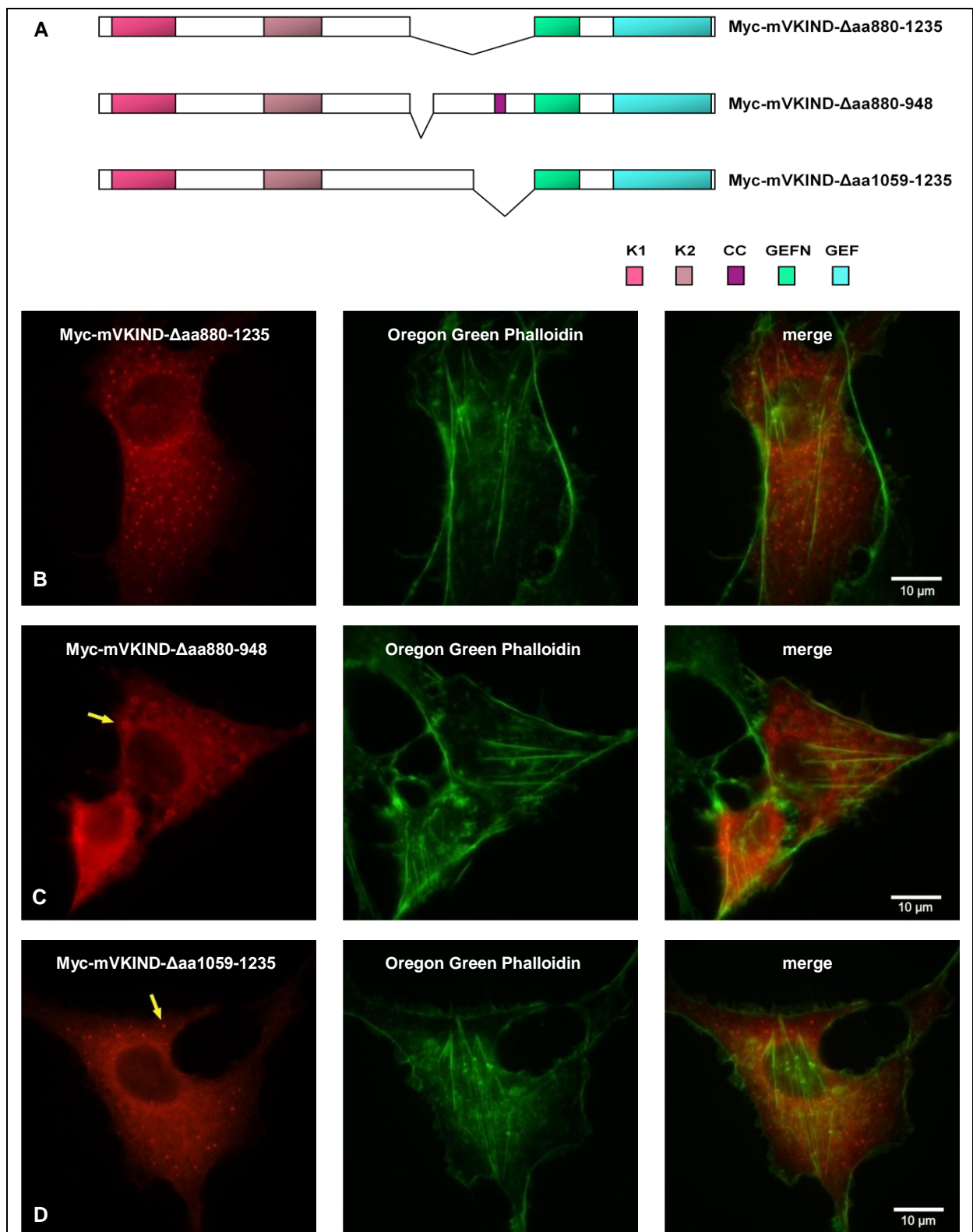
#### 4.9.5 | Transient expression mVKIND deletion mutants coding for Myc-mVKIND- $\Delta$ aa880-1235, Myc-mVKIND- $\Delta$ aa880-948 and Myc-mVKIND- $\Delta$ aa1059-1235

The alignment of the VKIND protein (Fig. 10) revealed two regions which were highly conserved among the species human, mouse, chicken and fugu. Region 1 spans amino acid residues 880 through 948, while region 2 spans amino acid residues 1059 through 1235, also harboring the coiled-coil motif (aa1121-1152). Since coiled-coil helices are known as mediators of protein-protein interactions and as structures responsible for protein stability and specificity (Singh & Hitchcock-DeGregori, 2006), the potential function of Region 1 and 2 were addressed here. Constructs coding for mVKIND depleted of Region 1 and Region 2, respectively were produced (Tab 6,  $\rightarrow$ 3.1.4.4) and transfected into NIH 3T3 cells ( $\rightarrow$ 3.3.2.1, 1  $\mu$ g DNA each). Cells were fixed 24 h later and immunostained using a primary antibody directed against the Myc tag epitope (9E10), located at the N-terminal of the fusion proteins and a TRITC-conjugated anti-mouse secondary antibody to detect the exogenous proteins. F-actin was stained with 2',7'-difluorofluorescein (Oregon Green 488 dye)-conjugated phalloidin and cells were fluorescently scanned ( $\rightarrow$ 3.3.3). Fig. 22A pictures a schematic outline of the transfected clones. The mutants were successfully expressed at high amounts in only few cells. Myc-mVKIND- $\Delta$ aa880-1235 which is depleted of both Region 1 and Region 2 is observed in the cytosol, forming structures of estimated diameter of 0.4  $\mu$ m in a speckled manner (Fig. 22B). Moreover, mVKIND- $\Delta$ aa880-1235 is not located in the nucleus and in the cell membrane. Its expression pattern matches the expression pattern of Myc-mVKIND- $\Delta$ aa1059-1235 (depleted of Region 2, including the coiled-coil) (Fig. 22D). Myc-mVKIND- $\Delta$ aa880-948 (harboring the Region 2 and the coiled-coil) on the other hand formed globular structures of estimated diameter of up to 1  $\mu$ m (Fig. 22C, golden arrow), while it is excluded from the nucleus and the plasma membrane. In addition the observed structures are not associated to actin filaments.

**Tab. 6| Overview of the Myc-tagged deletion mutants mVKIND- $\Delta$ aa880-1235, Myc-KIND- $\Delta$ aa880-948, Myc-mVKIND- $\Delta$ aa1059-1235. Detailed construct records are provided in Appendix II**

Construct	Depleted Coding Sequence	$\equiv$ Depleted Protein Sequence of Insert	Primer
pTopo-Myc-mVKIND- $\Delta$ aa880-1235	2639-3705 bp	aa880-1235	5'-873-879+1236-1242 3'-873-879+1236-1242
pTopo-Myc-mVKIND- $\Delta$ aa880-948	2639-2844 bp	aa880-948	5'-873-879+949-955 3'-873-879+949-955
pTopo-Myc-mVKIND- $\Delta$ 1059-1235	3175-3705 bp	aa1059-1235	5'-1052-1058+1236-1242 3'-1052-1058+1236-1242





**Fig. 22** NIH 3T3 cells transiently expressing Myc-tagged deletion mutants mVKIND- $\Delta$ aa880-1235, Myc-mVKIND- $\Delta$ aa880-948, Myc-mVKIND- $\Delta$ aa1059-1235.

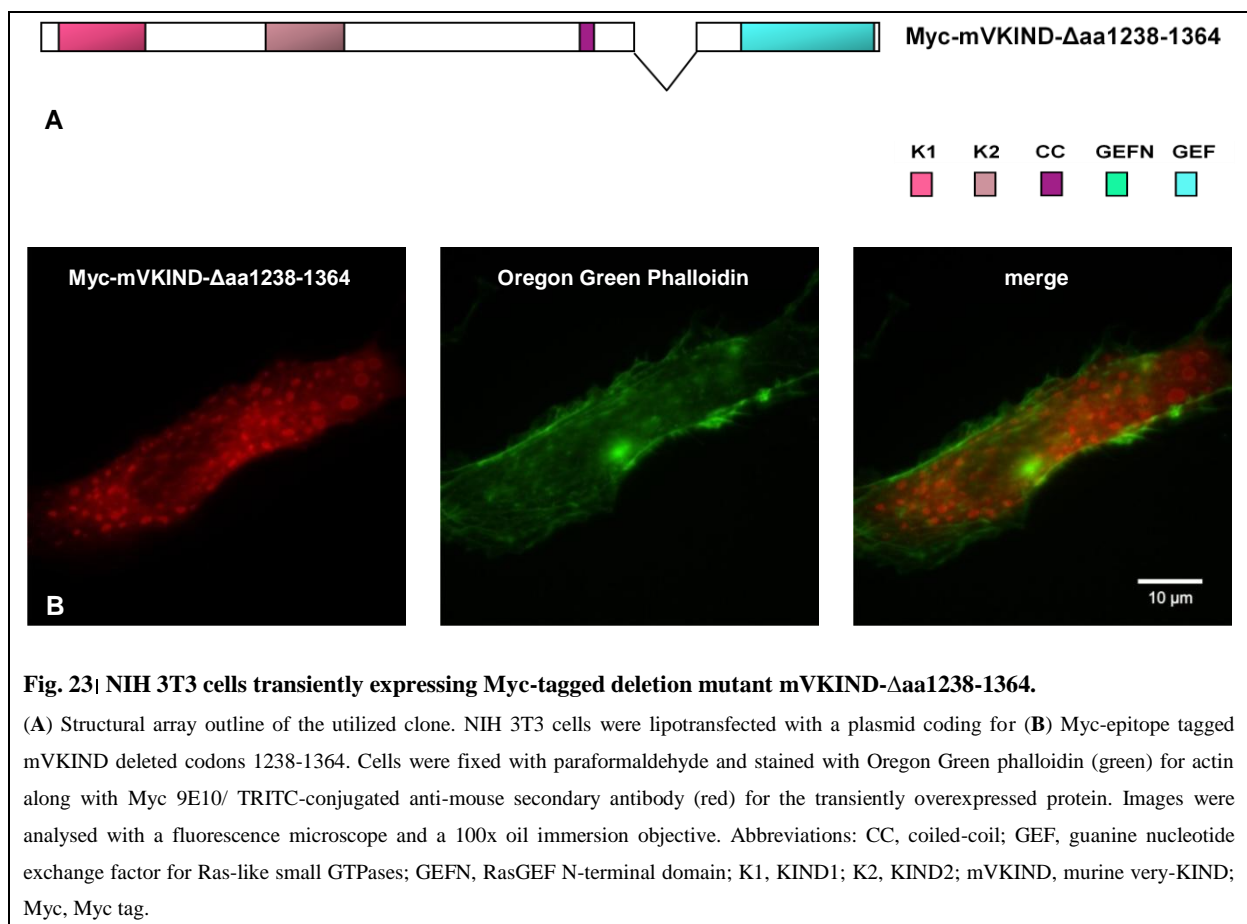
(A) Structural array outline of the utilized clones. NIH 3T3 cells were lipotransfected with vectors directing the expression of (B) Myc-epitope tagged mVKIND deleted codons 880-1235, (C) deleted codons 880-948 and (D) deleted codons 1059-1235. Cells were fixed with paraformaldehyde and stained with Oregon Green phalloidin (green) for their actin structures along with Myc 9E10/ TRITC-conjugated anti-mouse secondary antibody (red) for transiently overexpressed proteins. Subcellular accumulation is marked by arrows. Images were analysed with a fluorescence microscope and a 100x oil immersion objective. Abbreviations: CC, coiled-coil; GEF, guanine nucleotide exchange factor for Ras-like small GTPases; GEFN, RasGEF N-terminal domain; K1, KIND1; K2, KIND2; mVKIND, murine very-KIND; Myc, Myc tag.

#### 4.9.6 | Transient expression of mVKIND deletion mutants coding for Myc-mVKIND- $\Delta$ aa1238-1364

To investigate the influence and significance of the GEFN domain (amino acid residues 1238 through 1364) on the distribution of the mVKIND, a mutant depleted of the GEFN domain was created (Tab. 7,  $\rightarrow$ 3.1.4.4) and transfected into NIH 3T3 cells ( $\rightarrow$ 3.3.2.1). 24 h post transfection cells were fixed and immunostained using a primary antibody directed against the Myc tag epitope (9E10), located at the N-term of the fusion protein and a TRITC-conjugated anti-mouse secondary antibody to mark the exogenous protein. F-actin was visualized with 2',7'-difluorofluorescein (Oregon Green 488 dye)-conjugated phalloidin and stains were subjected to fluorescent microscopy ( $\rightarrow$ 3.3.3). Fig. 23A pictures a schematic outline of the clone. The mutant was successfully expressed in only few cells at high amounts. It accumulated in circular structures and distributed uniformly throughout the cytosol, being excluded from the nucleus and the cell membrane (Fig. 23B). Cells crafted cytosolic circular structures at low rates.

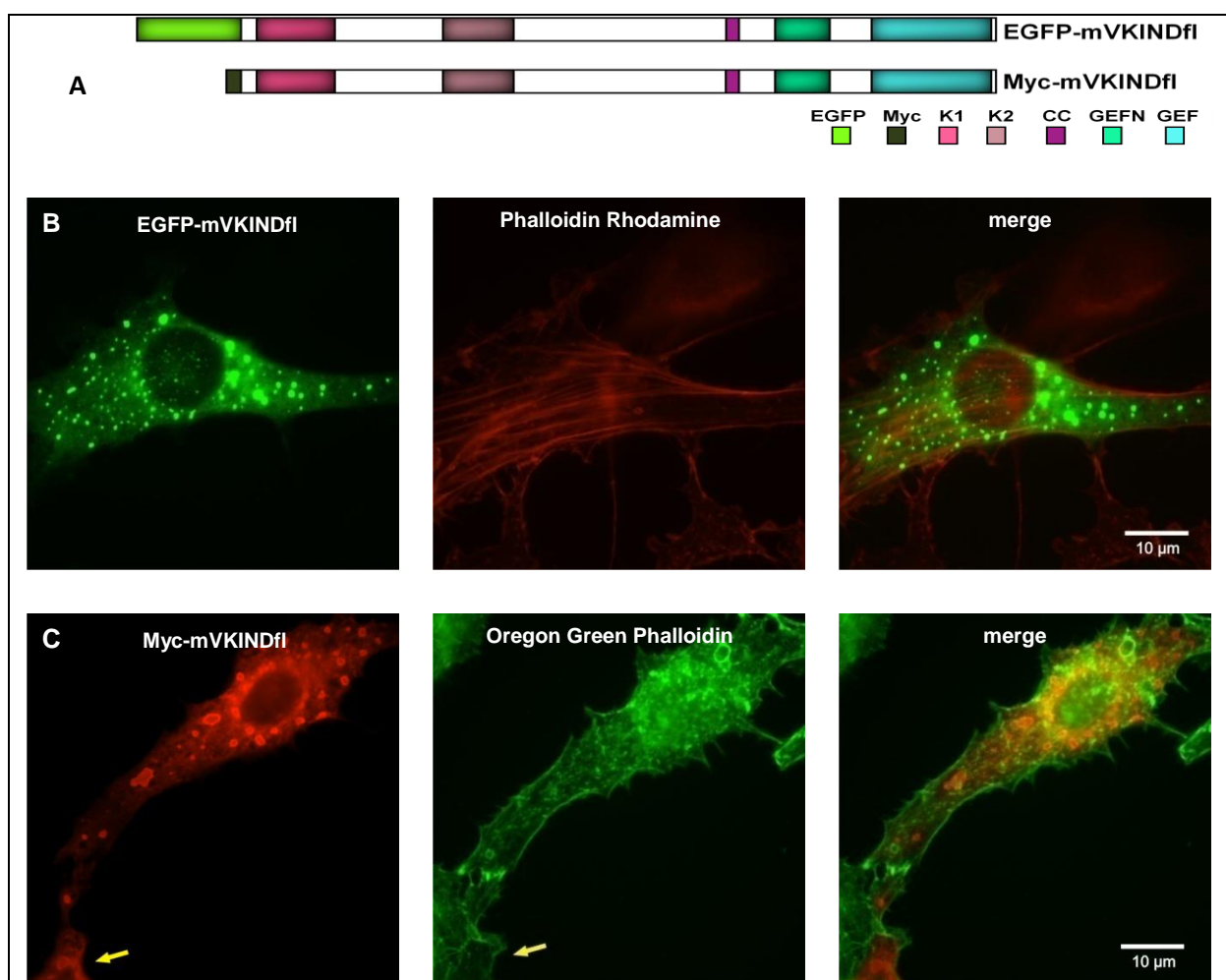
**Tab. 7 | Overview deletion mutant mVKIND- $\Delta$ aa1238-1364 construct. Detailed construct records are provided in Appendix II**

Construct	Depleted Coding Sequence	$\equiv$ Depleted Protein Sequence of Insert	Primer
pTopo-Myc-mVKIND-Aaa1238-1364	3712-4092 bp	aa1238-1364	5'-withoutRasGEFN 3'-withoutRasGEFN



#### 4.9.7 | Transient expression of mVKINDfl

Transiently expressed mVKINDfl in NIH 3T3 cells revealed the formation of distinguished circular structures which were dispersed throughout the cytosol (Fig. 18F). To address the influence of the liposomal transfection method with the Lipofectamine transfection reagent on the formation of these structures in NIH 3T3 cells, Myc-mVKINDfl and EGFP-mVKINDfl (Tab. 1 and Tab. 3) (Fig. 24A) were expressed by calcium phosphate transient transfection ( $\rightarrow$ 3.3.2.2). NIH 3T3 cells expressing Myc-mVKINDfl were fixed and immunostained using a primary antibody directed against the Myc tag epitope (9E10) located at the N-terminus of the Myc-fusion protein and a TRITC-conjugated anti-mouse secondary antibody to mark the exogenous protein 24 h post transfection. F-actin was visualized with 2',7'-difluorofluorescein (Oregon Green 488 dye)-conjugated phalloidin, whereas cells expressing EGFP-tagged mVKINDfl were fixed and F-actin was probed with tetramethylrhodamine-conjugated phalloidin. EGFP-mVKINDfl (Fig. 24B) as well as




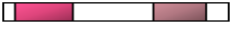






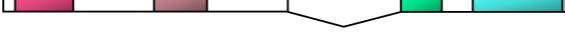
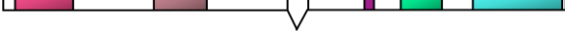
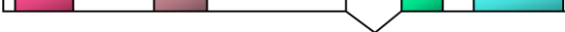
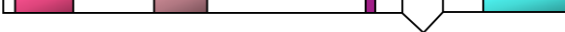
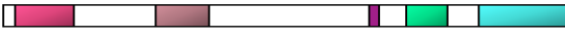

**Fig. 24|** NIH 3T3 cells transiently transfected with EGFP-mVKINDfl and Myc-mVKINDfl by DNA-calcium phosphate co-precipitation procedure.

(A) Structural array outline of utilized clones. NIH 3T3 cells were transfected with calcium-phosphate coprecipitation of a plasmid coding for (B) EGFP-fused mVKINDfl and (C) Myc-epitope tagged mVKINDfl. Cells were fixed with paraformaldehyde and cells expressing EGFP-fused mVKINDfl were probed with tetramethylrhodamine-conjugated phalloidin for F-actin, whereas cells expressing Myc-epitope tagged mVKINDfl were stained with Oregon Green phalloidin (green) for actin along with Myc 9E10/ TRITC-conjugated anti-mouse secondary antibody (red) for the transiently overexpressed protein. Images were analyzed with a fluorescence microscope and a 100x oil immersion objective. Golden arrow in pane C marks a second Myc-mVKINDfl expressing cell. Abbreviations: CC, coiled-coil; EGFP, Enhanced Green Fluorescent Protein; GEF, guanine nucleotide exchange factor for Ras-like small GTPases; GEFN, RasGEF N-terminal domain; K1, KIND1; K2, KIND2; mVKINDfl, murine very-KIND full length; Myc, Myc tag.

Myc-mVKINDfl (Fig. 24C) was found expressed at high levels. The expressed protein is accumulated in circular structures in the cytosol and excluded from nucleus and the cell membrane. Moreover, the spherical entities were not associated to the actin filament network. These findings are in good agreement with the results presented in 4.8.1.

#### 4.9.8 | Summary of the transient expression of mVKINDfl and mVKIND truncation mutants

Summarized subcellular distribution of the transiently expressed mVKINDfl and its truncation mutants in mouse NIH 3T3 fibroblast cells is presented in Fig. 25, as previously presented in Fig. 18, 19, 20, 21, 22, 23 and 24.

UTILIZED TRUNCATION MUTANTS		SUBCELLULAR DISTRIBUTION
	<b>A</b>	mVKIND-aa2-337; uniform nuclear and cytoplasmic distribution, faint accumulation in the perinuclear region and in actin based cell surface protrusions
	<b>B</b>	mVKIND-aa2-709; uniform cytoplasmic distribution, slight perinuclear and lamellipodial accumulation, enriched along actin bundles at the cell edges
	<b>C</b>	mVKIND-aa2-1204; formed uniformly distributed circular cytoplasmic structures
	<b>D</b>	mVKIND-aa2-1234; formed uniformly distributed circular cytoplasmic structures
	<b>E</b>	mVKIND-aa2-1349; formed uniformly distributed circular cytoplasmic structures
	<b>F</b>	mVKIND-aa456-1742; uniform cytoplasmic distribution
	<b>G</b>	mVKIND-aa614-1742; uniform cytoplasmic distribution
	<b>H</b>	mVKIND-aa1451-1742; uniform cytoplasmic distribution, enriched on actin bundles in the cell membrane
	<b>I</b>	mVKIND-Δaa880-1235; formed uniformly distributed circular cytoplasmic structures
	<b>J</b>	mVKIND-Δaa880-948; formed uniformly distributed circular cytoplasmic structures
	<b>K</b>	mVKIND-Δaa1059-1235; formed uniformly distributed circular cytoplasmic structures
	<b>L</b>	mVKIND-Δaa1238-1364; formed uniformly distributed circular cytoplasmic structures
	<b>M</b>	mVKINDfl; formed uniformly distributed circular cytoplasmic structures
		

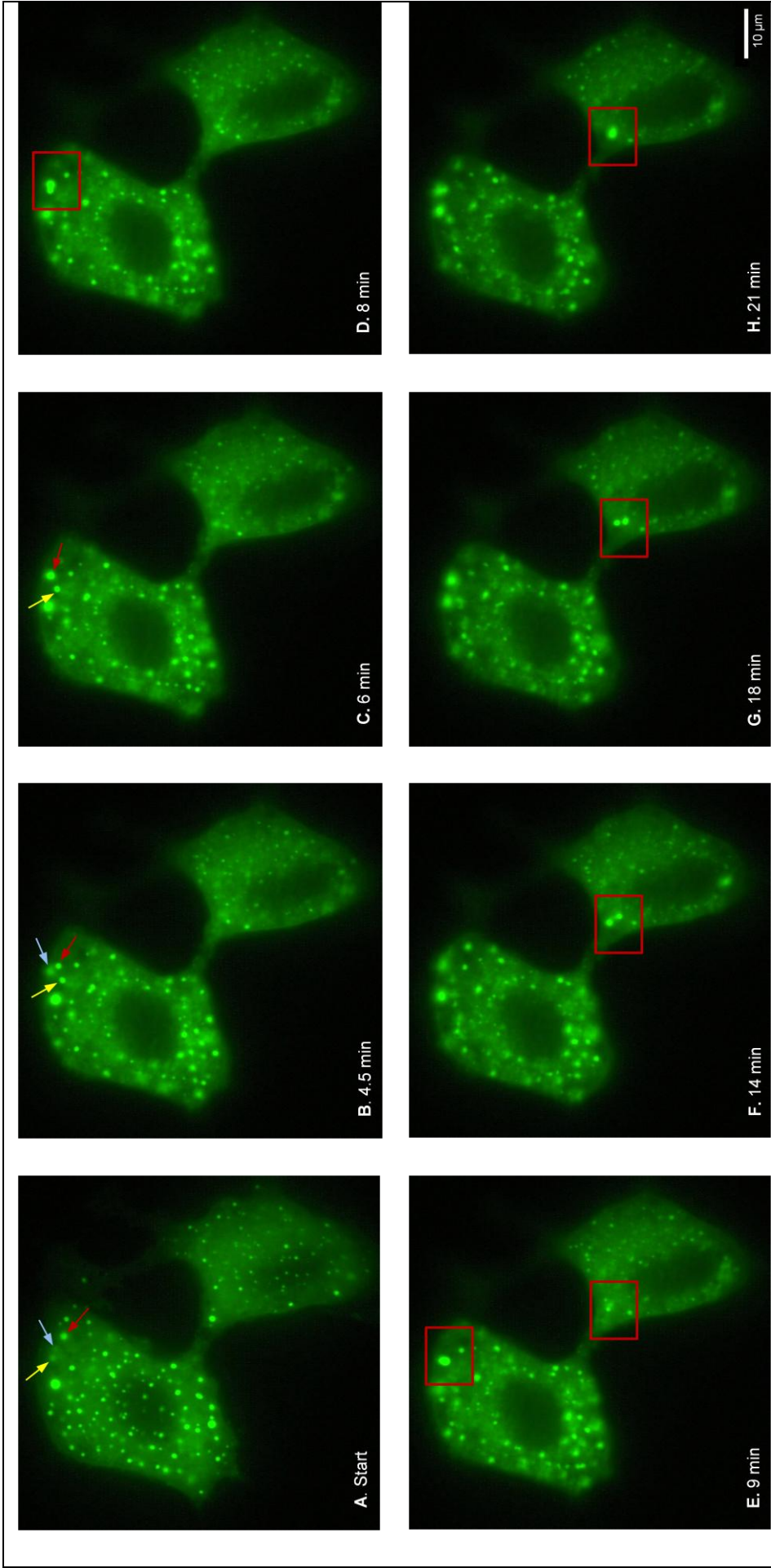
**Fig. 25 | Subcellular distribution of the transiently expressed mVKINDfl and its truncation mutants in mouse NIH 3T3 fibroblast cells**

Detailed construct records are provided in Appendix II. Abbreviations: CC, coiled-coil; GEF, guanine nucleotide exchange factor for Ras-like small GTPases; GEFN, RasGEF N-terminal domain; K1, KIND1; K2, KIND2; mVKINDfl, murine very-KIND full length.

#### 4.10 | Live cell imaging of EGFP-mVKINDfl transfected cells

Mouse fibroblast NIH 3T3 cells transiently expressing mVKINDfl revealed the occurrence of massive circular structures that ranged in size up to 10  $\mu\text{m}$  in a period of 24 h (Fig. 18 and 24). To monitor the formation and evolution of these structures, NIH 3T3 cells were lipotransfected with plasmids coding for EGFP-mVKINDfl (Tab. 3). A subsequent microscopic time-lapse imaging was carried out.

For the EGFP-mVKINDfl time lapse analysis, NIH 3T3 cells were plated on glass cover slips in growth medium in 35 mm-well plates. Cells were allowed to adhere for approximately 18 h and were subjected to Lipofectamine mediated EGFP-mVKINDfl transfection ( $\rightarrow$ 3.3.2.1, 1  $\mu\text{g}$  DNA). 5 h post transfection, cells were provided with fresh growth medium. Detection of the fluorescent signal from EGFP-mVKINDfl required approximately 6 h. Upon visual evidence of high levels transient expression of the EGFP-fused mouse VKIND, a cover slip carrying positively transfected NIH 3T3 cells was clamped in a cover slip chamber. Cells were overlaid with warm growth medium ( $\text{CO}_2$  free, *Gibco*) and immediately transferred to a fluorescent microscope (*Leica*) while being incubated at 37°C. Cells positive for EGFP fluorescence were selected and focused with a 100x oil immersion objective. Subsequently, a time-lapse fluorescent monitoring was initiated with images captured every 30 s for 22 min employing a digital camera (*Hamamatsu Orca*). Images (1024x1022 pixels) were optimized and light intensities were color-coded with *Openlab* imaging software (*Improvision*). QuickTime videos (.mov format) were generated using time series pictures ( $\rightarrow$ 3.3.4). The time-lapse analysis revealed a series of events by which the EGFP-carrying particles in the NIH 3T3 cytoplasm are in motion, make contact and eventually fuse. Fig. 26A illustrates three structures estimated to be up to 0.3  $\mu\text{m}$  in size (golden, red and blue arrows) at start. Fig. 26B shows the slight migration of these three structures 4.5 min later which ultimately results in the fusion of two structures, indicated by blue and red arrows (Fig. 26C, the resulting larger structure is indicated by red arrow). Fig. 26D and E demonstrate the subsequent contact and fusion of the two structures described above (upper cell, red rectangle). At the same time, the red rectangle in the lower cell points out two distinct entities which fuse within the following 12 min (Fig. 26, images E through H). In general, the nascent structures progressively grew over the time period of 21 min to significantly larger entities of approximately 2  $\mu\text{m}$  in size. Relocation of the structures throughout the cytoplasm was viewed to be in cases leading to particle fusion directed and highly dynamic.



**Fig. 26| EGFP-mVKIND1 video time-lapse analysis.**

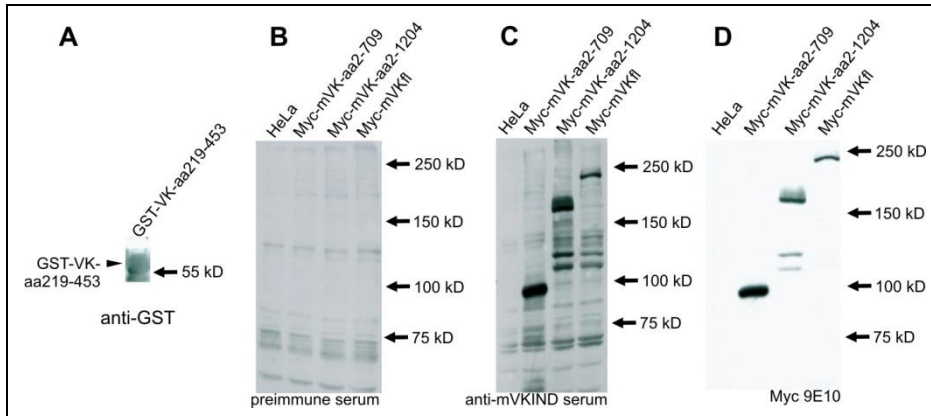
NIH 3T3 cells were lipotransfected with a vector coding for EGFP-fused mVKIND1. 6 h post transfection cells were examined on a fluorescent microscope and a time-lapse fluorescent monitoring was launched. Images were collected at 100x oil immersion objective every 30 s. (A, B) Initial three discrete structures are marked by arrows. (C) At 4.5 min blue and red marked structures fused first to one larger entity (red arrow) and eventually (D, red rectangle) joined the structure marked by the golden arrow which (E, upper red rectangle) completely fused at 9 min. (E, lower red rectangle) Additional circular mobile structures which (E, F, G and H) fused in the course of time.

## 4.11 | mVKIND antibody

For further characterization of the endogenous expression pattern of the mouse VKIND protein, an mVKIND polyclonal antibody was generated by rabbit immunization. A designated mVKIND peptide, encompassing amino acid residues 219 through 453 (poorly conserved), was fused to glutathione-S-transferase (GST) (pGEX-6P-1-mVKIND-aa219-453, Tab. 8, Fig. 29B). Recombinant GST-mVKIND-aa219-453 (Fig. 27A) protein was expressed in the *E. coli* host strain Rosetta (*Novagen*) (→3.2.2). The Rosetta strain contains a pRARE plasmid coding for all of the rarely used codons Arg, Ile, Gly, Leu and Pro, enabling high protein expression yields (Novy *et al.*, 2001). The GST-fusion protein was affinity purified on Glutathione Sepharose 4b beads (*Amersham*) under nondegrading conditions following the manufacturer's batch purification protocol. The buffer was exchanged by using NAP 10 columns to TBST buffer and supplemented with 20% glycerin (→3.2.3, 3.2.4). The immunization with the mVKIND antigen was performed by *immunoGlobe* and crude sera were stored at -20°C. A sample of the acquired anti-mVKIND serum was supplemented with 0.02% NaN<sub>3</sub> (v/v) and examined by western blot techniques. Initially, NIH 3T3 fibroblasts were lipotransfected with vectors coding for Myc-epitope tagged mVKIND-aa2-709, mVKIND-aa2-1204 and mVKINDfl (→3.3.2.1). Total cell lysates were separated by SDS-polyacrylamide gel electrophoresis (→3.1.1.1) and analyzed by immunoblotting with the preimmune serum (→3.2.1) (Fig. 27B), the anti-mVKIND serum (Fig. 27C) and the anti-Myc antibody 9E10 (Fig. 27D). The developed immunoblot showed a slight background signal with the preimmune serum, whereas the anti-mVKIND serum detected the transiently overexpressed mVKINDfl and its C-terminal truncation mutants. The mVKIND antiserum was further analyzed by western blot, employing C57BL/6 mouse tissue samples (→2.6.3). Total tissue lysates were separated by SDS-PAGE and subjected to immunodetection using the anti-mVKIND serum. The anti-mVKIND serum detected the endogenous mouse VKIND protein in the murine brain and cerebellum tissue samples, with an apparent molecular weight of approximately 200 kD (Fig. 28A and B, golden stars), along with an equal sized overexpressed exogenous Myc-tagged mVKINDfl (Fig. 28B, indicated by a red star). Next, the anti-mVKIND serum was tested by immunocytochemical analysis. NIH 3T3 mouse fibroblasts were transfected by lipofection with a vector coding for EGFP-mVKINDfl (→3.3.2.1). At 24 h post transfection, cells were fixed and EGFP-mVKINDfl was visualized by autofluorescence and staining with the anti-mVKIND serum along with a tetramethylrhodamine isothiocyanat (TRITC)-conjugated secondary antibody (red) (→3.3.3). EGFP-mVKINDfl accumulated in circular structures which were detected by the anti-mVKIND serum, along with a strong nonspecific background (Fig. 29).

**Tab. 8| Overview of the pGEX-6P-1-mVKIND-aa219-453 construct. Detailed construct records are illustrated in Appendix II**

Construct	Coding Sequence	≡ Protein Sequence of Insert	Primer	Restriction Site 5'/3'
pGEX-6P-1-mVKIND-aa219-453	655-1359 bp	aa219-453	5'-vKIND-BamHI-655bp 3'-vKIND-1340bp-EcoRI	BamHI/EcoRI

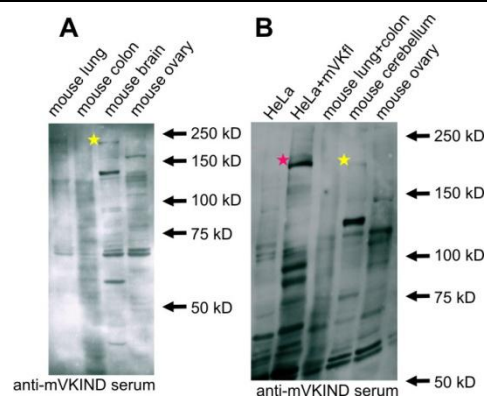


**Fig. 27| Anti-mVKIND serum tested by western blotting.**

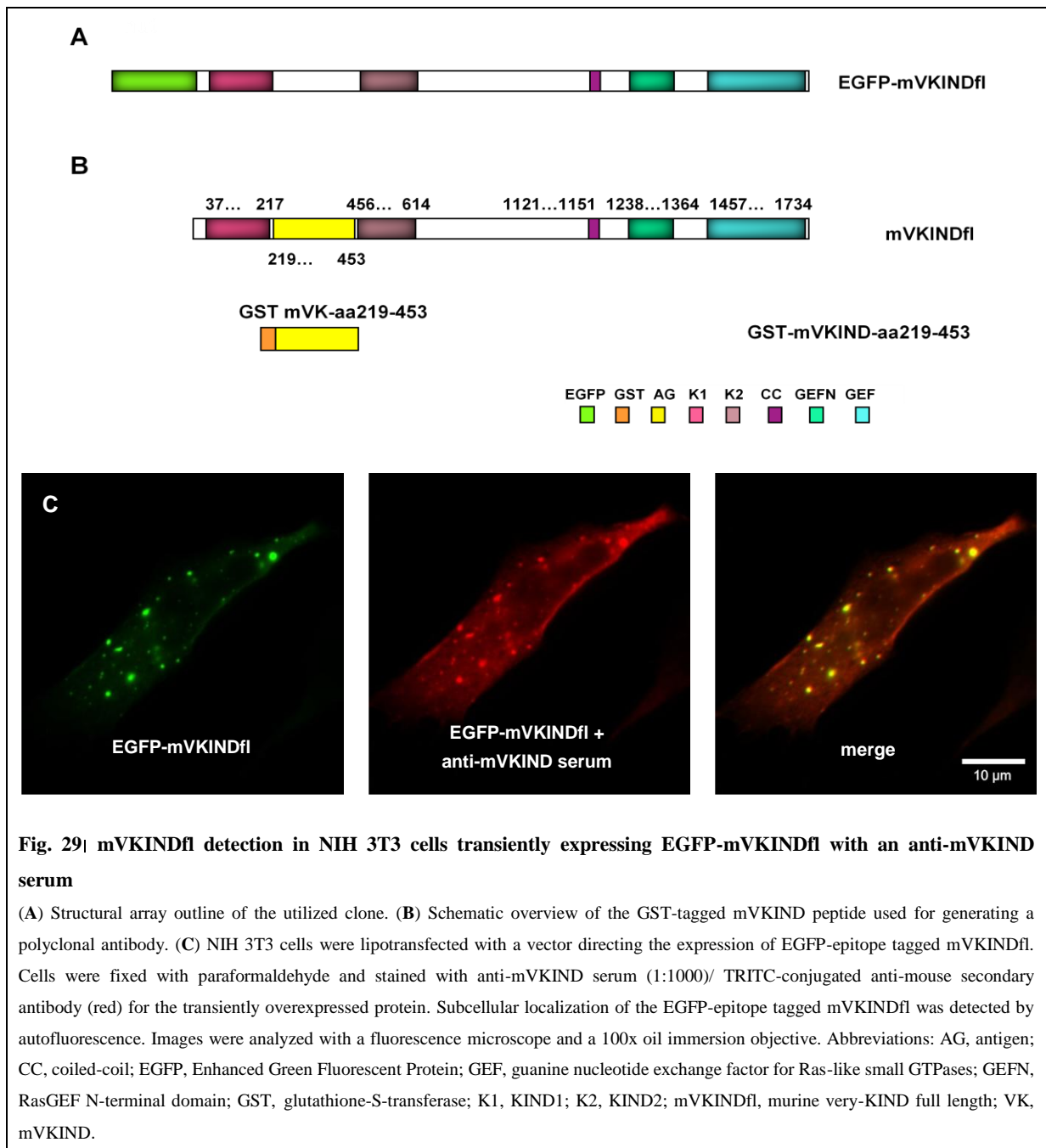
(A) Purified GST-mVKIND-aa219-453 with an apparent molecular weight of approximately 56 kD. (B) Western blots developed with preimmune rabbit serum (1:300), (C) anti-mVKIND serum (1:300) and (D) the Myc 9E10 antibody. Abbreviations: GST, glutathione-S-transferase; kD, kilo Dalton; VK, mVKIND; mVKINDfl, murine very-KIND full length; Myc, Myc tag.

**Fig. 28| WB mVKIND antiserum analysis, employing mouse tissue samples.**

(A) C57BL/6 mouse tissue total lysates of lung, colon, brain and ovary, along with (B) total tissue lysate of cerebellum and in HeLa cells exogenously overexpressed mVKINDfl were separated by SDS-PAGE and blotted onto nitrocellulose membrane. Immunoblots were developed with anti-mVKIND serum (1:300). Stars indicate immunodetected endogenous mVKIND. Abbreviations: kD, kilo Dalton; mVKfl, murine very-KIND full length .



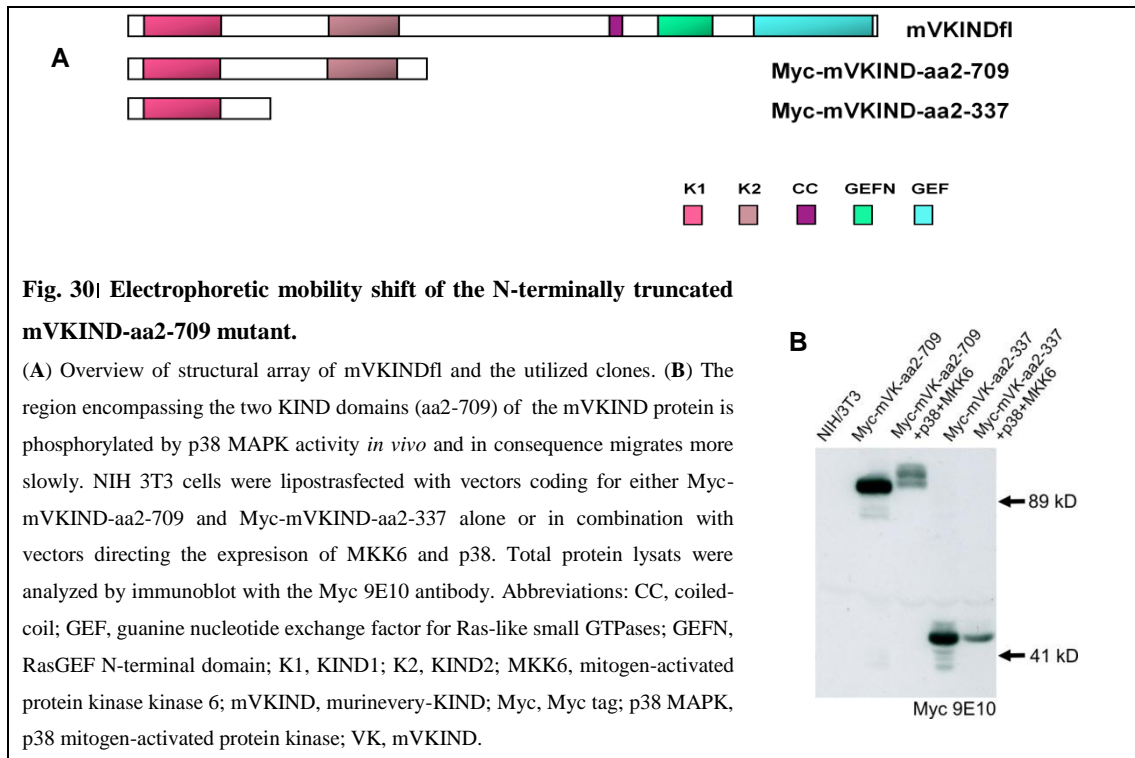




#### 4.12 | Murine VKIND protein phosphorylation by the p38 MAPK

Guanine nucleotide exchange factors (GEFs) are highly regulated (Mitin *et al.*, 2005). To determine if the mouse VKIND is a possible phosphorylation target of mitogen activated kinases, the phosphorylation of the mVKIND was investigated. NIH 3T3 mouse fibroblasts were transfected with plasmids either coding for Myc-mVKIND-aa2-709 alone (Tab. 1, computational calculated molecular weight of 78.49 kD), or along with plasmids coding for mitogen-activated protein kinase kinase 6 (MKK6, constitutively active) as well as p38 mitogen-activated protein kinase (MAPK), respectively ( $\rightarrow$ 3.3.2.1, 0.7  $\mu$ g pcDNA3-Myc-mVKIND-aa2-709 in combination with 0.4  $\mu$ g DNA of each kinase expressing construct). Additionally, Myc-mVKIND-aa2-337 (Tab. 1, computational calculated molecular weight of 40.3 kD) was expressed in NIH 3T3 alone, as well as cotransfected with MKK6 and p38 MAPK ( $\rightarrow$ 3.3.2.1, 0.7  $\mu$ g pcDNA3-Myc-mVKIND-aa2-337 in combination with 0.4  $\mu$ g DNA of each kinase expressing construct). Total cell lysates

were subjected to SDS-PAGE and western blotting ( $\rightarrow$ 3.2.1), revealing an electrophoretic mobility shift of the C-terminal truncation mutant mVKIND-aa2-709, suggesting an *in vivo* p38 phosphorylation (Fig. 30B), whereas mVKIND amino acids 2-337 were not phosphorylated.



---

## Chapter V | Discussion

	<b>Page</b>
<b>5.1</b>   Cloning and structure	67
<b>5.2</b>   mVKIND Antibody	69
<b>5.3</b>   <i>mVKIND</i> expression	70
<b>5.4</b>   Transient expression	71
<b>5.5</b>   mVKIND protein phosphorylation by the p38 MAPK	73
<b>5.6</b>   Outlook	73

## 5.1 | Cloning and structure

At present the kinase non-catalytic C-lobe domain is located at present in the N-terminal regions of three proteins: 1) the Spir family of actin organizers (Otto *et al.*, 2000; Ciccarelli *et al.*, 2003); 2) the non-receptor tyrosine phosphatases type 13 (PTP type 13) (Erdmann, 2003); and 3) the guanidine exchange factor of the Ras-like small guanosine GTPases (VKIND) (Mees *et al.*, 2005) (Fig. 3). A cDNA coding for the mouse VKIND was generated by cloning six RT-PCR fragments (Fig. 8, Tab. 1), employing cerebellum RNA of an adult C57BL/6 mouse as template. An open reading frame of 5229 base pairs (Fig. 9C) (with the endogenous stop codon) was deduced from sequenced cDNA fragments and the assembling accuracy was confirmed by DNA sequence analysis as well as endonucleolytic cleavage. The open reading frame translates into 1742 amino acid residues (Fig. 9D). The precise expression of the cloned Myc-epitope tagged full length mVKIND was confirmed by transient expression in NIH 3T3 mouse fibroblasts. The computational calculated size of 191,204 kD coincided with the observed apparent molecular weight of 205 kD (Fig. 12).

The novel KIND domain comprises the entire C-lobe of the protein kinase catalytic fold of p21 activated kinases (PAKs) except the N-lobe and the linker region (Ciccarelli *et al.*, 2003) (Fig. 1A). The absence of structures essential for enzymatic activity, i.e. the N-lobe, including the N-terminal subdomains I-IV primarily involved with nucleotide binding and orienting; the invariant Asp<sub>166</sub> and Asn<sub>171</sub> (as referenced to PAK) in C-lobe subdomain VIB, assigned with catalytic kinase activity; the invariant amino acid Asp<sub>184</sub> (as referenced to PAK) in the activation loop that is incorporated in the highly conserved DFG triplet in the C-lobe subdomain VII; and the deep cleft between the structurally independent lobes recognized as the site initiating the phosphotransfer supposedly deprives the KIND domain of any catalytic capacity (Hanks & Hunter, 1995; Knighton *et al.*, 1991a; Knighton *et al.*, 1991b) (Fig. 2). Homologous enzymes and nonenzymes sharing high sequence identity but not performing any similar functions have been described (Todd *et al.*, 2002). The KIND domain appears to be an adapted nonenzyme within a superfamily that otherwise embodies protein kinases. Given the kinase domain is apparently an ancient module which ancestor predates the divergence of Bacteria, Archaea and Eukaryotes (Leonard *et al.*, 1998), whereas the KIND domain is present only in Metazoa substantiates the assumption. An interaction and/or regulatory potential for the KIND domain is advocated since paired nonenzymes retain a ligand binding capacity (Todd *et al.*, 2002) and the PAK1 C-lobe communicates the substrate recognition (Knighton *et al.*, 1991a). In fact, recently we reported that the Spir family KIND domain mediates the inhibition of actin nucleation by Cappuccino family formins (Quinlan *et al.*, 2007). In an evolutionary conserved interaction the *Drosophila* and mammalian Spir KIND domains bind the formin homology 2 (FH2) domain of Cappuccino (or its mammalian homologue formin-2) at a ratio of 2:2 (two KIND monomers/one FH2 dimer) while competing with actin filaments and microtubules (Quinlan *et al.*, 2007). Moreover, the interaction of the Spir KIND domain with Cappuccino enhances the actin nucleation by Spir. The KIND domains of the protein VKIND, however, did not bind the Formin-2 FH2 domain, emphasizing the specificity of the interaction (Quinlan *et al.*, 2007).

In the VKIND protein two homologous KIND domains are arranged in the N-terminal region in a tandem like fashion (Fig. 3 & Fig 9C, D). The nomination of the novel eukaryotic protein is attributed to the dual occurrence of two KIND domains (KIND1/2) in its structure. Recently, the interaction capacity of the KIND2 domain was demonstrated as it binds to the microtubules-associated protein 2 (Huang *et al.*, 2007). While the precise purpose of the first KIND domain of the VKIND protein remains obscure, some roles can be hypothesized analyzing the protein composition. Remarkably, up to 80% of the eukaryotic genome account for multidomain proteins (Apic *et al.*, 2001a; Han *et al.*, 2007). In some occasions domains behave

in a cooperative manner, that is the folding of individual domains is influenced by its adjacent domains (Batey *et al.*, 2005; Zhou *et al.*, 2005). Still, in others domains fold independently (Scott *et al.*, 2002; Robertsson *et al.*, 2005). Notably, the Spir KIND domain does not form dimers (Quinlan *et al.*, 2007). It can be assumed that the folding of one KIND domain of VKIND may have stabilizing effects on the folding of the neighboring domain by interdomain interactions, given the KIND domains are separated by a linker of 239 amino acid residues (Fig. 9D). It has been shown that tandem domains attain stabilization while flanked by expanded non-native peptides (Randles *et al.*, 2007). Additionally, specific interdomain interactions may have essential biological significance, since multidomain proteins were assigned new functions combining evolutionary old building entities rather than inventing new ones (Apic *et al.*, 2001b). Special functional demands that appeared with the rising of Metazoa, such as complex signalling, cell adhesion along with regulatory mechanisms, were met by repeated domains of Metazoa-specific families (Apic *et al.*, 2001b). The cooperativity aspect of the KIND domains in VKIND remains to be elucidated, yet there is an indication that the functional ability of the KIND2 domain might be enhanced in the presence of the KIND1 domain (Huang *et al.*, 2007).

A coiled-coil helix was predicted in the central portion of mVKIND by *COILS* (version 2.2) (Lupas *et al.*, 1991) (Fig. 9D). The coiled-coil is a general and highly versatile assembly motif present in a wide range of structural and regulatory proteins (Lupas, 1996) that comprise estimated 2-8% of the genomic complement (Rose *et al.*, 2005). The coiled-coil functional variety ranges from assembling of macromolecular complexes to molecular recognition (Lupas *et al.*, 1991) indicating an essential biological activity. Short coiled-coils (up to 35 residues) are reported to be stable (Yu, 2002) and important for oligomerization (Hayward & Koronakis, 1999). Furthermore, short coiled-coils were found to be involved in mediating protein-protein interactions (Picking *et al.*, 2001). The coiled-coil of the eukaryotic protein Coronin, involved in actin rearrangements, is essential for its dimerization and ability to bind F-actin (Asano *et al.*, 2001). Indeed, the coiled-coil module is a prominent structural feature for many eukaryotic cytoskeletal proteins engaged in the association with and regulation of actin polymerization (e.g.  $\alpha$ -Actinin,  $\alpha$ -Catenin and VASP) (Delahay & Frankel, 2002). In the light of the ligands for coiled-coil interactions tending to be coiled-coil helices as well (Delahay & Frankel, 2002), there is a promising option for VKIND to interact with multiple partners (i.a. F-actin) via its coiled-coils motif. Moreover, interaction between coiled-coils and non-coiled-coils structures have also been described (Nusrat *et al.*, 2000). Phosphorylation events induce functional modification (stabilization or destabilization) of coiled-coil interactions (Szilak *et al.*, 1997) and display a means of VKIND regulation in the context of subcellular environment.

In the carboxy-terminus of VKIND a guanine nucleotide exchange factor for Ras-like small GTPases (RasGEF) with a structural motif attached at its N-terminal site (RasGEFN) was identified by *SMART* (Schultz *et al.*, 1998) (Fig. 9). The Ras subfamily comprises 36 members (e.g. H-Ras, Rap1, Rap2, RalA and B) and regulates signalling knots in respond to various extracellular stimuli (Vojtek & Der, 1998; Repasky *et al.*, 2004; Wennerberg *et al.*, 2005). Ras subfamily GTPases employ GEFs that share a catalytic domain with homology to the yeast RasGEF CDC25 (Ehrhardt *et al.*, 2002). Sequence alignment of the VKIND GEF domain with representatives of other GEF domains for Ras subfamily GTPases, such as RapGEFs, RalGEFs and the H-RasGEFs indicates that the VKIND RasGEF domain is a CDC25 like domain (Fig. 11). The closest relation of the VKIND RasGEF domain with average sequence identity of 23% is assigned to the RasGEF domains of exchange factors specific for Rap GTPases, such as the Epac, MR-GEF and RA-GEF (Fig. 11). Notably, the alignment shows that the VKIND enzymatic domain has a unique structure. It features two insertions, the first one of 24 amino acids in the N-terminal end of the domain (between helices  $\alpha$ A and  $\alpha$ B of the SOS1 RasGEF module) and the second one of 11 amino acids in the C-terminal part

(between, helices  $\alpha J$  and  $\alpha K$  of the Sos1 RasGEF module) (Boriack-Sjodin *et al.*, 1998) (Fig. 11). Nonetheless, recently VKIND was reported to operate as a GEF for the Ras GTPase (Huang *et al.*, 2007). The CDC25 homology domains of the Ras branch, however, have been shown to concurrently regulate the cycling of other Ras subfamily proteins (Mitin *et al.*, 2005). Thus, additional interaction partners of the VKIND RasGEF domain remain to be investigated.

To present knowledge the RasGEFN domain is mutual to all but one RasGEFs (Quilliam *et al.*, 2002; Bos *et al.*, 2007). The exceptional one is a dual specificity exchange factor for H-RAS and Rap 1A, PLCE1 (1-phosphatidylinositol-4,5-bisphosphate phosphodiesterase epsilon-1) (accession: Q9P212). In SOS RasGEFN interacts with one edge of a helical hairpin (helices  $\alpha H$  and  $\alpha I$ ) that projects from the main body of the CDC25 domain and is thereby loosely hinged to the core of the catalytic domain (Margarit *et al.*, 2003). The helical hairpin is responsible for the displacement of the Switch 1 segment of Ras during the guanine nucleotide exchange reaction (Margarit *et al.*, 2003). Interaction between the RasGEFN domain and the helical hairpin is critical for SOS function, since disruption of this interface reduces nucleotide exchange activity severely (Hall *et al.*, 2001) even though Ras and SOS interact entirely via the CDC25 domain (Sondermann *et al.*, 2004). Remarkably, in SOS the GEFN and GEF domains form an allosteric binding site for Ras•GTP (Margarit *et al.*, 2003). Upon binding of Ras•GTP to this distal site the Ras exchange activity is increased to maximal levels revealing a positive feedback loop (Margarit *et al.*, 2003). Additionally, it has been shown that Ras•GDP binds with lower affinity to the GEFN-GEF interface and sets an intermediate level of SOS activity (Sondermann *et al.*, 2004). Yet SOS nucleotide exchange activity is masked until so far undescribed signals trigger the displacement of the DH-PH unit as the DH domain operates as a autoinhibition element (Sondermann *et al.*, 2004). It has been proposed that the GEFN-GEF interface might be intrinsically unstable thus causing changes at the GEF active site and can be stabilized by Ras•GTP or Ras•GDP (Sondermann *et al.*, 2004). While the Ras distal allosteric site is not conserved among other RasGEFs (Margarit *et al.*, 2003) these findings indicate the significance of the interface between the GEFN and GEF domains for the proper GEF function of VKIND.

The structure of the VKIND protein is highly conserved among species. Sequence analysis of the human, mouse, chicken and fugu protein showed a high conservation within the predicted two KIND domains, the coiled-coil region, the RasGEFN and the RasGEF domains (Fig. 10). Moreover, the phylogenetic analysis yielded a distribution of the *VKIND* gene only in Vertebratae and Echinodermatae (*S. purpuratus* and *P. lividus*). Echinodermatae, like Chordatae, are Deuterostomia and thought to share a common ancestor and to be the most closely related of the major phyla to the Chordatae. Intriguingly, about 70% of sea urchin genes have a human counterpart compared for example to just 40% of fruit fly genes (Sodergren *et al.*, 2006a; Sodergren *et al.*, 2006b). Though invertebrate sea urchins exhibit a radically different morphological design from humans and other Vertebratae, basic similarities are displayed by their embryonic development. Notably, receptor tyrosine kinases for growth factors and over 90% of sea urchin small GTPases are expressed during their embryogenesis suggesting a comparable complexity of signaling through GTPases between sea urchins and Vertebratae (Sodergren *et al.*, 2006b). Analysis of the sea urchin genome also revealed genes involved in constructing neurons, transmitting signals and axon guidance (Sodergren *et al.*, 2006b). In the light of sea urchins bearing genes associated with taste, smell, hearing, balance and visual perception even without possessing eyes and ears (Sodergren *et al.*, 2006b), it is credible that the ancient gene *VKIND* was assigned an important role in processing of sensory information and development.

## 5.2 | mVKIND Antibody

The mVKIND polyclonal antibody was produced by a rabbit immunization employing a peptide encompassing amino acid residues 219 through 453. The protein region selection was based on its poor

conservation (Fig. 10), therefore higher specificity was predicted. When tested by western blotting the VKIND antibody was able to detect the exogenous and endogenous VKIND protein with a slight background signal (Fig. 26 & 27).

When tested by immunocytochemical analysis in NIH 3T3 mouse fibroblasts the VKIND antibody exhibited a strong nonspecific background suggesting further affinity purification procedures (Fig. 28).

### 5.3 | *mVKIND* expression

The highly restricted spatial expression pattern of the mammalian *VKIND* gene was revealed by a northern blot analysis. *VKIND* was not detected in adult murine tissues of the digestive, excretory, immune, male reproductive and respiration systems (Fig. 13). On the other hand, strong expression was found in the murine nervous system along with a low expression in the female reproductive system (Fig. 13). The mouse *VKIND* mRNA was found to possess the size of the published *VKIND*fl mRNA length (Fig. 9A). The northern blot analysis may also feature an indication of a second *VKIND* isoform (at the level of ~3 kb).

The *VKIND* gene expression in the brain and the neural tube was also confirmed during mouse embryogenesis by *in situ* hybridizations. At E14.5 a high *VKIND* expression was located in the mid- and hindbrain with just weak expression in the forebrain (Fig. 14A). In the time course there was a shift of the main expression towards the telencephalon at E17.5 (Fig. 14A, B). At E10.5 (Fig. 14C), an even earlier *VKIND* expression was traceable in the murine neural tube in the ventro-lateral part, where motoneurons are already positioned, and it was later prolonged to the dorsal part (Fig. 14C, F, I). Particularly, at E10.5 the *VKIND* expression pattern in the neural tube coincided in part with markers for post mitotic motoneurons within the neural tube and early post mitotic migrating neurons (Fig. 14D, E). *VKIND* expression in the developing DRG was detectable not before E12.5 (Fig. 14C), while by E14.5 *VKIND* expression was distributed throughout the entire neural tube except for the marginal layer, but only in a speckled pattern (Fig. 14I). The speckled pattern is indicative of a cell type specific and probably neuronal expression pattern.

In the developing vertebrate eye the expression of *VKIND* was restricted to the future neuronal cell layers and to the fetal stage E17.5 (Fig. 15A, B, C). Notably, the most specific expression of *mVKIND* in the retinal ganglion cells correlates with the high enrichment of rodent MAP2 mRNA in dendritic regions of the retina (Cristofanilli *et al.*, 2004). A relation between the abolished *VKIND* expression past E17.5 and the differential expression of distinct MAP2 isoforms both during development and adulthood (Dehmelt & Halpain, 2005) remains to be determined.

Intriguingly, in the adult mouse brain *VKIND* expression is most prominent in the cerebellum (Fig. 16A, B), however exclusively restricted to the granular and Purkinje cell layers indicating a very specific expression pattern (Fig. 16B, C). In addition, *mVKIND* was identified in cultured primary cerebellar cells of postnatal mice (Fig. 17).

During embryonic development, *VKIND* may play a role in the delicately synchronized neuronal proliferation, migration and differentiation required for the construction of functional synaptic circuits in the mammalian cerebral cortex (Weimer & Anton, 2006). Granule cells precursors tour a complex migration route: they arise from the dorsal hindbrain rhombic lip and during embryonic development stream across the outer surface of the cerebellum founding the external germinal layer (E13-14 in mice) (Wingate, 2001; Porcionatto, 2006). After birth during the first two weeks of age EGL cells undergo extensive proliferation, move inward along Bergmann glia and establish contacts with the Purkinje cells (Wechsler-Reya, 2003; Porcionatto, 2006). Differentiating granule cells continue inward migration through the molecular layer and past the Purkinje cell bodies to their very last destination, the internal granule layer (Wechsler-Reya, 2003) where they make synapses with mossy fibers and Golgi cell axons (Ito, 1997). On the other hand, Purkinje

cell progenitors arise via radial migration from the neuroepithelium between E13 and E17 (Alvarez Otero *et al.*, 1993).

Ras subfamily GTPases participate in every aspect of the orchestration of granule cell precursor proliferation, cell-cycle exit and differentiation, migration, axon extension and synapse formation (Pascual-Castroviejo *et al.*, 1994) all of which are influenced by dynamic rearrangements of the neural cytoskeleton (Weimer & Anton, 2006). Likewise, the expression of extracellular guidance factors, such as Netrin 1, and of their respective receptors (e.g. DCC and  $\alpha 6\beta 4$  integrin) is strictly regulated in time and space during the early cerebellar development (Cirulli & Yebra, 2007). Netrin 1 exerts a chemorepulsive effect on the axonal outgrowth and migration of granule cells (Alcantara *et al.*, 2000). The DCC/ $\alpha 6\beta 4$  integrin intracellular signalling response incorporates the Ras and AKT signaling pathways which are engaged in the control of cell migration and cell proliferation (Cirulli & Yebra, 2007). Conclusively, the expression pattern of the mVKIND protein during embryogenesis suggests its possible participation in the Ras GTPases regulated network of neuronal migration, process outgrowth (also retraction) along with nuclear translocation to ensure their correct positioning in the cerebellar cortex, eye and neural tube.

#### 5.4 | Transient expression

Subcellular distribution of high level constitutively expressed mVKIND protein was explored by EGFP-fused and Myc-epitope-tagged mVKINDfl and various C-terminal truncation mutants in NIH 3T3 mouse fibroblasts.

The KIND1 domain evenly distributed in the cell cytoplasm and in the nucleus, indicating no specific localization (both EGFP- and Myc-fused) (Fig. 18C & 19B). Additionally, the KIND1 domain was detected in actin based cell surface protrusions (Fig. 19B). The expression of KIND1/KIND2 domains displayed perinuclear and lamellipodial accumulation (both EGFP- and Myc-fused) (Fig. 18D & 19C). In addition, KIND1/KIND2 was observed at cell-cell contact interfaces (Fig. 19C). Intriguingly, mVKINDfl induced the development of large circular structures in the cytosol (both EGFP- and Myc-fused) (Fig. 18F & 24B, C). Likewise, the deletion mutants  $\Delta$ GEFN/ $\Delta$ GEF induced partially circular entities (Fig. 20B, C, D). The incorporation of expressed protein into these structures was observed to be forceful with a negligible fraction of transiently expressed protein remaining unbound in the cytosol and no detectable protein at the cell periphery (Fig. 18, 20 & 24). The overlapping expression pattern of EGFP- and Myc-tagged truncation mutants, suggests no distributional influence of the employed molecular tags (Fig. 24B, C). Moreover, the transfection method (with respect to transfection reagents) had no effect on the potential of mVKINDfl to form distinguished circular structures (Fig. 24B, C).

The mVKIND-aa2-1204 (Fig. 20B) and mVKIND-aa2-1349 (Fig. 20D) truncation mutants were expressed at high amounts, whereas the mVKIND-aa2-1234 (Fig. 20C) expression was observed only in few cells, indicating a probable instability of the protein product. These truncation mutants formed closed structures of estimated dimension of up to 10  $\mu$ m width and 7.7  $\mu$ m length dispersed in the cytosol and cell extensions (Fig. 20B, C, D). The truncation mutants exhibited no targeting to the nucleus and cell membrane. Conclusively, the data suggest the putative redundant role of GEFN and GEF domains and the fundamental involvement of the KIND1, KIND2, the adjacent two clusters of high conservation and the coiled-coil for the induction of the cytosolic circular structures as well as protein targeting.

The N-terminal truncation mutants mVKIND-aa456-1742 (Fig. 21B) and mVKIND-aa614-1742 (Fig. 21C) displayed a feasible protein instability in contrast to the mVKIND-aa1451-1742 (Fig. 21D). The mVKIND-aa456-1742 and mVKIND-aa614-1742 mutants distributed predominantly and evenly in the cell cytoplasm (Fig. 21B, C), whereas mVKIND-aa1451-1742 showed an additional nuclear and cell membrane distribution (Fig. 21D). The results advocate the crucial function of the KIND1 and KIND2 domains for the



construction of the cytosolic circular entities in combination with the central region of the VKIND domain. In addition, the key contribution of the KIND1 and KIND2 domains for the VKIND protein stability and targeting were revealed.

The VKIND includes two regions which are highly conserved among species. Selective depletions of either region 1 (aa880-948), region 2 (aa1059-1235, also harboring the coiled-coil motif) or the coiled-coil motif (aa1059-1235) influenced the expression level (to a low intensity) of the deletion mutants and reduced the size of the cytosolic spherical structures (0.4  $\mu\text{m}$ -1  $\mu\text{m}$ ) (Fig. 22B, C, D). The findings propose an implication of the coiled-coil helix for protein stability. Nevertheless, concave structures were formed, implying a possible role for these regions in mediating protein-protein interactions or/and oligomerization. This is supported also by the finding that the mVKIND truncation mutant  $\Delta\text{GEFN}$  crafted cytosolic circular structures of a larger size (Fig. 23B). Compromised structural stability of this truncation mutant was evident. The formation and evolution of the circular structures was studied by a time-lapse fluorescent monitoring of transiently expressed EGFP-fused mVKINDfl in NIH 3T3 mouse fibroblasts. A time-lapse analysis revealed a series of events by which the EGFP-carrying particles in the cytoplasm were in motion, made contact and eventually fused (Fig. 25). In the course of time the nascent structures progressively grew from up to 0.3  $\mu\text{m}$  to significantly larger entities of approximately 2  $\mu\text{m}$  in size. Notably, in cases leading to particle fusion, the relocation of the structures throughout the cytoplasm was directed and highly dynamic.

Punctuate distribution of VKIND has been recently concomitantly shown in dendrites of cerebellar granule cells (Huang *et al.*, 2007). VKIND is proposed to be targeted to MTs via KIND2 domain interactions with MAP2 and influence the development of dendritic arborization with regard to both extension and branching (Huang *et al.*, 2007). Thus VKIND is engaged in neurites differentiation which involves selective stimulation and inhibition of process outgrowth as well as the dynamic elaboration of the dendritic arbor (Cline, 2001). Neurite elongation requires assembly of tubulin into microtubules, whereas the propensity for branching is influenced by the stability of both the actin and microtubule cytoskeletons (Kiddie *et al.*, 2005). Destabilization of the microtubule bundles within the terminal neurite area promotes branching (Kobayashi & Mundel, 1998) that in turn is regulated by the brain microtubule associated proteins (Dehmelt & Halpain, 2005). Unphosphorylated MAP2 promotes and stabilizes microtubule assembly and bundling (Audesirk *et al.*, 1997). VKIND has been reported to induce MAP2 phosphorylation by the Ras pathway downstream effectors ERK and JNK1 (Huang *et al.*, 2007). During neuronal differentiation cytoplasmic JNK1 was found to be a dominant regulator of the dendritic shape (Bjorkblom *et al.*, 2005) by means of phosphorylating and modifying the MAP2 affinity for microtubules (Ozer & Halpain, 2000).

Furthermore, tubulin produced in the soma is delivered to the growth cone by diffusion as well as active transport (Kobayashi & Mundel, 1998). Also, neurons regulate the extent of their neurites by modifying the tubulin production at the soma relative to the active transport fraction (Graham *et al.*, 2006). Additionally, MAP2 mRNA, packed in complex macromolecular ribonucleoparticles, is specifically transported to dendrites along microtubules at an average velocity of 4-8  $\mu\text{m}/\text{min}$  (Huang *et al.*, 2003). Targeted transport of multiple mRNAs and proteins to dendrites, those modulating synaptic plasticity along with others that play more common roles in cellular metabolism, is crucial for the functions of the highly polarized neuronal cells (Zhong *et al.*, 2006). Furthermore, MAP2 proteins are employed in the kinesin- and dynein-dependent intracellular organelle transport along microtubules (Hagiwara *et al.*, 1994). Taken together, these findings imply a role for VKIND in organelle transport given the association and accumulation of VKIND to motile cytosolic particles. A possible correlation between VKIND and distant dendritic transport of RNA granules or/and membranous structures needs to be further investigated.

### 5.5 | mVKIND protein phosphorylation by the p38 MAPK

The p38 MAPK in combination with constitutively active MKK6 was able to phosphorylate *in vivo* exogenous truncation mutant mVKIND-aa2-709. An electrophoretic mobility shift of the C-terminal truncation mutant mVKIND-aa2-337 was not observed suggesting a possible p38 phosphorylation target sequence within the linker region between the KIND1 and KIND2 domains or/and the KIND2 domain. The p38 MAP kinase was found to induce neurite outgrowth in response to hyperosmotic shock by activation of CREB (Kano *et al.*, 2007). These findings are indicative for a potential counter play of the p38 pathway as a positive acting factor in dendrite growth upon VKIND which negatively controls dendrite growth (Huang *et al.*, 2007).

### 5.6 | Outlook

The further exploration of the mVKIND protein has the potential to be a rewarding venture. Since the interaction and regulatory functions of several KIND domains is determined (Quinlan *et al.*, 2007; Huang *et al.*, 2007) while the precise purpose of the VKIND KIND1 domain remains obscure, its interaction partners may be identified by a yeast two-hybrid screening. The confirmed expression of the VKIND gene in brain tissue (Mees *et al.*, 2005) suggests the further study of VKIND in neuronal cells. The localization of the subcellular distribution of endogenous mVKIND in cultured mouse hippocampal and cerebellar cells with the anti-VKIND antibody may reveal the role of VKIND during various stages of neuronal morphological differentiation. To study the effects of VKIND on neuronal morphogenesis, mouse hippocampal neurons also may be infected with adenoviral vectors encoding the mVKINDfl and its truncation mutants. Furthermore, establishing stable VKIND expressing cell lines may reveal the VKIND signal transduction pathway. Also, the putative effect of the Nerve Growth Factor (NGF) on VKIND activity and dendritic growth can be addressed in cultured neuronal cells by NGF stimulation. Moreover, the effect of the *in vivo* p38 phosphorylation of VKIND on dendritic growth may be determined by exposing neuronal VKIND expressing cells to specific inhibitors of MKK6. Since the VKIND catalytic RasGEF domain is a CDC25 like domain closest related to the RasGEF domains of exchange factors specific for Rap GTPases (Mees *et al.*, 2005), its catalytic activity towards Rap and other representatives of the Ras subfamily GTPases can be investigated by performing *in vitro* and *in vivo* GEF assays. In addition, the VKIND gene function can be studied by a phenotypic characterization of a transgenic knock-in mouse model.

## Appendix I | *mVKIND* Sequence

**Mus musculus mRNA for very-KIND protein sequence (*VKIND* gene); accession: AJ580324.**

```

1/1                               31/11
atg cag gcc atg gac cca gcc tcc cgg ggc ttc tac gag gaa gat ggc aag gac ttg ggc
M Q A M D P A S R G F Y E E D G K D L G
61/21                               91/31
ttc tac gac ttc gag ccg ctc ccc acc ctg ccg gag gat gag gaa aat gtg tct ctg gct
F Y D F E P L P T L P E D E E N V S L A
121/41                               151/51
gac atc ctc tcc ctg cgg gac aga ggc ctc agt gag cag gag gcc tgg gct gtg tgc cta
D I L S L R D R G L S E Q E A W A V C L
181/61                               211/71
gag tgc agc ctg tcc atg cgg agt gtc gcc cac gca gcc atc ttc cag acc ctg tgc atc
E C S L S M R S V A H A A I F Q T L C I
241/81                               271/91
aca cca gac acc ttg gcc ttc aac acc agt gga aac gtg tgc ttc atg gaa cag ctc agt
T P D T L A F N T S G N V C F M E Q L S
301/101                               331/111
gat gac ccc gag ggt gcc ttt gta ccc cca gag ttt gac ctg aca gga aac acc ttt gag
D D P E G A F V P P E F D L T G N T F E
361/121                               391/131
gct cac atc tac tcc ctg ggg gcc aca ctg aag gct gcc ctg gag tat gtc cca gaa cca
A H I Y S L G A T L K A A L E Y V P E P
421/141                               451/151
gag ctg gag ccc aag ctg agc aca gac ctg gag gga ctg ctg agc cag atg cag gca gaa
E L E P K L S T D L E G L L S Q M Q A E
481/161                               511/171
gac ccc aga gag cgg ccg gac ctg gcg agc atc ata gca ctg tgt gag gag aag atg cag
D P R E R P D L A S I I A L C E E K M Q
541/181                               571/191
cct gtg tcc tca tgc cgc ctg tgc cgc agt ctc tca gcc att gga aga agg gtg ctc tcc
P V S S C R L C R S L S A I G R R V L S
601/201                               631/211
att gag tcc ttc gga gca ttc cag gag ctc agc gag aac aca tgg agg gga agg cct gct
I E S F G A F Q E L S E N T W R G R P A
661/221                               691/231
cca aga aac gtg ggg ccc aag aag atg cca gga gac ctc agc act gac cca gag gca ctg
P R N V G P K K M P G D L S T D P E A L
721/241                               751/251
ttc cca tca aag ggc cta ctc cag cct cct gct tcc agg gat gcc gag cag gag gct ggg
F P S K G L L Q P P A S R D A E Q E A G
781/261                               811/271
cag agg ccc aga gcc cca tcc ccc aaa cca ctg ctg tca gcc cct gtg aga aat ggt gag
Q R P R A P S P K P L L S A P V R N G E
841/281                               871/291
aac cca gga cag gaa ggg ctg gct gac ctt gtc ctg gat gcc agg tgc ccc ctg ggc gag
N P G Q E G L A D L V L D A R C P L G E
901/301                               931/311
ctg gac aga gac aac ctc agg cga agc cgg ctg aaa aag gct cag acg ttt ccc agg cta
L D R D N L R R S R L K K A Q T F P R L
961/321                               991/331
ctg cag gaa agc aca gag acc agc acc ctc tgc ctg tca ctg aac ggc tcg aga aac cag
L Q E S T E T S T L C L S L N G S R N Q
1021/341                               1051/351
ctg gcc ata tct gag ttc ttt ccc cca gac cct agg aag ctc ttc ctg gaa ggg aaa aat
L A I S E F F P P D P R K L F L E G K N
1081/361                               1111/371
ggc ctt tct ggt ttc aaa aca cag tcc aaa agc aga ctg tgg cca gag cag gag cct gga
G L S G F K T Q S K S R L W P E Q E P G
1141/381                               1171/391
gtc cag ttg gat aag aca cca ggt gca ggc cgc aac cca cac agg agt cca ggg gcc tcg
V Q L D K T P G A G R N P H R S P G A S
1201/401                               1231/411
ggg caa cta gag gct tca tct cct agc cag gga tct gta gag tac aaa cct tca ccc agc
G Q L E A S S P S Q G S V E Y K P S P S
1261/421                               1291/431
cct gta gac gct gga gat tca gac cat gaa ggc cac ata cct agg agt gaa gag aag att
P V D A G D S D H E G H I P R S E E K I
1321/441                               1351/451
cca gaa gaa tcc aga caa cct gga agc aca gcc act gaa cag agc ctg tcc ctg aag gac
P E E S R Q P G S T A T E Q S L S L K D
1381/461                               1411/471
ctt ctg tct aag cta ggc cgg ccc ttc agg gag tac gag ctg tgg gca ctg tgc ctc tcc
L L S K L G R P F R E Y E L W A L C L S

```

1441/481  
 tgc ctt agc act ctg cag aca cac aag gag cac cca gct cac ctg tgc ctg gac aac gtg  
 C L S T L Q T H K E H P A H L C L D N V  
 1501/501  
 ttg gtg gcc gag gac ggg aca gtg ttc ttc gga ccg ccc cct gcc aat ggc gcc tac aac  
 L V A E D G T V F F G P P A N G A Y N  
 1561/521  
 tca ctc ttc ttg gct ccc gaa gtg tca gaa gag aag ctg gtg aca gag aag gcc tct gtg  
 S L F L A P E V S E E K L V T E K A S V  
 1621/541  
 tac tgt gtg gct gcg gtt ctg tgg aca gca gcc aag ttc agc gta ccc cga gac cac aaa  
 Y C V A A V L W T A A K F S V P R D H K  
 1681/561  
 ctg gcc ctg cca cgt aga ctc aaa aca ctc ctt ctg gac atg gcc aga cgc cat gcc tca  
 L A L P R R L K T L L L D M A R R H A S  
 1741/581  
 gaa ccg cca tct gca gcc gag gcc atc aag gtg tgc agc agc tac ctc ctt cag cga ggc  
 E R P S A A E A I K V C S S Y L L Q R G  
 1801/601  
 atg gac agc agc aag att cta gcc cac ctg cgg gca tcc acc tgc aag gtt cac cca gag  
 M D S S K I L A H L R A S T C K V H P E  
 1861/621  
 gag gag acc atc ggc ctc cag aac gcc ttc tca gtg gtt gaa ctg aaa tcc acc acg gca  
 E E T I G L Q N A F S V V E L K S T T A  
 1921/641  
 cct gct cct gag agt agt ccc ggc ttc ctg cag gtc agc aat gat acc aag ctg gtc gct  
 P A P E S S P G F L Q V S N D T K L V A  
 1981/661  
 gtc cca ggg cct gtg cct ggt ctg ccc ccc tgc tgc aaa gaa gcc tgt gag ctg cca gca  
 V P G P V P G L P P C C K E A C E L P A  
 2041/681  
 gcc ttc acc tct gag gcc act cac ttt aag ccc ata gtc ctg gct cag gac gca agt gtt  
 A F T S E A T H F K P I V L A Q D A S V  
 2101/701  
 acc aga gac cag ctt gcc ttg ccc tca gag tca aat gag aaa ccc aaa gag gga agt ggt  
 T R D Q L A L P S E S N E K P K E G S G  
 2161/721  
 cat ctg gac agg gag gga aca aga aag cag gca gcc ctg gag ctt gtt gag gcc act gac  
 H L D R E G T R K Q A A L E L V E A T D  
 2221/741  
 cta aag atg tcc aac cag ctg tca cct ggt cca gag ctg cag gga gca act cca gac cct  
 L K M S N Q L S P G P E L Q G A T P D P  
 2281/761  
 gat ggt gac tca ggg tcc ccc agc tca gcc acg gaa tgt tcc tgc ccc cat ggc cct gct  
 D G D S G S P S S A T E C S C P H G P A  
 2341/781  
 ctg gtc acc cag caa aaa gga aca tca ggg aca ccc agc tct cct gcc tct tcc ctg ccc  
 L V T Q Q K G T S G T P S S P A S S L P  
 2401/801  
 cct gag cac agg cca gat ggt gag gga cca cta ggc acc act gtg ctc cca ggg ccc acc  
 P E H R P D G E G P L G T T V L P G P T  
 2461/821  
 tca gcc agc cag ggc tct cga cac cca tgt aag cca ccc agg ggt agg gct gca gcg agt  
 S A S Q G S R H P C K P P R G R A A A S  
 2521/841  
 cca agc agc cct agg ggc tcg gat ggt cat cct gag aag cct cgg cca gca gac cgc aag  
 P S S P R G S D G H P E K P R P A D R K  
 2581/861  
 ctc tgt cca tcc agt gta gat acc tca tcc ccc cct aag atg aca gcc tgc ccc tcg ctt  
 L C P S S V D T S S P P K M T A C P S L  
 2641/881  
 cag gaa gcc atg cgc ctc atc cag gag gaa ttt gcc ttt gat ggc tac atg gac aac ggg  
 Q E A M R L I Q E E F A F D G Y M D N G  
 2701/901  
 cta gag gca ctg atc atg ggg gag tat att tac gcc ttg aaa gac ctc acc ttc gcc acc  
 L E A L I M G E Y I Y A L K D L T F A T  
 2761/921  
 ttc tgt ggt gcc ata tct gag aag ttt tgt gac cta tac tgg gat gag cag ctg cta aag  
 F C G A I S E K F C D L Y W D E Q L L K  
 2821/941  
 aac ctc ttc aag gtg gtc aat ggg cca gcc tca ccc tct gag agc act aat gag gag cct  
 N L F K V V N G P A S P S E S T N E E P  
 2881/961  
 gga tcc cag cca gaa cac tca ccc agc aga tgc tca ctg tcc agc aaa agg cct tcc ctg  
 G S Q P E H S P S R C S L S S K R P S L  
 2941/981  
 cat gga ctc ggc aag gag aag cca gcc acg acc tgg ggc agc ggg gga ccc tgc tcc ccc  
 H G L G K E K P A T T W G S G G P C S P

3001/1001  
 aca gca cta tca gat ata gac tcc gac acg ctc tct cag gga aac ttt gag gtt gga ttt  
 T A L S D I D S D T L S Q G N F E V G F  
 3061/1021  
 cgg tct cag aag tca ata aaa gtc acg cga gag caa caa cca gag gcc gaa gtg ggt ggg  
 R S Q K S I K V T R E Q Q P E A E V G G  
 3121/1041  
 cag cca ggt cca agc cag gac tca acc agc cat gcc tcg gac aca gtg gcc cgg cta gct  
 Q P G P S Q D S T S H A S D T V A R L A  
 3181/1061  
 aga tct gag gac ggt ggc cca gct ggg tct cca ggg gca tct gat ttc cag aac tgc agc  
 R S E D G G P A G S P G A S D F Q N C S  
 3241/1081  
 cct ggc tgg tcc agt gcc ttc tat gag gct gag tgc ttt gga gcc gat gtc tac aac tac  
 P G W S S A F Y E A D C F G A D V Y N Y  
 3301/1101  
 gtg aag gat ctg gag agg cag aag gcc aac ggg cac aca gaa ctg gaa gcc cag agt cca  
 V K D L E R Q K A N G H T E L E A Q S P  
 3361/1121  
 gag ctg gag cag cag ctc atg ata gag aag agg aac tac agg aag acc ctg aag ttt tac  
 E L E Q Q L M I E K R N Y R K T L K F Y  
 3421/1141  
 cag aaa ctc tta cag aag gaa aaa cgg aac aaa ggc tct gag gtc agg acc atg ttg tct  
 Q K L L Q K E K R N K G S E V R T M L S  
 3481/1161  
 aaa ctt cga gga cag ctg gat gaa atg aag tcc aag gtg cag ttc ctg agc ctg gtc aag  
 K L R G Q L D E M K S K V Q F L S L V K  
 3541/1181  
 aag tac ctc cag gtc atg tat gca gaa cgc tgg ggg ctg gag ccc tgt gct ctg ccg gtg  
 K Y L Q V M Y A E R W G L E P C A L P V  
 3601/1201  
 att gtg aac atc gca gca gcc ccc ttt gac aca ctg gat ttc agc ccc ctg gat gag tct  
 I V N I A A A P F D T L D F S P L D E S  
 3661/1221  
 tct tcc ctc atc ttc tac aat gtc aac aag cac cca ggc agc ggc cga cag aag aag gct  
 S S L I F Y N V N K H P G S G R Q K K A  
 3721/1241  
 cgc atc cta cag gct ggt aca cca ctg ggg ctc atg gcc tac ctc tac tcc agt gat gct  
 R I L Q A G T P L G L M A Y L Y S S D A  
 3781/1261  
 ttc ctc gag ggc tac gtg cag cag ttt ctc tac act ttc cgg tac ttt tgc aca ccg cac  
 F L E G Y V Q Q F L Y T F R Y F C T P H  
 3841/1281  
 gac ttc ctg cac ttc ctc ctg gac cgc atc agc agc act tta tcc agg gct cac cag gat  
 D F L H F L L D R I S S T L S R A H Q D  
 3901/1301  
 cct acc tcg act ttt gcc aag atc tac agg cga agc ctc tgc gtc ctg cag gcc tgg gtg  
 P T S T F A K I Y R R S L C V L Q A W V  
 3961/1321  
 gaa gac tgc tac acc gtg gac ttc ata agg aac cgc ggg ctg ctg gga cag ctg gag gac  
 E D C Y T V D F I R N A G L L G Q L E D  
 4021/1341  
 ttc atc tct tcc aag atc cta cct cta gat ggc act gcc gag cac ctg ctg gcc ctc tta  
 F I S S K I L P L D G T A E H L L A L L  
 4081/1361  
 gag gtg ggc act gag cgg cgg gct gac agt gcc tct cga ggt gca gac ctg gag gac cct  
 E V G T E R R A D S A S R G A D L E D P  
 4141/1381  
 aag gag gca gag gag gac acc aga ccc ttt aat gcc ctc tgc aag agg ttc tca gag gat  
 K E A E E D T R P F N A L C K R F S E D  
 4201/1401  
 ggc atc acc cgg aag agc ttc tct tgg aga ctg cct cgg ggc aac ggg cta gtg ctg cca  
 G I T R K S F S W R L P R G N G L V L P  
 4261/1421  
 cat cat aag gag cgc cag tac acc att gca tcc gcc ctg cct aag ccc tgc ttc ttc gaa  
 H H K E R Q Y T I A S A L P K P C F F E  
 4321/1441  
 gac ttc tat ggc ccc tat gcc aaa gcc agt gag aag ggt cct tac ttc ttg aca gag tac  
 D F Y G P Y A K A S E K G P Y F L T E Y  
 4381/1461  
 agc acc aac cag ctc ttc act cag cta aca cta ctg cag cag gaa ttg ttt caa aag tgc  
 S T N Q L F T Q L T L L Q Q E L F Q K C  
 4441/1481  
 cac cct gtc cac ttc cta aat tca cga gcc ctg ggt gtc atg gac aaa agt gca gcc att  
 H P V H F L N S R A L G V M D K S A A I  
 4501/1501  
 ccc aaa gcc agc tct tct gag tct ctt tct gcc aaa acc tgc agc ctc ttc cta ccc aat  
 P K A S S S E S L S A K T C S L F L P N

```

4561/1521          4591/1531
tac gtc cag gac aaa tat ctg cta cag ctt tta aga aac gca gat gat gtc agt acc tgg
Y   V   Q   D   K   Y   L   L   Q   L   L   R   N   A   D   D   V   S   T   W
4621/1541          4651/1551
gtg gct gct gaa att gtg acc agt cat acc tcc aag ctt cag gtg aac ttg ctg tcc aaa
V   A   A   E   I   V   T   S   H   T   S   K   L   Q   V   N   L   L   S   K
4681/1561          4711/1571
ttc ctg ctg att gca aaa tct tgc tac gaa cag agg aac ttt gca acg gcc atg caa atc
F   L   L   I   A   K   S   C   Y   E   Q   R   N   F   A   T   A   M   Q   I
4741/1581          4771/1591
ctg ggc ggg ctg gag cac ctg gct gtg agg cag tcc cct gct tgg aga atc ctg cct gcg
L   G   G   L   E   H   L   A   V   R   Q   S   P   A   W   R   I   L   P   A
4801/1601          4831/1611
aag att gct gag gtc atg gaa gag ctg aaa gct gtg gag gta ttc ctg aag agt gac agc
K   I   A   E   V   M   E   E   L   K   A   V   E   V   F   L   K   S   D   S
4861/1621          4891/1631
ctg tgt ctg atg gaa gga agg cgc ttc cgg gcc cag cct act cta ccc tcc gcc cac ctg
L   C   L   M   E   G   R   R   F   R   A   Q   P   T   L   P   S   A   H   L
4921/1641          4951/1651
ctg gcc atg cac atc cag cag ctg gag aca gga ggt ttc acc atg act aat gga gcc cat
L   A   M   H   I   Q   Q   L   E   T   G   G   F   T   M   T   N   G   A   H
4981/1661          5011/1671
aga tgg agc aaa ctg aga aac atc gcc aag gtg gca agc cag gtg cac gcg ttc caa gag
R   W   S   K   L   R   N   I   A   K   V   A   S   Q   V   H   A   F   Q   E
5041/1681          5071/1691
aac ccg tac aca ttc agc ccg gac ccc aag cta cag gcc cac ctc aag cag agg atc gcc
N   P   Y   T   F   S   P   D   P   K   L   Q   A   H   L   K   Q   R   I   A
5101/1701          5131/1711
cgc ttt agc ggc gct gat gtc tcc att tta gca gct gat aac agg gcc aac ttc cac cag
R   F   S   G   A   D   V   S   I   L   A   A   D   N   R   A   N   F   H   Q
5161/1721          5191/1731
atc cca gga gag aaa cac tca cgg aag atc caa gac aag ctg agg aga atg aag gct aca
I   P   G   E   K   H   S   R   K   I   Q   D   K   L   R   R   M   K   A   T
5221/1741
ttc cag tag
F   Q   *

```

## Appendix II | Clone Charts

### pcDNA3-Myc-mVKIND-aa2-337

<b>RT-PCR:</b>	template	mouse cerebellum total RNA
	primer	<p><b>5'-mKISN-XbaI/HindIII+Myc</b> <i>Myc</i> →  XbaI HindIII Transl Ini M E Q K L I S E E D  5'- gc <u>TCT AGA AAG CTT GCC GCC GCC</u> ATG GAG CAG AAG CTG ATC TCC GAG GAG GAC  L Q A M D P A S  CTG CAG GCC ATG GAC CCA GCC TCC - 3'  VKIND 2. Codon codon 8  start 4 bp 24 bp</p> <p><b>3'-mKISN-afterXhoI</b>  P D P R K L F  coding sequence 5'- CCA GAC CCT AGG AAG CTC TTC - 3'  start 1045 bp 1066 bp  codon 349 codon 355</p> <p>primer sequence 5'- GAA GAG CTT CCT AGG GTC TGG - 3'</p>
<b>Cloning:</b>	<p>1st step: RT-PCR-fragment (≈ 1 kb ) (purified) digested with XbaI/XhoI and cloned into pcDNA3, linearised by XbaI/XhoI, named pcDNA3-Myc-mVKIND-aa2-337(a)</p> <p>2nd step: inverting the fragment, pcDNA3-Myc-mVKIND-aa2-337(a) linearised by HindIII/BamHI and cloned into pcDNA3, linearised by HindIII/BamHI, named pcDNA3-Myc-mVKIND-aa2-337</p>	

### pcDNA3-Myc-mVKIND-aa2-709

<b>RT-PCR:</b>	template	mouse cerebellum total RNA
	primer	<p><b>5'-mVKIND-beforeXhoI</b>  S T L C L S  5'- CC AGC ACC CTC TGC CTG TCA C - 3'  start 980 bp 1000 bp  codon 328 codon 332</p> <p><b>3'-mVKIND-afterBstXI+BamHI</b>  Q L A L P S BamHI  coding sequence 5'- C CAG CTT GCC TTG CCC TCA GA <u>GGA TCC</u> cg - 3'  start 2109 bp 2129 bp  codon 704 codon 709</p> <p>primer sequence 5'- cg <u>GGA TCC</u> TCT GAG GGC AAG GCA AGC TGG - 3'</p>
<b>Cloning:</b>	<p>1st step: RT-PCR-fragment (≈ 1.1 kb ) (purified) digested with XhoI/BamHI and cloned into pcDNA3-Myc-mVKIND-aa2-337(a), linearised by XhoI/BamHI, named pcDNA3-Myc-mVKIND-aa2-709(a)</p> <p>2nd step: inverting the fragment, pcDNA3-Myc-mVKIND-aa2-709(a) linearised by HindIII/BamHI and cloned into pcDNA3, linearised by HindIII/BamHI, named pcDNA3-Myc-mVKIND-aa2-709</p>	

### pcDNA3-Myc-mVKIND-aa2-1204

<b>RT-PCR:</b>	template	mouse cerebellum total RNA
	primer	<p><b>5'-mVKIND-beforeBstXI</b>  E L P A A F T  5'- GAG CTG CCA GCA GCC TTC ACC - 3'  start 2029 bp 2049 bp  codon 677 codon 683</p> <p><b>3'-mVKIND-3'-rev+KpnI</b>  P V I V N I KpnI  coding sequence 5'- G CCG GTG ATT GTG AAC ATC GC <u>GGT ACC</u> ccg - 3'  start 3594 bp 3614 bp  codon 1199 codon 1204</p> <p>primer sequence 5'- ccg <u>GGT ACC</u> GCG ATG TTC ACA ATC ACC GGC - 3'</p>
<b>Cloning:</b>	<p>1st step: RT-PCR-fragment (≈ 1.5 kb ) (purified) digested with BstXI/KpnI and cloned into pcDNA3-Myc-aa2-709, linearised by BstXI/KpnI, named pcDNA3-Myc-mVKIND-aa2-1204(a)</p> <p>2nd step: inverting the fragment, pcDNA3-Myc-mVKIND-aa2-1204(a) linearised by KpnI, and pcDNA3 linearised by XhoI, both treated with Klenow pcDNA3-Myc-mVKIND-aa2-1204(a) (KpnI/Klenow) digested with HindIII and cloned into pcDNA3 (XhoI/Klenow), digested with HindIII, named pcDNA3-Myc-mVKIND-aa2-1204</p>	

**pcDNA3-Myc-mVKIND-2-1234**

<b>PCR:</b>	template	pcDNA3:Myc-VKINDfl
	primer	<p><b>5'-mKISNXbaI/HindIII-Myc</b> <i>Myc</i> →  XbaI HindIII Transl Ini M E Q K L I S E E D  5'-gc TCT AGA AAG CTT <b>GCC GCC GCC</b> ATG GAG CAG AAG CTG ATC TCC GAG GAG GAC  L <b>Q A M D P A S</b>  CTG CAG GCC ATG GAC CCA GCC TCC - 3'</p> <p><b>VKIND 2. Codon</b>  start 4 bp 24 bp</p> <hr/> <p><b>3'-ab3682bp+EcoRI</b>  V N K H P G S EcoRI  coding sequence 5'-GTC AAC AAG CAC CCA GGC AGC <b>GAA TTC</b> cg - 3'  start 3682 end 3702 bp  codon 1228 codon 1234</p> <hr/> <p>primer sequence 5'-cg <b>GAA TTC</b> GCT GCC TGG GTG CTT GTT GAC - 3'</p>
<b>Cloning:</b>	PCR-fragment (≈ 3.7 kb, codon2-1234) digested with HindIII/EcoRI cloned into pcDNA3 linearised by HindIII/EcoRI, named pcDNA3-Myc-mVKIND-aa2-1234	

**pcDNA3-Myc-mVKIND-aa2-1349**

<b>RT-PCR:</b>	template	mouse cerebellum total RNA
	primer	<p><b>5'-vKIND-before NheI</b>  D S T S H A S  5'- GAC TCA ACC AGC CAT GCC TCG - 3'  start 3139 bp 3135 bp  codon 1047 codon 1053</p> <hr/> <p><b>3'-vKIND-after XbaI</b>  A L L E V G T  coding sequence 5'- GCC CTC TTA GAG GTG GGC ACT - 3'  start 4072 bp 4092 bpP  codon 1358 codon 1364</p> <hr/> <p>primer sequence 5'- AGT GCC CAC CTC TAA GAG GGC - 3'</p>
<b>Cloning:</b>	PCR-fragment (≈ 1kb, codon 1047-1364) digested with NheI/XbaI, and cloned into pcDNA3-Myc-mVKIND-aa2-1204, digested with NheI/XbaI, dephosphorylated by CIP, named pcDNA3-Myc-mVKIND-aa2-1349	

**pSport1-Myc-mVKIND-aa2-1349**

<b>Cloning:</b>	Insert: pcDNA3-Myc-mVKIND-aa2-1349 digested with HindIII/XbaI and cloned into Vector pSport1, digested with HindIII/XbaI, named pSport1-Myc-mVKIND-aa2-1349
-----------------	---

**pSport1-mVKIND-aa1349-1742**

<b>RT-PCR:</b>	template	mouse cerebellum total RNA
	primer	<p><b>5'-vKIND-before XbaI</b>  G L L G Q L E  5'- GGG CTG CTG GGA CAG CTG GAG - 3'  start 3997 bp 4017 bp  codon 1333 codon 1339</p> <hr/> <p><b>3'-vKIND-Ende+EcoRI</b>  M K A T F Q stop EcoRI  coding sequence 5'- ATG AAG GCC ACA TTC CAG TAG <b>GAA TTC</b> cg - 3'  start 5209 bp 5229 bp  codon 1737 codon 1743</p> <hr/> <p>primer sequence 5'-cg <b>GAA TTC</b> CTA CTG GAA TGT GGC CTT CAT - 3'</p>
<b>Cloning:</b>	PCR fragment (≈ 1.2 kb, codon 1333-1742) digested with XbaI/EcoRI and cloned into pSport1, digested with XbaI/EcoRI, named pSport1-mVKIND-aa1349-1742	

**pSport1-Myc-mVKINDfl**

<b>Cloning:</b>	Insert: pSport1-mVKIND-aa1349-1742 digested with XbaI/EcoRI and cloned into Vector pSport1-Myc-mVKIND-aa2-1349 digested with XbaI/EcoRI, named pSport1-Myc-mVKINDfl
-----------------	---



**pcDNA3-Myc-mVKINDfl**

<b>Cloning:</b>	Insert: pSport1-Myc-mVKINDfl linearised by SnaBI, Vector pcDNA3 linearised by HindIII, both treated with Klenow; Insert: pSport1-Myc-mVKINDfl (SnaBI/Klenow) digested by EcoRI and cloned into Vector pcDNA3 (HindIII/Klenow), digested by EcoRI, named pcDNA3-Myc-mVKINDfl
-----------------	--

**pcDNA3-Doublecortin**

<b>RT-PCR:</b>	template	day 14.5 mouse embryo total RNA (C57BL/6)
	primer	<p><b>BamHI-m-Doublecortin-CT-5'</b>            BamHI S Y V C S S D            5'- GC <u>GGATCC</u> AGC TAT GTC TGC TCC TCA GAC - 3'            start 370 bp 390 bp</p> <p><b>m-Doublecortin-CT-EcoRI-3'</b>            S L G D S M stop EcoRI            coding sequence 5'- TCA CTT GGC GAT TCC ATG TGA <u>GAA TTC</u> gc - 3'            start 1063 bp 1082 bp</p> <p>primer sequence 5'- GC <u>GAA TTC</u> TCA CAT GGA ATC GCC AAG TGA - 3'</p>
<b>Cloning:</b>	PCR-fragment (712 bp, codon 124-360) digested with BamHI/EcoRI into pcDNA3 linearised by BamHI/EcoRI, named pcDNA3-Doublecortin	

**pcDNA3-Islet1**

<b>RT-PCR:</b>	template	day 14.5 mouse embryo total RNA (C57BL/6)
	primer	<p><b>BamHI-m-Islet1-CT-5'</b>            BamHI C R A D H D V            5'- GC <u>GGATCC</u> TGC CGT GCA GAC CAC GAT GTG - 3'            start 385 bp 405 bp</p> <p><b>m-Islet1-CT-EcoRI-3'</b>            A S P I E A stop EcoRI            coding sequence 5'- GCC AGT CCT ATT GAG GCA TGA <u>GAATTC</u> GC - 3'            start 1030 bp 1050 bp</p> <p>primer sequence 5'- GC <u>GAATTC</u> TCA TGC CTC AAT AGG ACT GGC - 3'</p>
<b>Cloning:</b>	PCR-fragment (661 bp, codon 129-350 ) digested with BamHI/EcoRI, cloned into pcDNA3 linearised by BamHI/EcoRI, named pcDNA3-Islet1	

**pEGFP-C1-mVKIND-aa2-355**

<b>PCR:</b>	template	pcDNA3-Myc-mVKIND-aa2-1204
	primer	<p><b>5'-fr.I+BglII</b>            BglII Q A M D P A S            5'- <u>ga AGA TCT</u> CAG GCC ATG GAC CCA GCC TCC - 3'            start 4 bp 24 bp            codon 2 codon 8</p> <p><b>3'-fr.I-afterXhoI+EcoRI</b>            P D P R K L F EcoRI            coding sequence 5'- CCA GAC CCT AGG AAG CTC TTC <u>GAA TTC</u> <u>cg</u>- 3'            start 1045 bp 1066 bp            codon 349 codon 355</p> <p>primer sequence 5'- <u>cg GAA TTC</u> GAA GAG CTT CCT AGG GTC TGG - 3'</p>
<b>Cloning:</b>	PCR-fragment (≈ 1 kb, codon 2-355) digested with BglIII/EcoRI cloned into pEGFP-C1 linearised by BglIII/EcoRI, named pEGFP-C1-mVKIND-aa2-355	

**pEGFP-C1-mVKIND-aa2-709**

<b>PCR:</b>	template	pcDNA3-Myc-mVKIND-aa2-1204
	primer	<p><b>5'-vKIND-beforeXhoI</b></p> <p style="text-align: center;">S T L C L S</p> <p>5'- CC AGC ACC CTC TGC CTG TCA C - 3'</p> <p style="text-align: center;">start 980 bp                                  1000 bp</p> <p style="text-align: center;">codon 32    codon 332</p> <hr/> <p><b>3'-vKIND-afterBstXI+BamHI</b></p> <p style="text-align: center;">  Q L A L P S           BamHI</p> <p>coding sequence      5'- C CAG CTT GCC TTG CCC TCA GA <u>GGA TCC</u> cg- 3'</p> <p style="text-align: center;">start 2109 bp    2129 bp</p> <p style="text-align: center;">codon 704    codon 709</p> <p>primer sequence     5'- cg <u>GGA TTC</u> TCT GAG GGC AAG GCA AGC TGG- 3'</p>
<b>Cloning:</b>	PCR-fragment (≈ 1.1 kb) digested with XhoI/BamHI into pEGFP-C1-mVKIND-aa2-355 linearised by XhoI/BamHI, named pEGFP-C1-mVKIND-aa2-709	

**pEGFP-C1-mVKIND-aa2-1204**

<b>Cloning:</b>	Insert: pcDNA3-Myc-mVKIND-aa2-1204 digested with BamHI/XbaI and cloned into Vector pEGFP-C1-mVKIND-aa2-709 linearised by BamHI/XbaI, named pEGFP-C1-mVKIND-aa2-1204
-----------------	---

**pEGFP-C1-mVKINDfl**

<b>Cloning:</b>	Insert: pSport1-Myc-mVKINDfl digested with SacI/KpnI and cloned into Vector pEGFP-C1-mVKIND-aa2-355 digested by SacI/KpnI, named pEGFP-C1-mVKINDfl
-----------------	--

**pcDNA3-Myc-mVKIND-456-1742**

<b>PCR:</b>	template	pcDNA3-Myc-mVKINDfl
	primer	<p><b>5'KpnI+Myc-ab1366</b>                                        <i>Myc</i> →</p> <p style="text-align: center;">KpnI            Transl Ini    M E Q K L I S E</p> <p>5'- gg <u>GGT ACC GGC GCC GCC</u> ATG GAG CAG AAG CTG ATC TCC GAG</p> <p style="text-align: center;">E D L L S L K D L L</p> <p>GAG GAC CTG CTG TCC CTG AAG GAC CTT CTG- 3'</p> <p style="text-align: center;">start1366 bp    1386 bp</p> <p style="text-align: center;">codon 456    codon 462</p> <hr/> <p><b>3'-vKIND-Ende+EcoRI</b></p> <p style="text-align: center;">  M K A T F Q stop EcoRI</p> <p>coding sequence      5'- ATG AAG GCT ACA TTC CAG TAG <u>GAA TTC</u> cg - 3'</p> <p style="text-align: center;">start 5209 bp    5229 bp</p> <p style="text-align: center;">codon 1737    codon 1743</p> <p>primer sequence     5'- cg <u>GAA TTC</u> CTA CTG GAA TGT GGC CTT CAT - 3'</p>
<b>Cloning:</b>	PCR-fragment (≈ 4.0 kb, codon 456-1742) digested with KpnI/EcoRI and cloned into pcDNA3 linearised by KpnI/EcoRI, named pcDNA3-Myc-mVKIND-aa456-1742	

**pcDNA3-Myc-mVKIND-aa614-1742**

<b>PCR:</b>	template	pcDNA3-Myc-mVKINDfl
	primer	<p><b>5'KpnI+Myc-ab1840</b>                                        <i>Myc</i> →</p> <p style="text-align: center;">KpnI            Transl Ini    M E Q K L I S E</p> <p>5'- gg <u>GGT ACC GGC GCC GCC</u> ATG GAG CAG AAG CTG ATC TCC GAG</p> <p style="text-align: center;">E D L T C K V H P E</p> <p>GAG GAC CTG ACC TGC AAG GTT CAC CCA GAG- 3'</p> <p style="text-align: center;">start 1840 bp    1860 bp</p> <p style="text-align: center;">codon 614    codon 620</p> <hr/> <p><b>3'-vKIND-Ende+EcoRI</b></p> <p style="text-align: center;">  M K A T F Q stop EcoRI</p> <p>coding sequence      5'- ATG AAG GCC ACA TTC CAG TAG <u>GAA TTC</u> cg - 3'</p> <p style="text-align: center;">start 5209 bp    5229 bp</p> <p style="text-align: center;">codon 1737    codon 1743</p> <p>primer sequence     5'- cg <u>GAA TTC</u> CTA CTG GAA TGT GGC CTT CAT - 3'</p>
<b>Cloning:</b>	PCR-fragment (≈ 3.4 kb, codon 614-620 ) digested with KpnI/EcoRI and cloned into pcDNA3 linearised by KpnI/EcoRI, named pcDNA3-Myc-mVKIND-aa614-1742	

**pcDNA3-Myc-mVKIND-aa1451-1742**

<b>RT-PCR:</b>	template	mouse cerebellum total RNA
	primer	<p><b>5'-Ras-GEF-BamHI+Myc</b> <i>Myc</i> →  BamHI Transl Ini M E Q K L I S E  5'- gc <u>GGA TCC GCC GCC GCC</u> ATG GAG CAG AAG CTG ATC TCC GAG  E D L E K G P Y F L  GAG GAC CTG GAG AAG GGT CCT TAC TTC TTG- 3'  start 4351 bp 4371 bp  codon 1451 codon 1457</p> <hr/> <p><b>3'-Ras-GEF-EcoRI</b>  M K A T F Q stop EcoRI  coding sequence 5'- ATG AAG GCC ACA TTC CAG TAG <u>GAA TTC</u> cg - 3'  start 5209 5229 bp  codon 1737 codon 1743</p> <p>primer sequence 5'- cg <u>GAA TTC</u> CTA CTG GAA TGT GGC CTT CAT - 3'</p>
<b>Cloning:</b>	RT-PCR-fragment (≈ 880 bp, codon 1451-1742) (purified) digested with BamHI/EcoRI and cloned into pcDNA3, linearised by BamHI/EcoRI, named pcDNA3-Myc-mVKIND-aa1451-1742	

**pSport1-mVKIND-Δaa880-1235**

<b>PCR:</b>	template	pSport1-Myc-mVKINDfl
	primer	<p><b>5'-873-879+1236-1242</b>  K M T A C P S R Q K K A R I  5'- AAG ATG ACA GCC TGC CCC TGC <u>CGA CAG AAG AAG GCT CGC ATC</u> -3'  start 2617 bp end 2638 bp <b>start 3706 bp end 3726 bp</b>  codon 873 codon 879 <b>codon 1236 codon 1242</b></p> <hr/> <p><b>3'-873-879+1236-1242</b>  K M T A C P S R Q K K A R I  coding sequence 5'- AAG ATG ACA GCC TGC CCC TGC <u>CGA CAG AAG AAG GCT CGC ATC</u> - 3'  start 2617 bp end 2638 bp <b>start 3706 bp end 3726 bp</b>  codon 873 codon 879 <b>codon 1236 codon 1242</b></p> <p>primer sequence 5'- GAT GCG AGC CTT CTT CTG TCG GCA GGG GCA GGC TGT CAT CTT - 3'</p>
<b>Cloning:</b>	PCR fragment (≈ 8.3 kb) digested with DpnI followed by bacterial transformation	

**pTopo-mVKIND-Δaa880-1235**

<b>PCR:</b>	template	pSport1-mVKIND-Δaa880-1235
	primer	<p><b>5'-Topo4delMut</b>  HindIII Transl Ini <i>Myc</i> →  5'- CACC <u>AAG CTT</u> GCC GCC GCC ATG GAG-3'</p> <hr/> <p><b>3'-Topo4delMut+E</b>  stop EcoRI  coding sequence 5'- atg aag gct aca ttc cag tag <u>GAA TTC</u> - 3'  start 5209 bp end 5229 bp  codon 1737 codon 1743</p> <p>primer sequence 5'- GAA TTC cta ctg gaa tgt agc ctt cat - 3'</p>
<b>Cloning:</b>	PCR fragment (≈ 4.2 kb) cloned into pcDNA3.1D/V5-His-Topo, named pTopo-mVKIND-Δaa880-1235	

**pSport1-mVKIND-Δaa880-948**

<b>PCR:</b>	template	pSport1-Myc-mVKINDfl
	primer	<p><b>5'-873-879+949-955</b>  K M T A C P S P A S P S E S  5'- AAG ATG ACA GCC TGC CCC TCG <u>CCA GCC TCA CCC TCT GAG AGC</u> -3'  start 2617 bp end 2638 bp <b>start 2845 bp end 2865 bp</b>  codon 873 codon 879 <b>codon 949 codon 955</b></p> <hr/> <p><b>3'-873-879+949-955</b>  K M T A C P S P A S P S E S  coding sequence 5'- AAG ATG ACA GCC TGC CCC TCG <u>CCA GCC TCA CCC TCT GAG AGC</u> - 3'  start 2617 bp end 2638 bp <b>start 2845 bp end 2865 bp</b>  codon 873 codon 879 <b>codon 949 codon 955</b></p> <p>primer sequence 5'- GCT CTC AGA GGG TGA GGC TGG CGA GGG GCA GGC TGT CAT CTT - 3'</p>
<b>Cloning:</b>	PCR fragment (≈ 9.2 kb) digested with DpnI followed by bacterial transformation	

**pTopo-mVKIND-Δaa880-948**

<b>PCR:</b>	template	pSport1- mVKIND-Δaa880-948
	primer	<p><b>5'-Topo4delMut</b> HindIII          TI          Myc → 5'- CACC <u>AAG CTT</u> GCC GCC GCC ATG GAG-3'</p> <p><b>3'-Topo4delMut+E</b> stop EcoRI coding sequence    5'- atg aag gct aca ttc cag tag <u>GAA TTC</u> - 3' start 5209 bp                                  5229 bp codon    codon 1743</p> <p>primer sequence    5'- GAA TTC cta ctg gaa tgt agc ctt cat - 3'</p>
<b>Cloning:</b>	PCR fragment (≈ 5 kb) cloned into pcDNA3.1D/V5-His-Topo, named pTopo:mVKIND-Δaa880-948	

**pSport-1-mVKIND-Δaa1059-1235**

<b>PCR:</b>	template	pSport1-Myc-mVKINDfl
	primer	<p><b>5'-1052-1058+1236-1242</b> A S D T V A R R Q K K A R I 5'- GCC TCG GAC ACA GTG GCC CGG <b>CGA CAG AAG AAG GCT CGC ATC</b> -3' start 3154 bp                                  end 3174 bp <b>start 3706 bp</b>                                  end 3726 bp codon 1052    codon 1058 <b>codon 1236</b>    codon 1242</p> <p><b>3'-1052-1058+1236-1242</b> A S D T V A R R Q K K A R I coding sequence    5'- GCC TCG GAC ACA GTG GCC CGG <b>CGA CAG AAG AAG GCT CGC ATC</b> - 3' start 3154 bp                                  end 3174 bp <b>start 3706 bp</b>                                  end 3726 bp codon 1052    codon1058 <b>codon 1236</b>    codon 1242</p> <p>primer sequence    5'- GAT GCG AGC CTT CTT CTG TCG CCG GGC CAC TGT GTC CGA GGC - 3'</p>
<b>Cloning:</b>	PCR fragment (≈ 8.9 kb) digested with DpnI followed by bacterial transformation	

**pTopo-mVKIND-Δaa1059-1235**

<b>PCR:</b>	template	pSport1- mVKIND-Δaa1059-1235
	primer	<p><b>5'-Topo4delMut</b> HindIII          TI          Myc → 5'- CACC <u>AAG CTT</u> GCC GCC GCC ATG GAG-3'</p> <p><b>3'-Topo4delMut+E</b> stop EcoRI coding sequence    5'- atg aag gct aca ttc cag tag <u>GAA TTC</u> - 3' start 5209 bp                                  5229 bp codon 1737    codon 1743</p> <p>primer sequence    5'- GAA TTC cta ctg gaa tgt agc ctt cat - 3'</p>
<b>Cloning:</b>	PCR fragment (≈ 4.7 kb) cloned into pcDNA3.1D/V5-His-Topo, named pTopo-mVKIND-Δ aa1059-1235	

**pSport1-mVKIND-Δaa1238-1364**

<b>PCR:</b>	template	pSport1-Myc-mVKINDfl
	primer	<p><b>5'-withoutRasGEFN</b> H P G S G R Q E R R A D S A 5'- CAC CCA GGC AGC GGC CGA CAG <b>GAG CGG CGG GCT GAC AGT GCC</b> -3' start 3691 bp                                  end 3711 bp <b>start 4093 bp</b>                                  end 4113 bp codon 1231    codon 1237 <b>codon 1365</b>    codon 1371</p> <p><b>3'-withoutRasGEFN</b> coding sequence    5'- CAC CCA GGC AGC GGC CGA CAG <b>GAG CGG CGG GCT GAC AGT GCC</b> -3' start 3691 bp                                  end 3711 bp <b>start 4093 bp</b>                                  end 4113 bp codon 1231    codon 1237 <b>codon 1365</b>    codon 1371</p> <p>primer sequence    5'- GGC ACT GTC AGC CCG CCG CTC CTG TCG GGC GCT GCC TGG GTG - 3'</p>
<b>Cloning:</b>	PCR fragment (≈ 9 kb) digested with DpnI followed by bacterial transformation	

**pTopo-mVKIND-Δaa1238-1364**

<b>PCR:</b>	template	pSport1: mVKIND-Δaa1238-1364
	primer	<p><b>5'-Topo4delMut</b> HindIII                      TI                      Myc → 5'- CACC <u>AAG CTT</u> GCC GCC GCC ATG GAG-3'</p> <hr/> <p><b>3'-Topo4delMut+E</b></p> <p>coding sequence                      stop    EcoRI 5'- atg aag gct aca ttc cag tag <u>GAA TTC</u> - 3' start 5209 bp                      end 5229 bp codon 1737                      codon 1743</p> <p>primer sequence                      5'- GAA TTC cta ctg gaa tgt agc ctt cat - 3'</p>
<b>Cloning:</b>	PCR fragment (≈ 4.8 kb) cloned into pcDNA3.1D/V5-His-Topo, named pTopo-mVKIND-Δaa1238-1364	

**pGEX-6P-1-mVKIND-aa219-453**

<b>PCR:</b>	template	pcDNA3:Myc-mVKINDfl
	primer	<p><b>5'-vKIND-BamHI-655bp</b> BamHI P A P R N V G 5'- gc <u>GGA TCC</u> CCT GCT CCA AGA AAC GTG GGG - 3' codon 219                      codon 225 start 655 bp                      765 bp</p> <hr/> <p><b>3'-vKIND-1340bp-EcoRI</b></p> <p>coding sequence                      P G S T A T E    EcoRI 5'- CCT GGA AGC ACA GCC ACT GAA <u>GAA TTC</u> cg- 3' start 1339 bp                      bp 1359bp codon 447                      codon 453</p> <p>primer sequence                      5'- cg <u>GAA TTC</u> TTC AGT GGC TGT GCT TCC AGG - 3'</p>
<b>Cloning:</b>	PCR-fragment (≈ 700 bp, codon 219-453) was digested by BamHI/EcoRI and cloned into pGEX-6P-1, primary digested by BamHI/EcoRI	

## Appendix III | Abbreviations

2-ME	ethylene glycol monomethyl ether
Abi1	Abl-Interactor-1, also E3B1
ACK	acetate kinase
ADP	adenosine diphosphate
AF6	ALL-1 fusion partner on chromosome 6
AKT	also PKB, protein kinase B
Arp 2/3	actin-related proteins 2 and 3
ATP	adenosine triphosphate
BGH pA	bovine growth hormone polyadenylation signal
BLAST	Basic Local Alignment Search Tool
bp	base pair
BPB	bromphenol blue
c	complementary
C57BL/6	C57 black 6
cam <sup>r</sup>	chloramphenicol resistance
cAPK	$\alpha$ cAMP-dependent protein kinase catalytic subunit, also PKA
Capu	Cappuccino
CBL	Casitas B-lineage lymphoma
CC	coiled-coil
CD1	cluster of differentiation 1
CDC25	cell division cycle 25
cDNA	complementary DNA
CH	calponin homology
CIP	calf intestinal phosphatase
CMV	Cytomegalovirus promotor
CNB	cyclic nucleotide-binding
CTP	cytidine triphosphate
DAG	diacylglycerol
DCC	deleted in colon cancer
DH	dibble homology
DMEM	Dulbecco's Modified Eagle Medium
DMSO	Dimethylsulfoxide
DNA	deoxyribonucleic acid
dNTPs	Desoxyribonukleosid-5'-triphosphate
DRG	dorsal root ganglia
dsDNA	double strand DNA
dT	oligo-dT, thymidine
e.g.	exempli gratia
ECL	enhanced chemiluminescence
EF-G	elongation factor G
EF-Tu	elongation factor Tu
EGF	epidermal growth factor
Eps8	epidermal growth factor receptor pathway substrate 8
ERK	extracellular signal-regulated kinase
EST	expressed sequence tag
FERM	four point one, Ezrin, Radaxin, and Moesin four point one, Ezrin, Radaxin, and Moesin

FH1 and FH2	formin homology domains
G force	standard gravity, 9.80665 m/s <sup>2</sup>
G proteins	guanine nucleotide binding proteins, GTP-binding proteins
GAP	GTPases-activating protein
GBP	guanylate-binding protein
GDP	guanosine diphosphate
GEF	guanine nucleotide exchange factor
GNBPs	guanine nucleotide binding proteins
GPCR	G-protein-coupled receptor
GRB2	growth factor receptor-bound protein 2
GTP	guanosine triphosphate
GTPases	small guanosine triphosphatases
HB-EGF	heparin-binding EGF
H-Ras	Harvey rat sarcoma
HRP-linked	horseradish peroxidase linked
i.a.	inter alia
i.e.	id est
IF-2	initiation factor 2
Inositol-P	inositol monophosphate
IPTG	isopropyl- $\beta$ -D-thiogalactopyranoside
IS	inhibitory switch
JNK	c-Jun N-terminal kinase
kb	kbp, kilo base pairs
kD	kilo Dalton
KI	kinase inhibitor
KIND	kinase non-catalytic C-lobe domain
K-Ras	Kirsten sarcoma
KSR	kinase suppressor of Ras
l	liter
lacI	lactose repressor gene
m	murine
MAP	mitogen-activated protein
MAPK	mitogen-activated protein kinase
MARK	microtubule affinity regulating kinase
MEK	mitogen and extracellular regulated kinase
mg	milligram
min	minute
MKK6	mitogen-activated protein kinase kinase 6
ml	milliliter
M-Myc	M-Myc epitope peptide
MP	metalloproteinase
mpH <sub>2</sub> O	millipore water
NaAC	sodium acetate
NF1	neurofibromin
NORE1	N-Oct-3 responsive element 1
N-Ras	Neuroblastoma sarcoma
OD	optical density
ori	origin
P loop	phosphate binding site
PAGE	Polyacrylamide gel electrophoresis

PAK	p21 <sup>rac/cdc42</sup> -activated kinase
PCR	polymerase chain reaction
PKD1	phosphatidylinositol-dependent kinase 1
PDZ	domain present in PSD-95, Dil and Zo-1/2
PFA	paraformaldehyde
pH	potential of hydrogen
PH	pleckstrin homology
PI3K	phosphatidylinositol 3-kinase
PIP	1-phosphatidylinositol phosphate
PIP <sub>2</sub>	1-phosphatidylinositol-4,5-bisphosphate
PIP <sub>3</sub>	phosphatidylinositol-3,4,5-triphosphate
PKA	cAMP-dependent protein kinase, protein kinase A
PKC	protein kinase C
PKC $\zeta$	Protein kinase C $\zeta$
PLC $\epsilon$	phospholipase Cepsilon
Pol	polymerase
PSI-BLAST	Position-Specific Iterative BLAST
PTP-BAS	PTP-Basophil
PTP-BL	protein-tyrosine phosphatase-BAS-like
Pyk2	proline-rich tyrosine kinase 2
Raf	rapidly growing fibrosarcoma
RalGDS	Ral guanine nucleotide dissociation stimulator
Rap	Ras-related protein
Ras	rat sarcoma
RasGRF	guanine nucleotide releasing factor
RasGRP	guanyl nucleotide releasing protein
RASSF	Ras association domain family
RBD	Ras binding domain
Rce1	Ras and a factor converting enzyme
REM	Ras exchanger motif, also RasGEFN
RF-3	release factor 3
Rin1	Ras interference 1
RNA	ribonucleic acid
RNAse	Ribonuclease
rpm	revolutions per minute
RT	room temperature
RTK	receptor tyrosine kinase
RT-PCR	Reverse Transcription Polymerase Chain Reaction
s	second
SH2	Src homology 2
SH3	Src homology 3
SHC	Src homologous and collagen-like
SMART	Simple Modular Architecture Research Tool
SOS	Son of sevenless
SP6	bacteriophage SP6 promotor
Src	Sarcomatoid renal carcinoma
SRP	SRP-R signal recognition particle, receptor
ssDNA	single strand DNA
TGF $\alpha$	transforming growth factor- $\alpha$
Tiam1	T lymphoma invasion and metastasis protein 1



---

T <sub>m</sub>	annealing temperature
U	unit
UV	ultra violet
VKIND	very-KIND
WB	western blot
WH2	Wiskott-Aldrich homology region 2

## Appendix IV | List of Publications

**Mees A**, Rock R, Ciccarelli FD, Leberfinger CB, Borawski JM, Bork P, Wiese S, Gessler M & Kerkhoff E. (2005) Very-KIND is a novel nervous system specific guanine nucleotide exchange factor for Ras GTPases. *Gene Expr Patterns* **6**(1): 79-85.

Quinlan ME, Hilgert S, **Bedrossian A**, Mullins RD & Kerkhoff E. (2007) Regulatory interactions between two actin nucleators, Spire and Cappuccino. *The Journal of cell biology* **179**(1): 117-28.

**Poster:**

Hilgert S, **Mees A**, Borawski JM, Leberfinger CB, Kerkhoff E (2004) The novel KIND motif mediates the interaction of the distinct actin organizers Spir and Cappuccino. Symposium on Visualising Cytoskeletal Architecture and Dynamics by Light and Electron Microscopy, Dresden, Oktober 2004

## Appendix V | Vita

### PERSONAL INFORMATION

---

Name	Anaid Bedrossian (formerly Mees)
Date of birth	23.05.1974
Place of birth	Sofia, Bulgaria

### EDUCATION

---

1994	Abitur (equivalent to High School Exam) Immanuel-Kant-Schule, Kelkheim/Ts, Germany
1994-1996	Undergraduate studies biology University Würzburg, Germany
1996	Vordiploma in biology (equivalent to B.Sc. degree) University Würzburg, Germany
1996-2002	Graduate studies biology University Würzburg, Germany
2001-2002	Diploma thesis: ‘Construction of Vectors for the Somatic Gene Therapy’ at the Institute of Biochemistry University Würzburg, Germany Supervisor: Prof. Dr. F. Grummt
2002	Diploma in biology (equivalent to M.Sc. degree) University Würzburg, Germany
2002-2008	Ph.D. work at the Institute for Medical Radiation and Cell Research University Würzburg, Germany Supervisors: Prof. Dr. E. Kerkhoff Prof. Dr. G. Krohne

## Bibliography

- Aghazadeh B, Lowry WE, Huang XY & Rosen MK. (2000) Structural basis for relief of autoinhibition of the Dbl homology domain of proto-oncogene Vav by tyrosine phosphorylation. *Cell* **102**(5): 625-33.
- Agutter PS, Malone PC & Wheatley DN. (1995) Intracellular transport mechanisms: a critique of diffusion theory. *Journal of theoretical biology* **176**(2): 261-72.
- Alcantara S, Ruiz M, De Castro F, Soriano E & Sotelo C. (2000) Netrin 1 acts as an attractive or as a repulsive cue for distinct migrating neurons during the development of the cerebellar system. *Development (Cambridge, England)* **127**(7): 1359-72.
- Altschul SF, Madden TL, Schaffer AA, Zhang J, Zhang Z, Miller W & Lipman DJ. (1997) Gapped BLAST and PSI-BLAST: a new generation of protein database search programs. *Nucleic acids research* **25**(17): 3389-402.
- Alvarez Otero R, Sotelo C & Alvarado-Mallart RM. (1993) Chick/quail chimeras with partial cerebellar grafts: an analysis of the origin and migration of cerebellar cells. *The Journal of comparative neurology* **333**(4): 597-615.
- Apic G, Gough J & Teichmann SA. (2001a) Domain combinations in archaeal, eubacterial and eukaryotic proteomes. *Journal of molecular biology* **310**(2): 311-25.
- Apic G, Gough J & Teichmann SA. (2001b) An insight into domain combinations. *Bioinformatics (Oxford, England)* **17 Suppl 1**: S83-9.
- Apolloni A, Prior IA, Lindsay M, Parton RG & Hancock JF. (2000) H-ras but not K-ras traffics to the plasma membrane through the exocytic pathway. *Molecular and cellular biology* **20**(7): 2475-87.
- Appel B, Korzh V, Glasgow E, Thor S, Edlund T, Dawid IB & Eisen JS. (1995) Motoneuron fate specification revealed by patterned LIM homeobox gene expression in embryonic zebrafish. *Development (Cambridge, England)* **121**(12): 4117-25.
- Aronheim A, Engelberg D, Li N, al-Alawi N, Schlessinger J & Karin M. (1994) Membrane targeting of the nucleotide exchange factor Sos is sufficient for activating the Ras signaling pathway. *Cell* **78**(6): 949-61.
- Asano S, Mishima M & Nishida E. (2001) Coronin forms a stable dimer through its C-terminal coiled coil region: an implicated role in its localization to cell periphery. *Genes Cells* **6**(3): 225-35.
- Audesirk G, Cabell L & Kern M. (1997) Modulation of neurite branching by protein phosphorylation in cultured rat hippocampal neurons. *Brain research* **102**(2): 247-60.
- Avarsson A. (1995) Structure-based sequence alignment of elongation factors Tu and G with related GTPases involved in translation. *Journal of molecular evolution* **41**(6): 1096-104.
- Bai Y, Edamatsu H, Maeda S, Saito H, Suzuki N, Satoh T & Kataoka T. (2004) Crucial role of phospholipase Cepsilon in chemical carcinogen-induced skin tumor development. *Cancer research* **64**(24): 8808-10.
- Bange G, Wild K & Sinning I. (2007) Protein Translocation: Checkpoint Role for SRP GTPase Activation. *Curr Biol* **17**(22): R980-2.
- Bar-Sagi D & Hall A. (2000) Ras and Rho GTPases: a family reunion. *Cell* **103**(2): 227-38.
- Barbacid M. (1987) ras genes. *Annual review of biochemistry* **56**: 779-827.
- Batey S, Randles LG, Steward A & Clarke J. (2005) Cooperative folding in a multi-domain protein. *Journal of molecular biology* **349**(5): 1045-59.
- Berken A, Thomas C & Wittinghofer A. (2005) A new family of RhoGEFs activates the Rop molecular switch in plants. *Nature* **436**(7054): 1176-80.
- Bjorkblom B, Ostman N, Hongisto V, Komarovski V, Filen JJ, Nyman TA, Kallunki T, Courtney MJ & Coffey ET. (2005) Constitutively active cytoplasmic c-Jun N-terminal kinase 1 is a dominant regulator of dendritic architecture: role of microtubule-associated protein 2 as an effector. *J Neurosci* **25**(27): 6350-61.
- Boguski MS & McCormick F. (1993) Proteins regulating Ras and its relatives. *Nature* **366**(6456): 643-54.
- Boriack-Sjodin PA, Margarit SM, Bar-Sagi D & Kuriyan J. (1998) The structural basis of the activation of Ras by Sos. *Nature* **394**(6691): 337-43.
- Bos JL. (2006) Epac proteins: multi-purpose cAMP targets. *Trends in biochemical sciences* **31**(12): 680-6.
- Bos JL, Rehmann H & Wittinghofer A. (2007) GEFs and GAPs: critical elements in the control of small G proteins. *Cell* **129**(5): 865-77.
- Boulton TG & Cobb MH. (1991) Identification of multiple extracellular signal-regulated kinases (ERKs) with antipeptide antibodies. *Cell regulation* **2**(5): 357-71.

- Bourne HR, Sanders DA & McCormick F. (1991) The GTPase superfamily: conserved structure and molecular mechanism. *Nature* **349**(6305): 117-27.
- Boyartchuk VL, Ashby MN & Rine J. (1997) Modulation of Ras and a-factor function by carboxyl-terminal proteolysis. *Science (New York, N.Y)* **275**(5307): 1796-800.
- Broek D, Toda T, Michaeli T, Levin L, Birchmeier C, Zoller M, Powers S & Wigler M. (1987) The *S. cerevisiae* CDC25 gene product regulates the RAS/adenylate cyclase pathway. *Cell* **48**(5): 789-99.
- Castrillon DH & Wasserman SA. (1994) Diaphanous is required for cytokinesis in *Drosophila* and shares domains of similarity with the products of the limb deformity gene. *Development (Cambridge, England)* **120**(12): 3367-77.
- Chardin P, Camonis JH, Gale NW, van Aelst L, Schlessinger J, Wigler MH & Bar-Sagi D. (1993) Human Sos1: a guanine nucleotide exchange factor for Ras that binds to GRB2. *Science (New York, N.Y)* **260**(5112): 1338-43.
- Cherfils J & Chardin P. (1999) GEFs: structural basis for their activation of small GTP-binding proteins. *Trends in biochemical sciences* **24**(8): 306-11.
- Chien Y & White MA. (2003) RAL GTPases are linchpin modulators of human tumour-cell proliferation and survival. *EMBO reports* **4**(8): 800-6.
- Chishti AH, Kim AC, Marfatia SM, Lutchman M, Hanspal M, Jindal H, Liu SC, Low PS, Rouleau GA, Mohandas N, Chasis JA, Conboy JG, Gascard P, Takakuwa Y, Huang SC, Benz EJ, Jr., Bretscher A, Fehon RG, Gusella JF, Ramesh V, Solomon F, Marchesi VT, Tsukita S, Hoover KB & et al. (1998) The FERM domain: a unique module involved in the linkage of cytoplasmic proteins to the membrane. *Trends in biochemical sciences* **23**(8): 281-2.
- Choy E, Chiu VK, Silletti J, Feoktistov M, Morimoto T, Michaelson D, Ivanov IE & Philips MR. (1999) Endomembrane trafficking of ras: the CAAX motif targets proteins to the ER and Golgi. *Cell* **98**(1): 69-80.
- Ciccarelli FD, Bork P & Kerkhoff E. (2003) The KIND module: a putative signalling domain evolved from the C lobe of the protein kinase fold. *Trends in biochemical sciences* **28**(7): 349-52.
- Cirulli V & Yebra M. (2007) Netrins: beyond the brain. *Nature reviews* **8**(4): 296-306.
- Cline HT. (2001) Dendritic arbor development and synaptogenesis. *Current opinion in neurobiology* **11**(1): 118-26.
- Clyde-Smith J, Silins G, Gartside M, Grimmond S, Etheridge M, Apolloni A, Hayward N & Hancock JF. (2000) Characterization of RasGRP2, a plasma membrane-targeted, dual specificity Ras/Rap exchange factor. *The Journal of biological chemistry* **275**(41): 32260-7.
- Colicelli J. (2004) Human RAS superfamily proteins and related GTPases. *Sci STKE* **2004**(250): RE13.
- Cox AD & Der CJ. (2002) Ras family signaling: therapeutic targeting. *Cancer biology & therapy* **1**(6): 599-606.
- Crews CM, Alessandrini A & Erikson RL. (1992) The primary structure of MEK, a protein kinase that phosphorylates the ERK gene product. *Science (New York, N.Y)* **258**(5081): 478-80.
- Cristofanilli M, Thanos S, Brosius J, Kindler S & Tiedge H. (2004) Neuronal MAP2 mRNA: species-dependent differential dendritic targeting competence. *Journal of molecular biology* **341**(4): 927-34.
- Cullen PJ & Lockyer PJ. (2002) Integration of calcium and Ras signalling. *Nature reviews* **3**(5): 339-48.
- Cully M, You H, Levine AJ & Mak TW. (2006) Beyond PTEN mutations: the PI3K pathway as an integrator of multiple inputs during tumorigenesis. *Nat Rev Cancer* **6**(3): 184-92.
- de Vos AM, Tong L, Milburn MV, Matias PM, Jancarik J, Noguchi S, Nishimura S, Miura K, Ohtsuka E & Kim SH. (1988) Three-dimensional structure of an oncogene protein: catalytic domain of human c-H-ras p21. *Science (New York, N.Y)* **239**(4842): 888-93.
- Dehmelt L & Halpain S. (2005) The MAP2/Tau family of microtubule-associated proteins. *Genome biology* **6**(1): 204.
- Dehmelt L, Smart FM, Ozer RS & Halpain S. (2003) The role of microtubule-associated protein 2c in the reorganization of microtubules and lamellipodia during neurite initiation. *J Neurosci* **23**(29): 9479-90.
- Delahay RM & Frankel G. (2002) Coiled-coil proteins associated with type III secretion systems: a versatile domain revisited. *Molecular microbiology* **45**(4): 905-16.
- Dent P, Haser W, Haystead TA, Vincent LA, Roberts TM & Sturgill TW. (1992) Activation of mitogen-activated protein kinase kinase by v-Raf in NIH 3T3 cells and in vitro. *Science (New York, N.Y)* **257**(5075): 1404-7.
- Dierssen M & Ramakers GJ. (2006) Dendritic pathology in mental retardation: from molecular genetics to neurobiology. *Genes, brain, and behavior* **5 Suppl 2**: 48-60.

- Downward J. (2003) Targeting RAS signalling pathways in cancer therapy. *Nat Rev Cancer* **3**(1): 11-22.
- Downward J, Riehl R, Wu L & Weinberg RA. (1990) Identification of a nucleotide exchange-promoting activity for p21ras. *Proceedings of the National Academy of Sciences of the United States of America* **87**(15): 5998-6002.
- Drewes G, Trinczek B, Illenberger S, Biernat J, Schmitt-Ulms G, Meyer HE, Mandelkow EM & Mandelkow E. (1995) Microtubule-associated protein/microtubule affinity-regulating kinase (p110mark). A novel protein kinase that regulates tau-microtubule interactions and dynamic instability by phosphorylation at the Alzheimer-specific site serine 262. *The Journal of biological chemistry* **270**(13): 7679-88.
- Ebinu JO, Bottorff DA, Chan EY, Stang SL, Dunn RJ & Stone JC. (1998) RasGRP, a Ras guanyl nucleotide- releasing protein with calcium- and diacylglycerol-binding motifs. *Science (New York, N.Y)* **280**(5366): 1082-6.
- Egea PF, Stroud RM & Walter P. (2005) Targeting proteins to membranes: structure of the signal recognition particle. *Current opinion in structural biology* **15**(2): 213-20.
- Ehrhardt A, Ehrhardt GR, Guo X & Schrader JW. (2002) Ras and relatives--job sharing and networking keep an old family together. *Experimental hematology* **30**(10): 1089-106.
- Eisenberg S & Henis YI. (2008) Interactions of Ras proteins with the plasma membrane and their roles in signaling. *Cellular signalling* **20**(1): 31-9.
- Emmons S, Phan H, Calley J, Chen W, James B & Manseau L. (1995) Cappuccino, a Drosophila maternal effect gene required for polarity of the egg and embryo, is related to the vertebrate limb deformity locus. *Genes & development* **9**(20): 2482-94.
- Erdmann KS. (2003) The protein tyrosine phosphatase PTP-Basophil/Basophil-like. Interacting proteins and molecular functions. *Eur J Biochem* **270**(24): 4789-98.
- Etienne-Manneville S & Hall A. (2002) Rho GTPases in cell biology. *Nature* **420**(6916): 629-35.
- Evangelista M, Blundell K, Longtine MS, Chow CJ, Adames N, Pringle JR, Peter M & Boone C. (1997) Bni1p, a yeast formin linking cdc42p and the actin cytoskeleton during polarized morphogenesis. *Science (New York, N.Y)* **276**(5309): 118-22.
- Feig LA, Urano T & Cantor S. (1996) Evidence for a Ras/Ral signaling cascade. *Trends in biochemical sciences* **21**(11): 438-41.
- Feinstein E. (2005) Ral-GTPases: good chances for a long-lasting fame. *Oncogene* **24**(3): 326-8.
- Felgner H, Frank R, Biernat J, Mandelkow EM, Mandelkow E, Ludin B, Matus A & Schliwa M. (1997) Domains of neuronal microtubule-associated proteins and flexural rigidity of microtubules. *The Journal of cell biology* **138**(5): 1067-75.
- Garcia-Mata R & Burrige K. (2007) Catching a GEF by its tail. *Trends in cell biology* **17**(1): 36-43.
- Garnett MJ, Rana S, Paterson H, Barford D & Marais R. (2005) Wild-type and mutant B-RAF activate C-RAF through distinct mechanisms involving heterodimerization. *Molecular cell* **20**(6): 963-9.
- Garrington TP & Johnson GL. (1999) Organization and regulation of mitogen-activated protein kinase signaling pathways. *Current opinion in cell biology* **11**(2): 211-8.
- Gibbs JB, Sigal IS, Poe M & Scolnick EM. (1984) Intrinsic GTPase activity distinguishes normal and oncogenic ras p21 molecules. *Proceedings of the National Academy of Sciences of the United States of America* **81**(18): 5704-8.
- Graham BP, Lauchlan K & McLean DR. (2006) Dynamics of outgrowth in a continuum model of neurite elongation. *Journal of computational neuroscience* **20**(1): 43-60.
- Hagiwara H, Yorifuji H, Sato-Yoshitake R & Hirokawa N. (1994) Competition between motor molecules (kinesin and cytoplasmic dynein) and fibrous microtubule-associated proteins in binding to microtubules. *The Journal of biological chemistry* **269**(5): 3581-9.
- Hall BE, Yang SS, Boriack-Sjodin PA, Kuriyan J & Bar-Sagi D. (2001) Structure-based mutagenesis reveals distinct functions for Ras switch 1 and switch 2 in Sos-catalyzed guanine nucleotide exchange. *The Journal of biological chemistry* **276**(29): 27629-37.
- Haller O, Staeheli P & Kochs G. (2007) Interferon-induced Mx proteins in antiviral host defense. *Biochimie* **89**(6-7): 812-8.
- Hamada K, Shimizu T, Matsui T, Tsukita S & Hakoshima T. (2000) Structural basis of the membrane-targeting and unmasking mechanisms of the radixin FERM domain. *The EMBO journal* **19**(17): 4449-62.
- Han JH, Batey S, Nickson AA, Teichmann SA & Clarke J. (2007) The folding and evolution of multidomain proteins. *Nature reviews* **8**(4): 319-30.
- Hancock JF. (2003) Ras proteins: different signals from different locations. *Nature reviews* **4**(5): 373-84.

- Hancock JF. (2006) Lipid rafts: contentious only from simplistic standpoints. *Nature reviews* **7**(6): 456-62.
- Hanks SK. (2003) Genomic analysis of the eukaryotic protein kinase superfamily: a perspective. *Genome biology* **4**(5): 111.
- Hanks SK & Hunter T. (1995) Protein kinases 6. The eukaryotic protein kinase superfamily: kinase (catalytic) domain structure and classification. *Faseb J* **9**(8): 576-96.
- Hanks SK & Quinn AM. (1991) Protein kinase catalytic domain sequence database: identification of conserved features of primary structure and classification of family members. *Methods in enzymology* **200**: 38-62.
- Hanks SK, Quinn AM & Hunter T. (1988) The protein kinase family: conserved features and deduced phylogeny of the catalytic domains. *Science (New York, N.Y)* **241**(4861): 42-52.
- Hannan AJ, Henke RC, Seeto GS, Capes-Davis A, Dunn J & Jeffrey PL. (1999) Expression of doublecortin correlates with neuronal migration and pattern formation in diverse regions of the developing chick brain. *Journal of neuroscience research* **55**(5): 650-7.
- Harada A, Teng J, Takei Y, Oguchi K & Hirokawa N. (2002) MAP2 is required for dendrite elongation, PKA anchoring in dendrites, and proper PKA signal transduction. *The Journal of cell biology* **158**(3): 541-9.
- Hayward RD & Koronakis V. (1999) Direct nucleation and bundling of actin by the SipC protein of invasive *Salmonella*. *The EMBO journal* **18**(18): 4926-34.
- Hely TA, Graham B & Ooyen AV. (2001) A computational model of dendrite elongation and branching based on MAP2 phosphorylation. *Journal of theoretical biology* **210**(3): 375-84.
- Hentschel HG & Fine A. (1996) Diffusion-regulated control of cellular dendritic morphogenesis. *Proceedings* **263**(1366): 1-8.
- Herrmann C. (2003) Ras-effector interactions: after one decade. *Current opinion in structural biology* **13**(1): 122-9.
- Herrmann L, Dittmar T & Erdmann KS. (2003) The protein tyrosine phosphatase PTP-BL associates with the midbody and is involved in the regulation of cytokinesis. *Molecular biology of the cell* **14**(1): 230-40.
- Higgs HN. (2005) Formin proteins: a domain-based approach. *Trends in biochemical sciences* **30**(6): 342-53.
- Huang J, Furuya A & Furuichi T. (2007) Very-KIND, a KIND domain containing RasGEF, controls dendrite growth by linking Ras small GTPases and MAP2. *The Journal of cell biology* **179**(3): 539-52.
- Huang YS, Carson JH, Barbarese E & Richter JD. (2003) Facilitation of dendritic mRNA transport by CPEB. *Genes & development* **17**(5): 638-53.
- Hunter T. (1987) A thousand and one protein kinases. *Cell* **50**(6): 823-9.
- Ingerman E & Nunnari J. (2005) A continuous, regenerative coupled GTPase assay for dynamin-related proteins. *Methods in enzymology* **404**: 611-9.
- Innocenti M, Frittoli E, Ponzanelli I, Falck JR, Brachmann SM, Di Fiore PP & Scita G. (2003) Phosphoinositide 3-kinase activates Rac by entering in a complex with Eps8, Abi1, and Sos-1. *The Journal of cell biology* **160**(1): 17-23.
- Innocenti M, Tenca P, Frittoli E, Faretta M, Tocchetti A, Di Fiore PP & Scita G. (2002) Mechanisms through which Sos-1 coordinates the activation of Ras and Rac. *The Journal of cell biology* **156**(1): 125-36.
- Ito M. (1997) Cerebellar microcomplexes. *International review of neurobiology* **41**: 475-87.
- Itoh K, Lisovsky M, Hikasa H & Sokol SY. (2005) Reorganization of actin cytoskeleton by FRIED, a Frizzled-8 associated protein tyrosine phosphatase. *Dev Dyn* **234**(1): 90-101.
- Kalcheva N, Albala J, O'Guin K, Rubino H, Garner C & Shafit-Zagardo B. (1995) Genomic structure of human microtubule-associated protein 2 (MAP-2) and characterization of additional MAP-2 isoforms. *Proceedings of the National Academy of Sciences of the United States of America* **92**(24): 10894-8.
- Kamata T & Feramisco JR. (1984) Epidermal growth factor stimulates guanine nucleotide binding activity and phosphorylation of ras oncogene proteins. *Nature* **310**(5973): 147-50.
- Kano Y, Nohno T, Shimada K, Nakagiri S, Hiragami F, Kawamura K, Motoda H, Numata K, Murai H, Koike Y, Inoue S & Miyamoto K. (2007) Osmotic shock-induced neurite extension via activation of p38 mitogen-activated protein kinase and CREB. *Brain Res* **1154**: 1-7.
- Katz M, Amit I & Yarden Y. (2007) Regulation of MAPKs by growth factors and receptor tyrosine kinases. *Biochimica et biophysica acta* **1773**(8): 1161-76.

- Kawasaki H, Springett GM, Toki S, Canales JJ, Harlan P, Blumenstiel JP, Chen EJ, Bany IA, Mochizuki N, Ashbacher A, Matsuda M, Housman DE & Graybiel AM. (1998) A Rap guanine nucleotide exchange factor enriched highly in the basal ganglia. *Proceedings of the National Academy of Sciences of the United States of America* **95**(22): 13278-83.
- Kerckhoff E. (2006) Cellular functions of the Spir actin-nucleation factors. *Trends in cell biology* **16**(9): 477-83.
- Kerckhoff E, Simpson JC, Leberfinger CB, Otto IM, Doerks T, Bork P, Rapp UR, Raabe T & Pepperkok R. (2001) The Spir actin organizers are involved in vesicle transport processes. *Curr Biol* **11**(24): 1963-8.
- Kholodenko BN. (2003) Four-dimensional organization of protein kinase signaling cascades: the roles of diffusion, endocytosis and molecular motors. *The Journal of experimental biology* **206**(Pt 12): 2073-82.
- Kiddie G, McLean D, Van Ooyen A & Graham B. (2005) Biologically plausible models of neurite outgrowth. *Progress in brain research* **147**: 67-80.
- Kim E, Ambroziak P, Otto JC, Taylor B, Ashby M, Shannon K, Casey PJ & Young SG. (1999) Disruption of the mouse Rce1 gene results in defective Ras processing and mislocalization of Ras within cells. *The Journal of biological chemistry* **274**(13): 8383-90.
- Klebe C, Prinz H, Wittinghofer A & Goody RS. (1995) The kinetic mechanism of Ran--nucleotide exchange catalyzed by RCC1. *Biochemistry* **34**(39): 12543-52.
- Knighton DR, Zheng JH, Ten Eyck LF, Ashford VA, Xuong NH, Taylor SS & Sowadski JM. (1991a) Crystal structure of the catalytic subunit of cyclic adenosine monophosphate-dependent protein kinase. *Science (New York, N.Y)* **253**(5018): 407-14.
- Knighton DR, Zheng JH, Ten Eyck LF, Xuong NH, Taylor SS & Sowadski JM. (1991b) Structure of a peptide inhibitor bound to the catalytic subunit of cyclic adenosine monophosphate-dependent protein kinase. *Science (New York, N.Y)* **253**(5018): 414-20.
- Kobayashi N & Mundel P. (1998) A role of microtubules during the formation of cell processes in neuronal and non-neuronal cells. *Cell and tissue research* **291**(2): 163-74.
- Koradi R, Billeter M & Wuthrich K. (1996) MOLMOL: a program for display and analysis of macromolecular structures. *Journal of molecular graphics* **14**(1): 51-5, 29-32.
- Kranenburg O, Verlaan I & Moolenaar WH. (1999) Dynamin is required for the activation of mitogen-activated protein (MAP) kinase by MAP kinase kinase. *The Journal of biological chemistry* **274**(50): 35301-4.
- Krengel U, Schlichting I, Scherer A, Schumann R, Frech M, John J, Kabsch W, Pai EF & Wittinghofer A. (1990) Three-dimensional structures of H-ras p21 mutants: molecular basis for their inability to function as signal switch molecules. *Cell* **62**(3): 539-48.
- Kyriakis JM. (2007) The integration of signaling by multiprotein complexes containing Raf kinases. *Biochimica et biophysica acta* **1773**(8): 1238-47.
- Kyriakis JM, App H, Zhang XF, Banerjee P, Brautigan DL, Rapp UR & Avruch J. (1992) Raf-1 activates MAP kinase-kinase. *Nature* **358**(6385): 417-21.
- Lambert JM, Lambert QT, Reuther GW, Malliri A, Siderovski DP, Sondek J, Collard JG & Der CJ. (2002) Tiam1 mediates Ras activation of Rac by a PI(3)K-independent mechanism. *Nature cell biology* **4**(8): 621-5.
- Leevers SJ, Paterson HF & Marshall CJ. (1994) Requirement for Ras in Raf activation is overcome by targeting Raf to the plasma membrane. *Nature* **369**(6479): 411-4.
- Lei M, Lu W, Meng W, Parrini MC, Eck MJ, Mayer BJ & Harrison SC. (2000) Structure of PAK1 in an autoinhibited conformation reveals a multistage activation switch. *Cell* **102**(3): 387-97.
- Lei M, Robinson MA & Harrison SC. (2005) The active conformation of the PAK1 kinase domain. *Structure* **13**(5): 769-78.
- Leimeister C, Bach A & Gessler M. (1998) Developmental expression patterns of mouse sFRP genes encoding members of the secreted frizzled related protein family. *Mechanisms of development* **75**(1-2): 29-42.
- Lenzen C, Cool RH, Prinz H, Kuhlmann J & Wittinghofer A. (1998) Kinetic analysis by fluorescence of the interaction between Ras and the catalytic domain of the guanine nucleotide exchange factor Cdc25Mm. *Biochemistry* **37**(20): 7420-30.
- Leonard CJ, Aravind L & Koonin EV. (1998) Novel families of putative protein kinases in bacteria and archaea: evolution of the "eukaryotic" protein kinase superfamily. *Genome Res* **8**(10): 1038-47.
- Lewis SA & Cowan N. (1990) Microtubule bundling. *Nature* **345**(6277): 674.



- Lewis SA, Ivanov IE, Lee GH & Cowan NJ. (1989) Organization of microtubules in dendrites and axons is determined by a short hydrophobic zipper in microtubule-associated proteins MAP2 and tau. *Nature* **342**(6249): 498-505.
- Lewis SA, Wang DH & Cowan NJ. (1988) Microtubule-associated protein MAP2 shares a microtubule binding motif with tau protein. *Science (New York, N.Y)* **242**(4880): 936-9.
- Li HY, Cao K & Zheng Y. (2003) Ran in the spindle checkpoint: a new function for a versatile GTPase. *Trends in cell biology* **13**(11): 553-7.
- Libersat F & Duch C. (2004) Mechanisms of dendritic maturation. *Molecular neurobiology* **29**(3): 303-20.
- Liu P, Ying Y & Anderson RG. (1997) Platelet-derived growth factor activates mitogen-activated protein kinase in isolated caveolae. *Proceedings of the National Academy of Sciences of the United States of America* **94**(25): 13666-70.
- Llorca O, Arias-Palomo E, Zugaza JL & Bustelo XR. (2005) Global conformational rearrangements during the activation of the GDP/GTP exchange factor Vav3. *The EMBO journal* **24**(7): 1330-40.
- Lobo S, Greentree WK, Linder ME & Deschenes RJ. (2002) Identification of a Ras palmitoyltransferase in *Saccharomyces cerevisiae*. *The Journal of biological chemistry* **277**(43): 41268-73.
- Lopez LA & Sheetz MP. (1993) Steric inhibition of cytoplasmic dynein and kinesin motility by MAP2. *Cell motility and the cytoskeleton* **24**(1): 1-16.
- Lupas A. (1996) Coiled coils: new structures and new functions. *Trends in biochemical sciences* **21**(10): 375-82.
- Lupas A, Van Dyke M & Stock J. (1991) Predicting coiled coils from protein sequences. *Science (New York, N.Y)* **252**(5009): 1162-4.
- Malliri A, van der Kammen RA, Clark K, van der Valk M, Michiels F & Collard JG. (2002) Mice deficient in the Rac activator Tiam1 are resistant to Ras-induced skin tumours. *Nature* **417**(6891): 867-71.
- Malmendal A, Halpain S & Chazin WJ. (2003) Nascent structure in the kinase anchoring domain of microtubule-associated protein 2. *Biochemical and biophysical research communications* **301**(1): 136-42.
- Malumbres M & Barbacid M. (2003) RAS oncogenes: the first 30 years. *Nat Rev Cancer* **3**(6): 459-65.
- Marais R, Light Y, Paterson HF & Marshall CJ. (1995) Ras recruits Raf-1 to the plasma membrane for activation by tyrosine phosphorylation. *The EMBO journal* **14**(13): 3136-45.
- Marchler-Bauer A, Anderson JB, Derbyshire MK, DeWeese-Scott C, Gonzales NR, Gwadz M, Hao L, He S, Hurwitz DI, Jackson JD, Ke Z, Krylov D, Lanczycki CJ, Liebert CA, Liu C, Lu F, Lu S, Marchler GH, Mullokandov M, Song JS, Thanki N, Yamashita RA, Yin JJ, Zhang D & Bryant SH. (2007) CDD: a conserved domain database for interactive domain family analysis. *Nucleic acids research* **35**(Database issue): D237-40.
- Margarit SM, Sondermann H, Hall BE, Nagar B, Hoelz A, Pirruccello M, Bar-Sagi D & Kuriyan J. (2003) Structural evidence for feedback activation by Ras.GTP of the Ras-specific nucleotide exchange factor SOS. *Cell* **112**(5): 685-95.
- Marrari Y, Crouthamel M, Irannejad R & Wedegaertner PB. (2007) Assembly and trafficking of heterotrimeric G proteins. *Biochemistry* **46**(26): 7665-77.
- Matsuda S, Kosako H, Takenaka K, Moriyama K, Sakai H, Akiyama T, Gotoh Y & Nishida E. (1992) Xenopus MAP kinase activator: identification and function as a key intermediate in the phosphorylation cascade. *The EMBO journal* **11**(3): 973-82.
- Matus A. (1990) Microtubule-associated proteins and the determination of neuronal form. *Journal de physiologie* **84**(1): 134-7.
- McAllister AK, Katz LC & Lo DC. (1999) Neurotrophins and synaptic plasticity. *Annual review of neuroscience* **22**: 295-318.
- McCormick F. (1993) Signal transduction. How receptors turn Ras on. *Nature* **363**(6424): 15-6.
- Mees A, Rock R, Ciccarelli FD, Leberfinger CB, Borawski JM, Bork P, Wiese S, Gessler M & Kerkhoff E. (2005) Very-KIND is a novel nervous system specific guanine nucleotide exchange factor for Ras GTPases. *Gene Expr Patterns* **6**(1): 79-85.
- Memon AR. (2004) The role of ADP-ribosylation factor and SAR1 in vesicular trafficking in plants. *Biochimica et biophysica acta* **1664**(1): 9-30.
- Menezes JR & Luskin MB. (1994) Expression of neuron-specific tubulin defines a novel population in the proliferative layers of the developing telencephalon. *J Neurosci* **14**(9): 5399-416.
- Milburn MV, Tong L, deVos AM, Brunger A, Yamaizumi Z, Nishimura S & Kim SH. (1990) Molecular switch for signal transduction: structural differences between active and inactive forms of protooncogenic ras proteins. *Science (New York, N.Y)* **247**(4945): 939-45.

- Mitin N, Rossman KL & Der CJ. (2005) Signaling interplay in Ras superfamily function. *Curr Biol* **15**(14): R563-74.
- Moodie SA, Willumsen BM, Weber MJ & Wolfman A. (1993) Complexes of Ras.GTP with Raf-1 and mitogen-activated protein kinase kinase. *Science (New York, N.Y)* **260**(5114): 1658-61.
- Mor A & Philips MR. (2006) Compartmentalized Ras/MAPK signaling. *Annual review of immunology* **24**: 771-800.
- Morrison DA. (1977) Transformation in Escherichia coli: cryogenic preservation of competent cells. *Journal of bacteriology* **132**(1): 349-51.
- Nakahira M, Tanaka T, Robson BE, Mizgerd JP & Grusby MJ. (2007) Regulation of signal transducer and activator of transcription signaling by the tyrosine phosphatase PTP-BL. *Immunity* **26**(2): 163-76.
- Nakayama M, Iida M, Koseki H & Ohara O. (2006) A gene-targeting approach for functional characterization of KIAA genes encoding extremely large proteins. *Faseb J* **20**(10): 1718-20.
- Nichols A, Camps M, Gillieron C, Chabert C, Brunet A, Wilsbacher J, Cobb M, Pouyssegur J, Shaw JP & Arkinstall S. (2000) Substrate recognition domains within extracellular signal-regulated kinase mediate binding and catalytic activation of mitogen-activated protein kinase phosphatase-3. *The Journal of biological chemistry* **275**(32): 24613-21.
- Nie Z, Hirsch DS & Randazzo PA. (2003) Arf and its many interactors. *Current opinion in cell biology* **15**(4): 396-404.
- Niu S, Renfro A, Quattrocchi CC, Sheldon M & D'Arcangelo G. (2004) Reelin promotes hippocampal dendrite development through the VLDLR/ApoER2-Dab1 pathway. *Neuron* **41**(1): 71-84.
- Niv H, Gutman O, Kloog Y & Henis YI. (2002) Activated K-Ras and H-Ras display different interactions with saturable nonraft sites at the surface of live cells. *The Journal of cell biology* **157**(5): 865-72.
- Novy R, Drott D, Yaeger K & Mierendorf R. (2001) Overcoming the codon bias of E. coli for enhanced protein expression. *inNovations* **12**: 1-3
- Nusrat A, Chen JA, Foley CS, Liang TW, Tom J, Cromwell M, Quan C & Mrsny RJ. (2000) The coiled-coil domain of occludin can act to organize structural and functional elements of the epithelial tight junction. *The Journal of biological chemistry* **275**(38): 29816-22.
- Otto IM, Raabe T, Rennfahrt UE, Bork P, Rapp UR & Kerkhoff E. (2000) The p150-Spir protein provides a link between c-Jun N-terminal kinase function and actin reorganization. *Curr Biol* **10**(6): 345-8.
- Ozer RS & Halpain S. (2000) Phosphorylation-dependent localization of microtubule-associated protein MAP2c to the actin cytoskeleton. *Molecular biology of the cell* **11**(10): 3573-87.
- Pai EF, Kabsch W, Krengel U, Holmes KC, John J & Wittinghofer A. (1989) Structure of the guanine-nucleotide-binding domain of the Ha-ras oncogene product p21 in the triphosphate conformation. *Nature* **341**(6239): 209-14.
- Pardo CA & Eberhart CG. (2007) The neurobiology of autism. *Brain pathology (Zurich, Switzerland)* **17**(4): 434-47.
- Park HO & Bi E. (2007) Central roles of small GTPases in the development of cell polarity in yeast and beyond. *Microbiol Mol Biol Rev* **71**(1): 48-96.
- Park RK, Liu Y & Durden DL. (1996) A role for Shc, Grb2, and Raf-1 in FcγRI signal relay. *The Journal of biological chemistry* **271**(23): 13342-8.
- Pascual-Castroviejo I, Gutierrez M, Morales C, Gonzalez-Mediero I, Martinez-Bermejo A & Pascual-Pascual SI. (1994) Primary degeneration of the granular layer of the cerebellum. A study of 14 patients and review of the literature. *Neuropediatrics* **25**(4): 183-90.
- Pearson MA, Reczek D, Bretscher A & Karplus PA. (2000) Structure of the ERM protein moesin reveals the FERM domain fold masked by an extended actin binding tail domain. *Cell* **101**(3): 259-70.
- Picking WL, Coye L, Osiecki JC, Barnoski Serfis A, Schaper E & Picking WD. (2001) Identification of functional regions within invasion plasmid antigen C (IpaC) of Shigella flexneri. *Molecular microbiology* **39**(1): 100-11.
- Porcionatto MA. (2006) The extracellular matrix provides directional cues for neuronal migration during cerebellar development. *Brazilian journal of medical and biological research = Revista brasileira de pesquisas medicas e biologicas / Sociedade Brasileira de Biofisica ... [et al]* **39**(3): 313-20.
- Praefcke GJ & McMahon HT. (2004) The dynamin superfamily: universal membrane tubulation and fission molecules? *Nature reviews* **5**(2): 133-47.
- Prior IA, Muncke C, Parton RG & Hancock JF. (2003) Direct visualization of Ras proteins in spatially distinct cell surface microdomains. *The Journal of cell biology* **160**(2): 165-70.
- Pruyne D, Evangelista M, Yang C, Bi E, Zigmund S, Bretscher A & Boone C. (2002) Role of formins in actin assembly: nucleation and barbed-end association. *Science (New York, N.Y)* **297**(5581): 612-5.

- Quilliam LA, Rebhun JF & Castro AF. (2002) A growing family of guanine nucleotide exchange factors is responsible for activation of Ras-family GTPases. *Progress in nucleic acid research and molecular biology* **71**: 391-444.
- Quinlan ME, Heuser JE, Kerkhoff E & Mullins RD. (2005) Drosophila Spire is an actin nucleation factor. *Nature* **433**(7024): 382-8.
- Quinlan ME, Hilgert S, Bedrossian A, Mullins RD & Kerkhoff E. (2007) Regulatory interactions between two actin nucleators, Spire and Cappuccino. *The Journal of cell biology* **179**(1): 117-28.
- Rajalingam K, Schreck R, Rapp UR & Albert S. (2007) Ras oncogenes and their downstream targets. *Biochimica et biophysica acta* **1773**(8): 1177-95.
- Raman EP, Barsegov V & Klimov DK. (2007) Folding of tandem-linked domains. *Proteins* **67**(4): 795-810.
- Randles LG, Batey S, Steward A & Clarke J. (2007) Distinguishing specific and non-specific inter-domain interactions in multidomain proteins. *Biophys J*.
- Rangarajan A, Hong SJ, Gifford A & Weinberg RA. (2004) Species- and cell type-specific requirements for cellular transformation. *Cancer cell* **6**(2): 171-83.
- Rapp UR, Goldsborough MD, Mark GE, Bonner TI, Groffen J, Reynolds FH, Jr. & Stephenson JR. (1983) Structure and biological activity of v-raf, a unique oncogene transduced by a retrovirus. *Proceedings of the National Academy of Sciences of the United States of America* **80**(14): 4218-22.
- Rapp UR & Todaro GJ. (1980) Generation of oncogenic mouse type C viruses: in vitro selection of carcinoma-inducing variants. *Proceedings of the National Academy of Sciences of the United States of America* **77**(1): 624-8.
- Reddy EP, Reynolds RK, Santos E & Barbacid M. (1982) A point mutation is responsible for the acquisition of transforming properties by the T24 human bladder carcinoma oncogene. *Nature* **300**(5888): 149-52.
- Regier DS, Higbee J, Lund KM, Sakane F, Prescott SM & Topham MK. (2005) Diacylglycerol kinase iota regulates Ras guanyl-releasing protein 3 and inhibits Rap1 signaling. *Proceedings of the National Academy of Sciences of the United States of America* **102**(21): 7595-600.
- Rehmann H, Das J, Knipscheer P, Wittinghofer A & Bos JL. (2006) Structure of the cyclic-AMP-responsive exchange factor Epac2 in its auto-inhibited state. *Nature* **439**(7076): 625-8.
- Reiss Y, Goldstein JL, Seabra MC, Casey PJ & Brown MS. (1990) Inhibition of purified p21ras farnesyl:protein transferase by Cys-AAX tetrapeptides. *Cell* **62**(1): 81-8.
- Repasky GA, Chenette EJ & Der CJ. (2004) Renewing the conspiracy theory debate: does Raf function alone to mediate Ras oncogenesis? *Trends in cell biology* **14**(11): 639-47.
- Robertsson J, Petzold K, Lofvenberg L & Backman L. (2005) Folding of spectrin's SH3 domain in the presence of spectrin repeats. *Cellular & molecular biology letters* **10**(4): 595-612.
- Rocks O, Peyker A & Bastiaens PI. (2006) Spatio-temporal segregation of Ras signals: one ship, three anchors, many harbors. *Current opinion in cell biology* **18**(4): 351-7.
- Rodriguez-Viciano P, Warne PH, Dhand R, Vanhaesebroeck B, Gout I, Fry MJ, Waterfield MD & Downward J. (1994) Phosphatidylinositol-3-OH kinase as a direct target of Ras. *Nature* **370**(6490): 527-32.
- Roger B, Al-Bassam J, Dehmelt L, Milligan RA & Halpain S. (2004) MAP2c, but not tau, binds and bundles F-actin via its microtubule binding domain. *Curr Biol* **14**(5): 363-71.
- Romero F, Martinez AC, Camonis J & Rebollo A. (1999) Aiolos transcription factor controls cell death in T cells by regulating Bcl-2 expression and its cellular localization. *The EMBO journal* **18**(12): 3419-30.
- Rose A, Schraegle SJ, Stahlberg EA & Meier I. (2005) Coiled-coil protein composition of 22 proteomes--differences and common themes in subcellular infrastructure and traffic control. *BMC evolutionary biology* **5**: 66.
- Rost B, Sander C & Schneider R. (1994) PHD--an automatic mail server for protein secondary structure prediction. *Comput Appl Biosci* **10**(1): 53-60.
- Rotblat B, Prior IA, Muncke C, Parton RG, Kloog Y, Henis YI & Hancock JF. (2004) Three separable domains regulate GTP-dependent association of H-ras with the plasma membrane. *Molecular and cellular biology* **24**(15): 6799-810.
- Roy S, Plowman S, Rotblat B, Prior IA, Muncke C, Grainger S, Parton RG, Henis YI, Kloog Y & Hancock JF. (2005) Individual palmitoyl residues serve distinct roles in H-ras trafficking, microlocalization, and signaling. *Molecular and cellular biology* **25**(15): 6722-33.
- Rubin GM, Yandell MD, Wortman JR, Gabor Miklos GL, Nelson CR, Hariharan IK, Fortini ME, Li PW, Apweiler R, Fleischmann W, Cherry JM, Henikoff S, Skupski MP, Misra S, Ashburner M, Birney

- E, Boguski MS, Brody T, Brokstein P, Celniker SE, Chervitz SA, Coates D, Cravchik A, Gabrielian A, Galle RF, Gelbart WM, George RA, Goldstein LS, Gong F, Guan P, Harris NL, Hay BA, Hoskins RA, Li J, Li Z, Hynes RO, Jones SJ, Kuehl PM, Lemaitre B, Littleton JT, Morrison DK, Mungall C, O'Farrell PH, Pickeral OK, Shue C, Vossball LB, Zhang J, Zhao Q, Zheng XH & Lewis S. (2000) Comparative genomics of the eukaryotes. *Science (New York, N.Y)* **287**(5461): 2204-15.
- Sakagami K, Ishii A, Shimada N & Yasuda K. (2003) RaxL regulates chick ganglion cell development. *Mechanisms of development* **120**(8): 881-95.
- Saraste M, Sibbald PR & Wittinghofer A. (1990) The P-loop--a common motif in ATP- and GTP-binding proteins. *Trends in biochemical sciences* **15**(11): 430-4.
- Schultz J, Milpetz F, Bork P & Ponting CP. (1998) SMART, a simple modular architecture research tool: identification of signaling domains. *Proceedings of the National Academy of Sciences of the United States of America* **95**(11): 5857-64.
- Scott KA, Steward A, Fowler SB & Clarke J. (2002) Titin; a multidomain protein that behaves as the sum of its parts. *Journal of molecular biology* **315**(4): 819-29.
- Silvius JR. (2002) Mechanisms of Ras protein targeting in mammalian cells. *The Journal of membrane biology* **190**(2): 83-92.
- Singh A & Hitchcock-DeGregori SE. (2006) Dual requirement for flexibility and specificity for binding of the coiled-coil tropomyosin to its target, actin. *Structure* **14**(1): 43-50.
- Singh A, Sowjanya AP & Ramakrishna G. (2005) The wild-type Ras: road ahead. *Faseb J* **19**(2): 161-9.
- Smith MR, DeGudicibus SJ & Stacey DW. (1986) Requirement for c-ras proteins during viral oncogene transformation. *Nature* **320**(6062): 540-3.
- Smotrys JE & Linder ME. (2004) Palmitoylation of intracellular signaling proteins: regulation and function. *Annual review of biochemistry* **73**: 559-87.
- Sodergren E, Shen Y, Song X, Zhang L, Gibbs RA & Weinstock GM. (2006a) Shedding genomic light on Aristotle's lantern. *Developmental biology* **300**(1): 2-8.
- Sodergren E, Weinstock GM, Davidson EH, Cameron RA, Gibbs RA, Angerer RC, Angerer LM, Arnone MI, Burgess DR, Burke RD, Coffman JA, Dean M, Elphick MR, Etensohn CA, Foltz KR, Hamdoun A, Hynes RO, Klein WH, Marzluff W, McClay DR, Morris RL, Mushegian A, Rast JP, Smith LC, Thorndyke MC, Vacquier VD, Wessel GM, Wray G, Zhang L, Elsik CG, Ermolaeva O, Hlavina W, Hofmann G, Kitts P, Landrum MJ, Mackey AJ, Maglott D, Panopoulou G, Poustka AJ, Pruitt K, Sapojnikov V, Song X, Souvorov A, Solovyev V, Wei Z, Whittaker CA, Worley K, Durbin KJ, Shen Y, Fedrigo O, Garfield D, Haygood R, Primus A, Satija R, Severson T, Gonzalez-Garay ML, Jackson AR, Milosavljevic A, Tong M, Killian CE, Livingston BT, Wilt FH, Adams N, Belle R, Carbonneau S, Cheung R, Cormier P, Cosson B, Croce J, Fernandez-Guerra A, Geneviere AM, Goel M, Kelkar H, Morales J, Mulner-Lorillon O, Robertson AJ, Goldstone JV, Cole B, Epel D, Gold B, Hahn ME, Howard-Ashby M, Scally M, Stegeman JJ, Allgood EL, Cool J, Judkins KM, McCafferty SS, Musante AM, Obar RA, Rawson AP, Rossetti BJ, Gibbons IR, Hoffman MP, Leone A, Istrail S, Materna SC, Samanta MP, Stolc V, Tongprasit W, Tu Q, Bergeron KF, Brandhorst BP, Whittle J, Berney K, Bottjer DJ, Calestani C, Peterson K, Chow E, Yuan QA, Elhaik E, Graur D, Reese JT, Bosdet I, Heesun S, Marra MA, Schein J, Anderson MK, Brockton V, Buckley KM, Cohen AH, Fugmann SD, Hibino T, Loza-Coll M, Majeske AJ, Messier C, Nair SV, Pancer Z, Terwilliger DP, Agca C, Arboleda E, Chen N, Churcher AM, Hallbook F, Humphrey GW, Idris MM, Kiyama T, Liang S, Mellott D, Mu X, Murray G, Olinski RP, Raible F, Rowe M, Taylor JS, Tessmar-Raible K, Wang D, Wilson KH, Yaguchi S, Gaasterland T, Galindo BE, Gunaratne HJ, Juliano C, Kinukawa M, Moy GW, Neill AT, Nomura M, Raisch M, Reade A, Roux MM, Song JL, Su YH, Townley IK, Voronina E, Wong JL, Amore G, Branno M, Brown ER, Cavalieri V, Duboc V, Duloquin L, Flytzanis C, Gache C, Lapraz F, Lepage T, Locascio A, Martinez P, Matassi G, Matranga V, Range R, Rizzo F, Rottinger E, Beane W, Bradham C, Byrum C, Glenn T, Hussain S, Manning G, Miranda E, Thomason R, Walton K, Wikramanayake A, Wu SY, Xu R, Brown CT, Chen L, Gray RF, Lee PY, Nam J, Oliveri P, Smith J, Muzny D, Bell S, Chacko J, Cree A, Curry S, Davis C, Dinh H, Dugan-Rocha S, Fowler J, Gill R, Hamilton C, Hernandez J, Hines S, Hume J, Jackson L, Jolivet A, Kovar C, Lee S, Lewis L, Miner G, Morgan M, Nazareth LV, Okwuonu G, Parker D, Pu LL, Thorn R & Wright R. (2006b) The genome of the sea urchin *Strongylocentrotus purpuratus*. *Science (New York, N.Y)* **314**(5801): 941-52.
- Sondermann H, Soisson SM, Boykevisch S, Yang SS, Bar-Sagi D & Kuriyan J. (2004) Structural analysis of autoinhibition in the Ras activator Son of sevenless. *Cell* **119**(3): 393-405.

- Sprang SR. (1997) G protein mechanisms: insights from structural analysis. *Annual review of biochemistry* **66**: 639-78.
- Sudol M, Recinos CC, Abraczinskas J, Humbert J & Farooq A. (2005) WW or WoW: the WW domains in a union of bliss. *IUBMB life* **57**(12): 773-8.
- Symons M, Derry JM, Karlak B, Jiang S, Lemahieu V, McCormick F, Francke U & Abo A. (1996) Wiskott-Aldrich syndrome protein, a novel effector for the GTPase CDC42Hs, is implicated in actin polymerization. *Cell* **84**(5): 723-34.
- Szilak L, Moitra J & Vinson C. (1997) Design of a leucine zipper coiled coil stabilized 1.4 kcal mol<sup>-1</sup> by phosphorylation of a serine in the e position. *Protein Sci* **6**(6): 1273-83.
- Takai Y, Sasaki T & Matozaki T. (2001) Small GTP-binding proteins. *Physiological reviews* **81**(1): 153-208.
- Tall GG, Barbieri MA, Stahl PD & Horazdovsky BF. (2001) Ras-activated endocytosis is mediated by the Rab5 guanine nucleotide exchange activity of RIN1. *Developmental cell* **1**(1): 73-82.
- Therrien M, Chang HC, Solomon NM, Karim FD, Wassarman DA & Rubin GM. (1995) KSR, a novel protein kinase required for RAS signal transduction. *Cell* **83**(6): 879-88.
- Therrien M, Michaud NR, Rubin GM & Morrison DK. (1996) KSR modulates signal propagation within the MAPK cascade. *Genes & development* **10**(21): 2684-95.
- Thomas C, Fricke I, Scrima A, Berken A & Wittinghofer A. (2007) Structural evidence for a common intermediate in small G protein-GEF reactions. *Molecular cell* **25**(1): 141-9.
- Todd AE, Orengo CA & Thornton JM. (2002) Sequence and structural differences between enzyme and nonenzyme homologs. *Structure* **10**(10): 1435-51.
- Tognon CE, Kirk HE, Passmore LA, Whitehead IP, Der CJ & Kay RJ. (1998) Regulation of RasGRP via a phorbol ester-responsive C1 domain. *Molecular and cellular biology* **18**(12): 6995-7008.
- Toker A. (1998) Signaling through protein kinase C. *Front Biosci* **3**: D1134-47.
- Tommasi S, Dammann R, Jin SG, Zhang Xf XF, Avruch J & Pfeifer GP. (2002) RASSF3 and NORE1: identification and cloning of two human homologues of the putative tumor suppressor gene RASSF1. *Oncogene* **21**(17): 2713-20.
- Tong LA, de Vos AM, Milburn MV & Kim SH. (1991) Crystal structures at 2.2 Å resolution of the catalytic domains of normal ras protein and an oncogenic mutant complexed with GDP. *Journal of molecular biology* **217**(3): 503-16.
- Trahey M & McCormick F. (1987) A cytoplasmic protein stimulates normal N-ras p21 GTPase, but does not affect oncogenic mutants. *Science (New York, N.Y)* **238**(4826): 542-5.
- Trahey M, Wong G, Halenbeck R, Rubinfeld B, Martin GA, Ladner M, Long CM, Crosier WJ, Watt K, Kohts K & et al. (1988) Molecular cloning of two types of GAP complementary DNA from human placenta. *Science (New York, N.Y)* **242**(4886): 1697-700.
- Turner M & Billadeau DD. (2002) VAV proteins as signal integrators for multi-subunit immune-recognition receptors. *Nat Rev Immunol* **2**(7): 476-86.
- Van Aelst L, Barr M, Marcus S, Polverino A & Wigler M. (1993) Complex formation between RAS and RAF and other protein kinases. *Proceedings of the National Academy of Sciences of the United States of America* **90**(13): 6213-7.
- Verhey KJ & Rapoport TA. (2001) Kinesin carries the signal. *Trends in biochemical sciences* **26**(9): 545-50.
- Vestal DJ. (2005) The guanylate-binding proteins (GBPs): proinflammatory cytokine-induced members of the dynamin superfamily with unique GTPase activity. *J Interferon Cytokine Res* **25**(8): 435-43.
- Vetter IR & Wittinghofer A. (2001) The guanine nucleotide-binding switch in three dimensions. *Science (New York, N.Y)* **294**(5545): 1299-304.
- Vojtek AB & Der CJ. (1998) Increasing complexity of the Ras signaling pathway. *The Journal of biological chemistry* **273**(32): 19925-8.
- Walker SA, Lockyer PJ & Cullen PJ. (2003) The Ras binary switch: an ideal processor for decoding complex Ca<sup>2+</sup> signals? *Biochemical Society transactions* **31**(Pt 5): 966-9.
- Wansink DG, Peters W, Schaafsma I, Suttmuller RP, Oerlemans F, Adema GJ, Wieringa B, van der Zee CE & Hendriks W. (2004) Mild impairment of motor nerve repair in mice lacking PTP-BL tyrosine phosphatase activity. *Physiol Genomics* **19**(1): 50-60.
- Waters SB, Yamauchi K & Pessin JE. (1995) Insulin-stimulated disassociation of the SOS-Grb2 complex. *Molecular and cellular biology* **15**(5): 2791-9.
- Wechsler-Reya RJ. (2003) Analysis of gene expression in the normal and malignant cerebellum. *Recent progress in hormone research* **58**: 227-48.

- Weimer JM & Anton ES. (2006) Doubling up on microtubule stabilizers: synergistic functions of doublecortin-like kinase and doublecortin in the developing cerebral cortex. *Neuron* **49**(1): 3-4.
- Weis K. (2003) Regulating access to the genome: nucleocytoplasmic transport throughout the cell cycle. *Cell* **112**(4): 441-51.
- Wellington A, Emmons S, James B, Calley J, Grover M, Tolia P & Manseau L. (1999) Spire contains actin binding domains and is related to ascidian posterior end mark-5. *Development (Cambridge, England)* **126**(23): 5267-74.
- Wennerberg K & Der CJ. (2004) Rho-family GTPases: it's not only Rac and Rho (and I like it). *Journal of cell science* **117**(Pt 8): 1301-12.
- Wennerberg K, Rossman KL & Der CJ. (2005) The Ras superfamily at a glance. *Journal of cell science* **118**(Pt 5): 843-6.
- Wetzker R & Bohmer FD. (2003) Transactivation joins multiple tracks to the ERK/MAPK cascade. *Nature reviews* **4**(8): 651-7.
- Whitford KL, Dijkhuizen P, Polleux F & Ghosh A. (2002) Molecular control of cortical dendrite development. *Annual review of neuroscience* **25**: 127-49.
- Willingham MC, Pastan I, Shih TY & Scolnick EM. (1980) Localization of the src gene product of the Harvey strain of MSV to plasma membrane of transformed cells by electron microscopic immunocytochemistry. *Cell* **19**(4): 1005-14.
- Willumsen BM, Christensen A, Hubbert NL, Papageorge AG & Lowy DR. (1984) The p21 ras C-terminus is required for transformation and membrane association. *Nature* **310**(5978): 583-6.
- Wingate RJ. (2001) The rhombic lip and early cerebellar development. *Current opinion in neurobiology* **11**(1): 82-8.
- Wittinghofer A & Pai EF. (1991) The structure of Ras protein: a model for a universal molecular switch. *Trends in biochemical sciences* **16**(10): 382-7.
- Wittinghofer F, Krengel U, John J, Kabsch W & Pai EF. (1991) Three-dimensional structure of p21 in the active conformation and analysis of an oncogenic mutant. *Environmental health perspectives* **93**: 11-5.
- Wolf E, Kim PS & Berger B. (1997) MultiCoil: a program for predicting two- and three-stranded coiled coils. *Protein Sci* **6**(6): 1179-89.
- Wolfman A & Macara IG. (1990) A cytosolic protein catalyzes the release of GDP from p21ras. *Science (New York, N.Y)* **248**(4951): 67-9.
- Yu YB. (2002) Coiled-coils: stability, specificity, and drug delivery potential. *Advanced drug delivery reviews* **54**(8): 1113-29.
- Zeller R, Haramis AG, Zuniga A, McGuigan C, Dono R, Davidson G, Chabanis S & Gibson T. (1999) Formin defines a large family of morphoregulatory genes and functions in establishment of the polarising region. *Cell and tissue research* **296**(1): 85-93.
- Zerial M & McBride H. (2001) Rab proteins as membrane organizers. *Nature reviews* **2**(2): 107-17.
- Zhang FL & Casey PJ. (1996) Protein prenylation: molecular mechanisms and functional consequences. *Annual review of biochemistry* **65**: 241-69.
- Zhang Z, Rehmann H, Price LS, Riedl J & Bos JL. (2005) AF6 negatively regulates Rap1-induced cell adhesion. *The Journal of biological chemistry* **280**(39): 33200-5.
- Zhao Q, Kho A, Kenney AM, Yuk Di DI, Kohane I & Rowitch DH. (2002) Identification of genes expressed with temporal-spatial restriction to developing cerebellar neuron precursors by a functional genomic approach. *Proceedings of the National Academy of Sciences of the United States of America* **99**(8): 5704-9.
- Zhong J, Zhang T & Bloch LM. (2006) Dendritic mRNAs encode diversified functionalities in hippocampal pyramidal neurons. *BMC neuroscience* **7**: 17.
- Zhou Z, Feng H, Zhou H, Zhou Y & Bai Y. (2005) Design and folding of a multidomain protein. *Biochemistry* **44**(36): 12107-12.